


March 2015

Aggregation and Interfacial Behavior of Charged Surfactants in Ionic Liquids

Lang Chen
University of Massachusetts - Amherst

Follow this and additional works at: https://scholarworks.umass.edu/dissertations_2

 Part of the [Analytical Chemistry Commons](#), [Fluid Dynamics Commons](#), [Materials Chemistry Commons](#), [Physical Chemistry Commons](#), and the [Polymer Chemistry Commons](#)

Recommended Citation

Chen, Lang, "Aggregation and Interfacial Behavior of Charged Surfactants in Ionic Liquids" (2015).
Doctoral Dissertations. 294.
https://scholarworks.umass.edu/dissertations_2/294

This Open Access Dissertation is brought to you for free and open access by the Dissertations and Theses at ScholarWorks@UMass Amherst. It has been accepted for inclusion in Doctoral Dissertations by an authorized administrator of ScholarWorks@UMass Amherst. For more information, please contact scholarworks@library.umass.edu.

AGGREGATION AND INTERFACIAL BEHAVIOR OF CHARGED
SURFACTANTS IN IONIC LIQUIDS

A Dissertation Presented

By

LANG CHEN

Submitted to the Graduate School of the
University of Massachusetts Amherst in partial fulfillment
of the requirements for the degree of

DOCTOR OF PHILOSOPHY

February 2015

Polymer Science and Engineering

© Copyright by Lang Chen 2015

All Rights Reserved

AGGREGATION AND INTERFACIAL BEHAVIOR OF CHARGED
SURFACTANTS IN IONIC LIQUIDS

A Dissertation Presented

By

LANG CHEN

Approved as to style and content by:

Harry Bermudez, Chair

Thomas J. McCarthy, Member

Anthony D. Dinsmore, Member

David A. Hoagland, Department Head

Polymer Science and Engineering

DEDICATION

To my grandparents, parents, brother, sister in law
and my little nephew Zhenan.

Love the people who treat you right and forget about the ones who do not.

ACKNOWLEDGEMENTS

“Research is to see what everybody else has seen and to think what nobody else has thought.” Even as for now, I am not sure if I can say I have grown up to be a good researcher, but I have kept in my mind that critical thinking is so important that it starts to be my everyday habit. This dissertation is the result of many years of hard work in the lab as well as valuable support of many people who deserve thanks and acknowledgement during my graduate career.

To my thesis advisor, Dr. Harry Bermudez, I thank you for the constant support and guidance in the last six years. You are always full of passion and patience in research discussion. You are able to explain complicate concepts in simple words with funny analogy. Every time after our meeting, I immediately feel I gain energy and motivation again to do the work. With respect to your extensive knowledge, patience, dedication and kindness, you are definitely a role model to me.

To my committee members, Dr. Thomas McCarthy and Dr. Anthony Dinsmore, I thank you for the constructive comments and scientific recommendations. Your expertise in relevant areas are very helpful in my research.

To my collaborators, Dr. Silvina Matysiak and Dr. Helim Aranda-Espinoza, both from the University of Maryland, and their students, I thank you for participating in this interesting project. I really enjoyed our Skype meetings and occasionally site visiting. I learned completely different point of view of the project such as simulation studies. Our collaborations are really fruitful and have strengthened my dissertation.

To my past and present group members in Bermudez's group, Ronald Lerum, Treniece Terry, Adam Hathorne, Jung Won Keum, Andreas Kourouklis, Ploy Charoenphol, Sandipan Dawn, Purnendu Nayak, Stephen Strassburg, and Laura Lanier, I thank you for all your questions during the group meetings and warm friendship throughout my PhD. Thanks also goes to the undergraduate students I have mentored: Joel Brown, Annuli Okoye, and Thang Nguyen, I thank you for the hard work and fresh mind.

To the PSE faculty and staff members, I thank you for teaching courses, training instruments, and charging my paychecks and other documents. Thanks to Jack, Weiguo, Lisa, Maria, my life in Amherst is much easier.

To my manager Tim Butler and all the great people at Genzyme Biomaterials Group, Sneha, Bo, Jessica, Laura, Mike, Bob, Grace, Magnus, Luis, Joyce, Paul, Steve, Kanwen, Keith, Jeff, Erika, Rubina, Olga and Vish, I am grateful for all the help during my co-op. I really enjoyed my first industrial experience.

To the class 2008, UMass Pingpong Club, and my friends in Amherst, especially Dayong, Weiyin, Xiaodan, Li, Tsunghan, Henry, Yu, Feng, Mike, Xinyu, Ji, Yongping, Jun, Peiwen, Dian, Wei, Yan, Yujie, Xiaobo, Yingyong, Minchao, Cheng, Hsin-wei, Zhuoya, Yucheng, George, Yue, Dong, Bing, Xiaolin, Hunt, Ying, Fangfang, Ranran and Zhujun, I thank you for all the help to make me quickly get used to the life here. Those moments of sharing our happiness and frustration will be my best memory in Amherst.

Lastly, to my entire family in China, especially my grandparents, parents, brother, sister in law and my nephew, I would like to express my love to all of you. Thank you for all the untiring support and unconditional love in my whole life. You are always my best motivators.

Earning a Ph.D. degree is never the end or culmination, but a new start of my future career. With many years of scientific training, and full of love, I will begin with my new journey...

ABSTRACT

AGGREGATION AND INTERFACIAL BEHAVIOR OF CHARGED SURFACTANTS IN IONIC LIQUIDS

FEBRUARY 2015

LANG CHEN

B.S., UNIVERSITY OF SCIENCE AND TECHNOLOGY OF CHINA

M.S., UNIVERSITY OF MASSACHUSETTS AMHERST

PH.D., UNIVERSITY OF MASSACHUSETTS AMHERST

Directed by: Professor Harry Bermudez

Room-temperature ionic liquids (ILs) exhibit a unique set of properties, leading to opportunities for numerous applications such as green solvents, batteries and lubricants. Their properties can be greatly tuned and controlled by addition of surfactants. It is therefore critical to obtain a better understanding of the aggregation and interfacial behavior of surfactants within ILs.

Firstly, the phase diagram and aggregation isotherms of surfactants in several distinct ILs were investigated by solubility and tensiometry. A connection between solubility of the surfactant and the physical properties of the underlying ionic liquid was established. We found that the interfacial energy was crucial in determining

aggregation behavior while electrostatic interactions could be largely ignored. This finding could provide the general prediction of solubility and the first indication of how to choose ILs with desired properties. *Secondly*, this study was extended to include mixtures of cationic and anionic surfactants where our data further demonstrated near-complete charge screening. The critical micelle concentration (CMC) and mixed micelle composition were found to be close to ideal behavior. This so-called charge screening in IL is in sharp contrast to that of aqueous solution and can be explained by Debye theory. *Moreover*, our pulsed-field gradient spin-echo (PGSE)-NMR data confirmed the existence of micelle formation and showed evidence that the IL anion partially incorporates into surfactant micelles, resulting in slower diffusion when the surfactant concentration is above the *CMC*. *Lastly*, through use of X-ray photoelectron spectroscopy (XPS), the roles of surfactant alkyl chain length, concentration, and probing depth on interfacial properties were investigated. Depending on the chain length and concentration, surfactants can alter the IL interface to varying extents, highlighting a simple route to manipulate interfacial properties. XPS is further demonstrated to be a direct measurement of the surface activity and ion-exchange behavior in surfactant-ionic liquid system.

The results here give insight into the interaction between solutes and IL solvents and the nature of self-assembly of surfactants in ILs. This study could significantly broaden the potential application of ionic liquids such as novel solvents for protein storage and electrolytes for Li-ion batteries.

TABLE OF CONTENTS

	Page
ACKNOWLEDGEMENTS	v
ABSTRACT.....	viii
LIST OF TABLES	xiv
LIST OF FIGURES	xvi
CHAPTER	
1 INTRODUCTION	1
1.1 Overview	1
1.2 Room Temperature Ionic Liquids	2
1.2.1 History.....	2
1.2.2 Characteristics and Applications.....	3
1.3 Self-assembly of Surfactants in ILs.....	4
1.4 Techniques*	6
1.4.1 Tensiometry	6

1.4.2	X-ray Photoelectron Spectroscopy (XPS).....	9
1.4.3	Pulsed-field Gradient Spin-Echo (PGSE) NMR.....	12
1.4.4	Other Techniques.....	14
1.5	Thesis Outline	15
1.6	References	16
2	SOLUBILITY AND AGGREGATION OF CHARGED SURFACTANTS IN IONIC LIQUIDS*	22
2.1	Introduction.....	22
2.2	Experimental Section	24
2.3	Results and Discussion.....	27
2.4	Conclusions	41
2.5	References	42
3	CHARGE SCREENING BETWEEN ANIONIC AND CATIONIC SURFACTANTS IN IONIC LIQUIDS*	46
3.1	Introduction.....	46

3.2	Experimental Section	48
3.3	Results and Discussion	50
3.4	Conclusions	62
3.5	References	62
4	SHORT IONIC LIQUIDS PLAY ROLES AS BOTH SOLVENT AND CO-SURFACTANT IN MICELLIZATION*	66
4.1	Introduction	66
4.2	Experimental Section	67
4.3	Results and Discussion	71
4.4	Conclusions	79
4.5	References	79
5	PROBING THE INTERFACE OF CHARGED SURFACTANTS IN IONIC LIQUIDS BY XPS*	82
5.1	Introduction	82
5.2	Experimental	85

5.3	Results and Discussion.....	90
5.3.1	Chain Length Effect.....	94
5.3.2	Concentration Effect.....	96
5.3.3	Information Depth Effect.....	101
5.4	Conclusions.....	102
5.5	References.....	103
6	CONCLUSIONS AND OUTLOOK.....	109

APPENDICES

A.	PRELIMINARY RESULTS FOR EFFECT OF CHARGE PRESENTATION AND COUNTERIONS.....	111
B.	PROPOSED EXPERIMENTS.....	121
C.	PROCEDURES FOR XPS MEASUREMENTS.....	130
D.	PROCEDURES FOR PGSE-NMR MEASUREMENTS.....	135
	BIBLIOGRAPHY.....	139

LIST OF TABLES

Table	Page
2.1 Physical Properties of Ionic Liquids and Water at Room Temperature	25
2.2 Elemental Ratio of Neat Ionic Liquids from XPS, Recorded at Takeoff Angle of 45° (Following the procedures in Chapter 5)	25
2.3 Krafft Temperature (°C) of C _n TAB in I, III, IV, V and Water	29
2.4 Surface Properties of C _n TAB in [BMIM][BF ₄], III at 90°C	34
2.5 Surface Properties of C _n TAB in [EMIM][EtSO ₄], I at 90°C	34
2.6 Surface Properties of C _n TAB in [BMPyr][DCA], IV at 90°C	34
2.7 Summary of CMC Analysis of Data from Figure 2.9	39
3.1 Krafft Temperatures of SDS/DTAB Mixtures in [EMIM][EtSO ₄]	51
3.2 Maximum Surface Excess Concentration (Γ_m) of SDS/DTAB Mixtures in [EMIM][EtSO ₄]	59
3.3 Interaction Parameter of SDS/DTAB Mixtures in Water and [EMIM][EtSO ₄]	60

4.1 cmc, γ_{cmc} and Surface Properties (Surface Pressure at cmc (Π_{cmc}), Surface Excess Concentration (Γ_1) and the Interfacial Area per Molecule (A_1)) of SDS in Water (20°C) and [EMIM][EtSO ₄] (90°C) Obtained by Tensiometry.....	72
4.2 Diffusion Coefficient Value ($\times 10^{-10}$ m ² /s) of SDS in [EMIM][EtSO ₄] at Various Concentrations	73
4.3 Slopes from Figure 3 (i.e., $D_f\eta$ or $D_M\eta$) and their Ratio α	76
4.4 Viscosity η (mPa·s) of SDS in [EMIM][EtSO ₄] at Various Concentrations.....	78
5.1 Alkyltrimethylammonium Bromide Transition Concentrations, in mM, Determined by Tensiometry at room temperature.....	93
A.1 Surface Properties of SB-12, 1:1 DTAB/SDS, and DTADS in Water (20°C) and [EMIM][EtSO ₄] (90°C) (For the 1:1 DTAB/SDS system, cmc ₁₂ is used)	118

LIST OF FIGURES

Figure	Page
1.1 Chemical structures of common IL cations (red) and anions (blue) reprinted from Castner et al. ⁶	3
1.2 (a) Langmuir-Blodgett Trough setup as tensiometry and (b) surfactant aggregation process.....	8
1.3 Phase diagrams for binary mixtures, reprinted from Inoue et al. ⁴⁸	9
1.4 Schematic of X-ray photoelectron spectroscopy. Adapted from Chen et al. ⁵⁸	11
1.5 (a) XPS spectra of [EMIM][EtSO ₄], recorded at $\theta = 45^\circ$ emission angle. (b) XPS C1s regional spectra of (C ₈ TAB) on [EMIM][EtSO ₄]. Adapted from reference ⁵⁹	12
1.6 Schematic of diffusion NMR spectroscopy. Reprinted from reference ⁶¹	13
2.1 Structures of ionic liquids considered in this study.	25
2.2 Krafft temperature measurements by solubility for octyl, dodecyl, tetradecyl, and hexadecyltrimethylammonium bromides in [BMIM][BF ₄], III	28
2.3 Krafft temperature measurements by solubility for octyl, dodecyl, tetradecyl, and hexadecyltrimethylammonium bromides in [EMIM][EtSO ₄], I	28

2.4 Krafft temperature for hexyl, dodecyl, tetradecyl, and hexadecyltrimethylammonium bromides in [BMPyr][DCA], IV	29
2.5 Isotherms of C ₁₄ TAB in different subphase at 20°C (a, in H ₂ O, I , and II) and at 90°C (b, in I , III , and IV).	31
2.6 Isotherms of C _n TAB in [BMIM][BF ₄], III , at 90°C.	32
2.7 Isotherms of C _n TAB in [EMIM][EtSO ₄], I at 90°C.	32
2.8 Isotherms of C _n TAB in [BMPyr][DCA], IV at 90°C.	33
2.9 Dependence of chain length of surfactant on CMC in different solvents at temperatures higher than their Krafft temperatures.	36
3.1 Structures of SDS, DTAB and [EMIM][EtSO ₄].	49
3.2 Isotherms of SDS/DTAB Mixtures with different mole fraction of a component in the mixture, α_1 , in water at 20°C.	52
3.3 Isotherms of SDS/DTAB Mixtures with different mole fraction of a component in the mixture, α_1 , in [EMIM][EtSO ₄] at 90°C.	53
3.4 Critical micelle concentrations (CMC ₁₂) for SDS/DTAB mixtures in (a) water (solid circles) at 20°C and (b) [EMIM][EtSO ₄] (solid squares) at 90°C. The dashed lines represent cmc_{12}^{id} from Equation (3.1).	53

3.5 CMC calculation of SDS/DTAB mixtures ($\alpha_1 = 0.75$) in [EMIM][EtSO ₄] by fluorescence spectroscopy. Inset is fluorescence of DiO in the surfactant-IL solutions with different concentrations (the arrow indicates increasing concentrations). The CMC was determined to be 208mM.....	54
3.6 ¹ H NMR spectrum at 90°C obtained for (a) [EMIM][EtSO ₄] and (b) SDS/DTAB mixtures ($\alpha_1 = 0.75$) in [EMIM][EtSO ₄].	54
3.7 Plots of δ for surfactants protons as a function of SDS/DTAB mixtures ($\alpha_1 = 0.75$) concentration in [EMIM][EtSO ₄].	55
3.8 Surface tensions at CMC (γ_{CMC}) for SDS/DTAB mixtures in (a) water (open circles) at 20°C and (b) [EMIM][EtSO ₄] (open squares) at 90°C.	58
3.9 SDS mole fraction in micelles (x_1) from Equation 3.3 for SDS/DTAB mixtures in (a) water (solid circles) and (b) [EMIM][EtSO ₄] (solid squares), evaluated from Equation 3.3 at the CMC. The dashed lines represent x_1^{id} from Equation 3.2.....	60
4.1 ¹ H-NMR spectra of SDS in [EMIM][EtSO ₄] at SDS concentration of 575 mM...	70
4.2 Isotherms of SDS in water at 20 °C (solid square) and in [EMIM][EtSO ₄] at 90 °C (solid circle).	71

4.3 Diffusion coefficient of SDS in D ₂ O at 20 °C (empty squares, data taken from Pettersson et al. ⁶²) and [EMIM][EtSO ₄] at 90 °C (solid circles) as a function of SDS concentration.....	72
4.4 The product of diffusion coefficient, viscosity, and total SDS concentration ($D\eta C_t$) for [EMIM] (solid squares), [EtSO ₄] (solid circles) and SDS (solid triangles) as function of total SDS concentration. The solid lines are best fits corresponding to Equations 4.3 (a) and 4.3 (b).....	75
4.5 The product of diffusion coefficient, viscosity, and total SDS concentration ($D\eta C_t$) for SDS as function of total SDS concentration in D ₂ O. The dash lines are best fits corresponding to Equations 4.3 (a) and 4.3 (b). Taken from Pettersson et al. ⁶² Note: the solid square data are from our own PGSE-NMR measurements.....	78
5.1 Structures of the ionic liquids and surfactants in this study.....	85
5.2 XPS spectra of neat [EMIM][EtSO ₄] (black, down) and [BHEDMA][MeSO ₃] (red, up), recorded at $\theta=45^\circ$ takeoff angle.....	88
5.3 XPS regional spectra (a) C1s, (b) N1s, and (c) Si2p, for neat [EMIM][EtSO ₄] after 7.5 min of Ar ⁺ ion bombardment. Note that silicon content is minimal, reflective of minimal impurities.....	90

5.4 Isotherms of C₁₄TAB in [EMIM][EtSO₄] at different temperatures: 20°C (black squares) and 90°C (red circles). The surface tensions of neat IL at different temperatures are shown as the first points before the break. The Krafft temperature for this system is T_k = 75°C.⁶⁵92

5.5 (a) Surface fractions, x_i^{surf} , (C_nTA⁺ (black squares), [EMIM]⁺ (red circles), [EtSO₄]⁻ (blue triangles), and Br⁻ (dark cyan triangles) and overall surface charge ratios (inset) and (b) surface enrichment of C_nTAB on [EMIM][EtSO₄]. Overall surface charge is defined as the ratio of total surface cations to total surface anions. Surface enrichment is defined as the ratio $\epsilon_i = x_i^{surf} / x_i^{bulk}$, where x_i^{surf} are taken over the XPS information depth $d \approx 3.2$ nm.....92

5.6 Surface fractions (C_nTA⁺ (black squares), [EMIM]⁺ (red circles), [EtSO₄]⁻ (blue triangles), and Br⁻ (dark cyan triangles) and surface charge ratios (inset) of (a) C₈TAB and (b) C₁₄TAB in [EMIM][EtSO₄]. The open symbols represent samples that exhibit a semi-solid surface film.....98

5.7 Detailed X-ray photoelectron spectra of (a, b, c) C₈TAB and (d, e, f) C₁₄TAB in [EMIM][EtSO₄] at two different surfactant concentrations. The black solid lines represent $C \approx 30C_a < CMC$, while the red dashed lines represent $C > CMC$. The spectra were taken with an emission angle of 45° (information depth $d \approx 3.2$ nm)..... 100

5.8 Surface fraction difference of cations $\Delta x^+ = C_nTA^+ - [EMIM]^+$, for (a) C_8TAB and (b) $C_{14}TAB$ in $[EMIM][EtSO_4]$. The emission angles of 75° (black squares) and 30° (red circles) correspond to information depths d of 1.2 nm and 3.9 nm, respectively. The open symbols represent samples that exhibit a semi-solid surface film. 102

A.1 Surfactants with different charge presentation..... 112

A.2 Isotherms of (a) zwitterionic surfactant SB-12 (black squares), 1:1 DTAB/SDS mixture (red upward triangles), and DTADS (with Si impurity) in $[EMIM][EtSO_4]$ (green downward triangles) at $90^\circ C$ and (b) zwitterionic surfactant SB-12 (black squares) at $20^\circ C$, and DTADS in water (green downward triangles, data from reference¹⁵⁶, at $25^\circ C$). The isotherm for the 1:1 DTAB/SDS mixture in water is not available because of its multiphase character. Please note that the DTADS in this Figure has residual amount of Si..... 115

A.3 Isotherms of (a) zwitterionic surfactant SB-12 (black squares), 1:1 DTAB/SDS mixture (red upward triangles), and DTADS (without Si impurity) in $[EMIM][EtSO_4]$ (blue circles) at $90^\circ C$ and (b) zwitterionic surfactant SB-12 (black squares) at $20^\circ C$, and DTADS in water (blue downward triangles, data from reference¹⁵⁶, at $25^\circ C$). The isotherm for the 1:1 DTAB/SDS mixture in water is not available because of its multiphase character. 115

CHAPTER 1

INTRODUCTION

1.1 Overview

Ionic liquids (ILs), or molten salts, are a class of organic fused salts with melting point below 100 °C. Many of them are liquids at room temperature and have a wide liquid range. ILs often comprise large organic cations paired with organic or inorganic anions. In the last few years, the physical and chemical properties of ionic liquids have attracted interest among chemists, biologists, physicists, and nanotechnologists for extremely diverse applications. Ionic liquids are considered to be the next generation of “green” solvent mainly due to their negligible vapor pressure. A better understanding about this class of “green” solvents would not only provide us a new window to reexamine our past experience and knowledge on material science, but also could broaden the range of future industrial applications. In this project, charged surfactants were introduced into ILs resulting in a neither aqueous nor molecular organic solvent system. In this “sea of ions” system, the aggregation and interfacial self-assembly of surfactants will take place and be characterized. In this introduction, the history and basic physiochemical properties of neat ILs will be firstly discussed. More complicated surfactant/IL systems will be reviewed with respect to their self-assembly and aggregation behavior. The techniques used here and other general techniques in this

research area will also be summarized. At the end of the introduction, the organization of this thesis will be addressed.

1.2 Room Temperature Ionic Liquids

1.2.1 History

The term "ionic liquid" in the general sense was used as early as 1943.¹ But one of the earliest truly room temperature ionic liquid, ethylammonium nitrate, with melting point of 12°C, was synthesized and described by Walden in 1914.² Since then, ILs are continuing to receive intense attention as a result of their unusual and diverse properties due to the charged character. In the 1970s and 1980s, ionic liquids were developed for electrochemical applications such as electrolytes in battery applications.³⁻⁴ And from the mid-1980s, ILs were proposed and widely studied as new unique green solvents for organic reactions.⁵ In recent years, the number of ILs synthesized has been expanding rapidly and the potential ILs could be vast because of huge numbers of combination of different cations and anions (Figure 1.1). The possible combinations places chemists in the position to design and fine-tune physical and chemical properties by introducing or combining structural motifs and thereby, making tailor-made materials and solutions. Moreover, the huge numbers of ILs lead to the question of how to design optimal ILs by useful guidance.

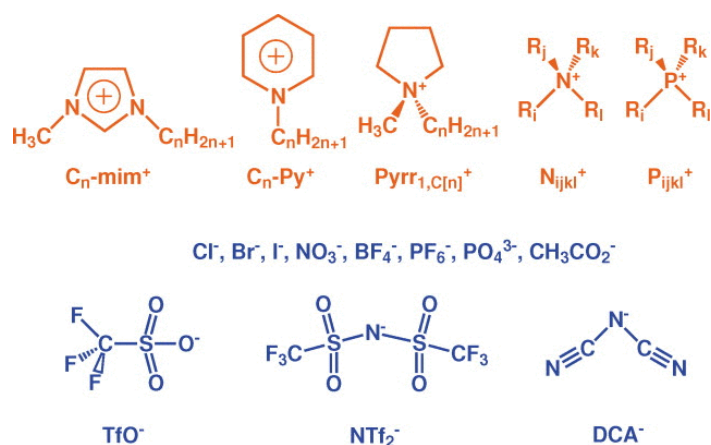


Figure 1.1 Chemical structures of common IL cations (red) and anions (blue) reprinted from Castner *et al.*⁶.

1.2.2 Characteristics and Applications

As bulk solvents, ILs generally demonstrate negligible vapor pressure, high thermal stability, outstanding catalytic properties, and a wide range of solubility for various compounds.⁷⁻⁸ As mentioned, their properties can be readily adjusted by variation of cation and anion species.⁹ The bulk properties of ILs have been exploited to achieve self-assembly of micelles and vesicles which can be applied in separations, formulations, drug delivery, etc..¹⁰⁻¹² The interfacial properties of ILs are of central importance in applications such as lubrication, (heterogeneous) catalysis, chromatography, and even fuel cells.¹³⁻¹⁷ Therefore, ILs are considered as the next generation of “designer” solvents comparing to traditional molecular volatile organic solvents (VOCs).^{8, 18-19}

1.3 Self-assembly of Surfactants in ILs

Although ILs are referred to as "designer" solvents due to their seemingly endless diversity, achieving desired properties remains largely empirical. This state of affairs motivates the synthesis and characterization of many new IL compounds to build and validate structure-property relationships. However, simple mixing is a traditional route to bypassing the iterative procedure of synthesis and characterization. One form of such mixing (and tuning of properties) is the introduction of surfactants to ILs. The self-assembly of surfactants will take place at both bulk and interface and eventually the two will reach equilibrium.

The self-assembly of surfactants in ILs is of fundamental interest in the field of colloid and interface science.²⁰⁻²⁴ The ability of surfactants to self-aggregate depends on many factors.²⁰ In an aqueous solution, as surfactant molecules are added, surfactants form a layer at the liquid-air interface. When the surface becomes saturated with surfactant monomers, molecules begin to aggregate in the bulk phase.²⁵ This process happens in IL systems as well.²¹ The transition concentration during the process is referred to as the critical micelle concentration (CMC). Due to the reconstruction of the species in the solution, many properties such as surface tension, conductivity, NMR chemical shift, have a sharp transition at this concentration.

The driving force of micellization in aqueous solution is the hydrophobic effect.²² The electrostatic interactions between the head groups determine their relative

positions and separations in aggregates.²⁶ From a physical point of view, ionic liquids are more complex than aqueous solution because they combine properties from two vastly different types of materials: molten salts and organic liquids.²⁷ Therefore, the micellization of surfactant in ionic liquids is expected to differ from that in aqueous solutions.

It is well-established that the CMC for charged surfactants in aqueous solutions is reduced as the ionic strength increases.²⁸ Intuitively, the presence of salt in water screens the electrostatic repulsion between charged headgroups, facilitating aggregation between surfactants and thereby lowering the CMC. The corresponding situation in ILs is not readily apparent, and from the argument above it might be anticipated that CMCs in ILs are much lower than in aqueous solutions. However, many experiments have shown that CMCs in ILs tend to be higher than in water,^{20, 24, 29-31} a result attributed to "solvatophobicity" or "solvophobicity". To gain further insight on solubility and aggregation behavior, in this project we will examine two series of common ionic surfactants (alkyl trimethylammonium bromides (C_n TAB) and sodium alkylsulfate (SC_nS)) and their mixtures in five distinct ionic liquids. The resulting CMCs not only vary substantially, but can have values either higher or lower than water. These results suggest an ability to rationally tune the CMC for any given surfactant by the appropriate choice of ionic liquid.

Besides the aggregation of surfactants in bulk solution, the introduction of surfactants can also extend the versatility of interfacial properties, with the possibility of greater control. The neat IL-vapor³² and IL-solid³³ interfaces have been probed with both experimental³⁴⁻⁴⁰ and modeling approaches⁴¹⁻⁴⁵, revealing unique features, such as (i) the preferential orientation of cations^{34-36, 42, 45} and (ii) the existence of surface layers^{37, 40, 42-44}. The above two properties suggested an interesting context to explore the behavior of surface-active molecules. In particular, by pairing charged surfactants with ILs, a wide variety of interfacial behavior should become possible due to the interplay of electrostatic and surface forces.

1.4 Techniques*

* This section was partially published in [Chen, L. G.; Strassburg S. H.; Bermudez, H., "Characterization of Self-assembled Amphiphiles in Ionic Liquids", Invited Book Chapter]⁴⁶

1.4.1 Tensiometry

The balance of forces at the free boundary of liquids reveals a net inward force towards the bulk, known as surface tension γ . Thus, surface tension is a property intimately related to both the bulk and the interface. Surface tension, also referred to as surface free energy, which represents the solvophobic interaction, is the main property of any liquid–gas interface. To modify the surface tension of a given liquid, surfactants are often used as additives, primarily because the bulk properties of the liquid remain

relatively unchanged. Other approaches to changing surface tension (e.g., temperature, solvent mixing) have the undesired effect that they alter both interfacial and bulk properties simultaneously.

With respect to neat ionic liquids, their surface tensions span the range of organic solvents and in some cases approach the value of water.^{27,47} Such a wide range is expected, given the organic character of IL ions and potential for hydrogen-bonding interactions.

Several methods are available to measure surface tension, differing in sensitivity and ease of use. The most basic (and crude) is the capillary rise method, where a capillary of known radius, r , is partially immersed into the liquid. The height, h , of the liquid column inside the capillary is related to the surface tension γ by: $\frac{2\gamma(\cos\theta)}{r} = gh(\Delta\rho)$, where θ is the contact angle between the liquid and capillary, g is the gravitational constant and $\Delta\rho$ is the density difference between the inner and the surrounding fluid. In the case of ideal wetting and with air as the surrounding fluid, the above equation can be approximated as: $\gamma = \rho ghr/2$. Other approaches include the bubble pressure, pendant-drop and Wilhelmy plate methods. The Wilhelmy plate method is perhaps the most sensitive and relies on the downward force applied to a probe by surface tension γ and the force due to buoyancy:

$$F = m_p g - m_l g + \gamma L \cos\theta \quad (1.1)$$

where F is the force on the plate, $m_p g$ and $m_l g$ are the weight of plate and the buoyancy force on the plate. L is the wetted perimeter (NOT the height of the plate), θ is the contact angle.

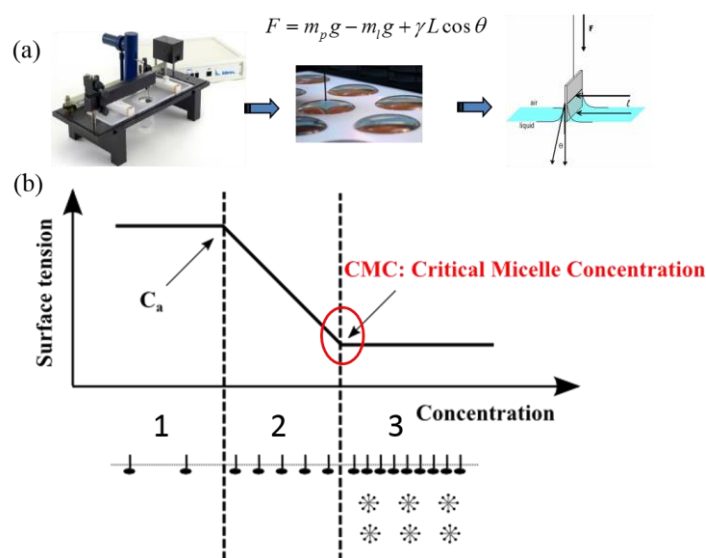


Figure 1.2 (a) Langmuir-Blodgett Trough setup as tensiometry and (b) surfactant aggregation process.

In our study, Langmuir-Blodgett Trough is used as tensiometry by the Wilhelmy method (Figure 1.2 (a)). Monitoring the surface tension as a function of surfactant concentration at constant temperature yields a so-called "isotherm" and can be used to calculate interfacial properties as well as the onset of aggregation (Figure 1.2 (b)). From isotherm curve, a decrease of surface tension indicates that the surfactant is absorbed at the air/solution interface.²¹ After the break point of an abrupt change in the slope, the surface tension of the solutions remains unchanged with further addition of surfactant, indicating the saturation of surfactant monomers and the formation of aggregates. The CMC is identified by the sharp transition between a window of gradual decrease and a

plateau in the surface tension. During the decrease of surface tension, the Gibbs equation and thermodynamic analysis yield characteristics such as maximum surface excess concentration Γ , molecular area A , and free energies of micellization and adsorption.²⁸

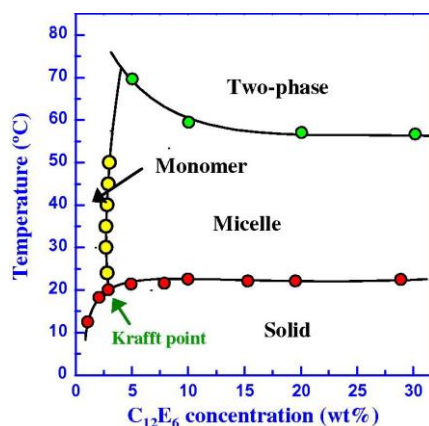


Figure 1.3 Phase diagrams for binary mixtures, reprinted from Inoue et al.⁴⁸.

The CMC is an important characteristic of a surfactant in solution. But not all CMCs can be determined at room temperature, especially in IL. The Krafft point, or Krafft Temperature (T_k), is a minimum temperature above which surfactants form micelles.⁴⁹ Micellization only takes place above the T_k , which itself depends on the nature of surfactant and the solvent. T_k can be determined by visual observation based on its phase diagram (Figure 1.3).^{48, 50}

1.4.2 X-ray Photoelectron Spectroscopy (XPS)

Among all the surface-sensitive techniques, X-ray photoelectron spectroscopy (XPS) is arguably the most common and prominent UHV-based tool to provide unique

information on chemical composition, chemical state identification and even composition depth profiles of the near-surface region. The negligible vapor pressure of ILs enables the use of low-pressure techniques, including XPS, to directly probe the surface composition of the resulting interfaces.^{9, 51-56} Recently, Lovelock et al. published a comprehensive review article on photoelectron spectroscopy applied to IL interfaces.⁵⁷ The first experimental investigation of the air-IL interface using XPS was reported by Smith et al. in 2005.⁵¹ This technique is based on the kinetic energy and number of photoelectrons that are irradiated by a beam of X-rays at the emission angle of θ (Figure 1.4).⁵⁸ The electron binding energy of each of the emitted electrons is given by

$$E_{binding} = E_{xray} - E_{kinetic} \quad (1.2)$$

where $E_{binding}$ is the binding energy of the electron, E_{xray} is the energy of X-ray being used, $E_{kinetic}$ is the kinetic energy of the electron measured. Different elements or the same element with different chemical environments will have different characteristic binding energy. The XPS signal originates from the top 1 to 10 nm of the sample depending on the emission angle θ .

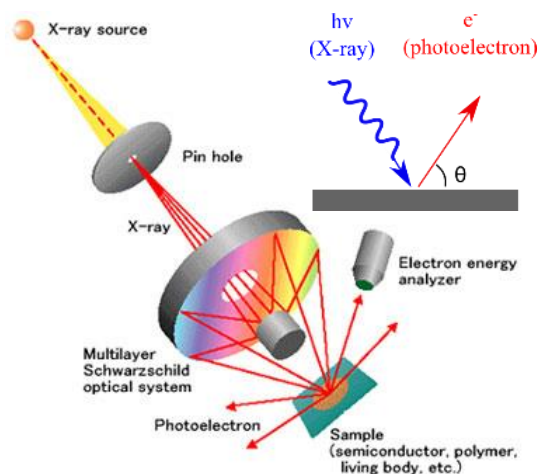


Figure 1.4 Schematic of X-ray photoelectron spectroscopy. Adapted from Chen et al.⁵⁸.

Atomic compositions were obtained by using known sensitivity factors for the instrument and setup. Molecular compositions are also determined by performing atomic mass balances using chemical formulas of each species (see Chapter 5 for details).⁵⁹ Besides of elemental composition of the surface, XPS can also be used to measure the elements that contaminate a surface. For example, Figure 1.5 (a) is the XPS survey spectrum for the IL [EMIM][EtSO₄].⁵⁹ The presence of C, N, O, S atoms confirms the formula and absence of other impurity at the air-IL interface. A series of XPS studies on the influence of anions and substituents for neat ILs have been reported by Lovelock et al..⁵⁴⁻⁵⁶

As expected, most XPS studies have focused exclusively on neat ILs. However, the interfacial self-assembly of surfactants in IL have also been investigated by using XPS. For example, our group examined the influence of positively-charged surfactants alkyltrimethylammonium bromide (C_nTAB) on the 1-ethyl-3-methyl imidazolium

ethylsulfate ([EMIM][EtSO₄]) interface by XPS.⁶⁰ Figure 1.5 (b) shows the C1s regional XPS scan of C₈TAB on [EMIM][EtSO₄].

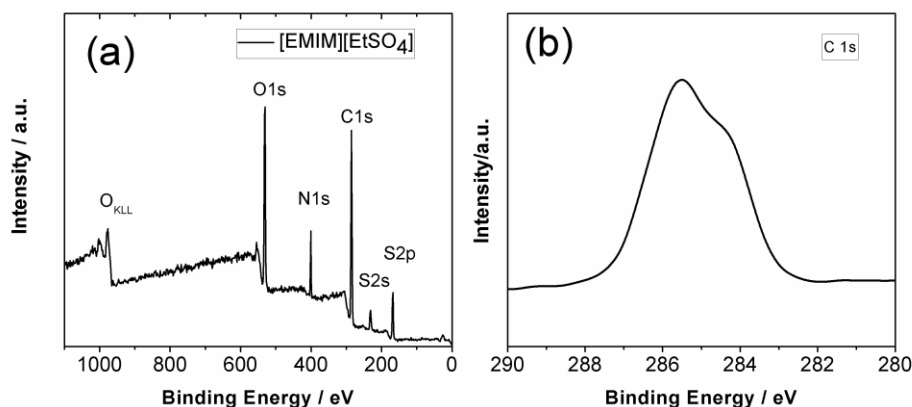


Figure 1.5 (a) XPS spectra of [EMIM][EtSO₄], recorded at $\theta = 45^\circ$ emission angle. (b) XPS C1s regional spectra of (C₈TAB) on [EMIM][EtSO₄]. Adapted from reference ⁵⁹.

1.4.3 Pulsed-field Gradient Spin-Echo (PGSE) NMR

Molecules can move in liquid or solution, known as Brownian molecular motion and is simply called diffusion or self-diffusion. Diffusion NMR experiments can resolve different compounds in a mixture based on their diffusion coefficients, depending on physical parameters such as: size and shape of the molecules, temperature, and viscosity. Assuming a spherical size of the molecule, the hydrodynamic radius R_h can be obtained from the Stokes-Einstein equation:

$$R_h = \frac{kT}{6\pi\eta D} \quad (1.3)$$

where k is the Boltzmann constant, T is the temperature and η is the viscosity.

The diffusion NMR technique is often referred to as Diffusion Ordered Spectroscopy (DOSY) or Pulsed-field Gradient Spin-Echo (PGSE) NMR. By use of a gradient, molecules can be spatially labeled depending on their position in the sample tube. If they move after diffusion time Δ , their new position can be decoded by a second gradient. The NMR signal intensity is attenuated depending on the diffusion time Δ and the gradient parameters by $I = I_0 e^{-D\gamma^2 g^2 \delta^2 (\Delta - \delta/3)}$, where I is the observed intensity, I_0 the reference intensity (unattenuated signal intensity), D the diffusion coefficient, γ the gyromagnetic ratio of the observed nucleus, g the gradient strength, δ the length of the gradient, and Δ the diffusion time. To simplify the equation by combining some parameters, we have:

$$I = I_0 e^{-DQ} \quad \text{or} \quad \ln\left(\frac{I}{I_0}\right) = -DQ \quad (1.4)$$

In other words, a series of NMR diffusion spectra are acquired as a function of the gradient strength g (Figure 1.6) and the slope of the peak linear decay ($\ln(I/I_0)$ vs. Q) is used to obtain the diffusion coefficient D .

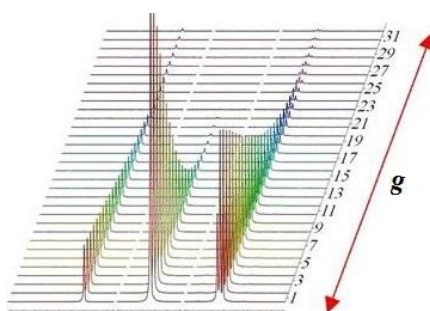


Figure 1.6 Schematic of diffusion NMR spectroscopy. Reprinted from reference ⁶¹.

Diffusion NMR can indicate the formation of aggregates (e.g., micelles, emulsions). Moreover, the CMC values can be obtained from the transition of D vs. surfactant concentration plot. Because of the dynamic equilibrium between monomer and micelle, the observed diffusion coefficient is the mean value of the two states.⁶²

Diffusion NMR studies have also been performed on the self-aggregation of neat IL with or without the presence of salt.⁶³⁻⁶⁴ To our knowledge, surfactant aggregation in IL has not been studied yet by using PGSE-NMR although the analysis in aqueous solution can be also applied in surfactant-IL systems. Chapter 4 of this thesis will discuss our investigation on the diffusion and size of surfactant aggregates in [EMIM][EtSO₄] by PGSE-NMR.

1.4.4 Other Techniques

Even though we are mainly using the above three techniques, many other surface or bulk liquid techniques have been conducted in different types of ILs or their complex systems such as Neutron Reflectivity (NR), Sum Frequency Generation (SFG), Atomic Force Microscopy (AFM), Fluorescence Spectroscopy, Polarized Optical Microscopy (POM), Scatterings (dynamic light scattering, SAXS, SANS), NMR, TEM, etc. To the best of our knowledge, a comprehensive review focusing on these techniques applied to the surfactant-IL systems has not been published yet. For the information of readers, we have reviewed these techniques with examples applied to both interface and the bulk as seen in reference⁴⁶.

1.5 Thesis Outline

Ionic liquids provide us a new window to reexamine our past understanding about solubility, micelle aggregation and interfacial self-assembly. In this thesis, I will describe some interesting phenomenon and the unusual behavior of surfactant in ionic liquid systems, in contrast to the aqueous solution. Chapter 2-4 will focus on the bulk aggregation, while Chapter 5 will discuss the interfacial behavior. This study could potentially broaden the future application of ILs in the areas of formulation, separation, drug delivery, and Li-ion batteries.

In Chapter 2, charged surfactants with different hydrocarbon chain length were introduced into several different ionic liquids. A connection between the solubility of the surfactant and the physical properties of the underlying ionic liquid was established. Interfacial energy was found to be the major factor affecting the surfactant aggregation process. The results here give insight into explaining the nature of self-assembly of surfactants at IL interfaces and the interaction between solutes and IL solvents.

In Chapter 3, the study was extended to include the mixtures of anionic and cationic surfactants in the same IL. Our experiments showed nearly ideal mixing of the two surfactant components over the entire composition range and suggested that charge screening is prominent in ILs. This behavior is in sharp contrast to the strong electrostatic attraction and a multiphase composition gap in water. Two models by Clint

and Rubingh, which describe ideal and nonideal micellar behavior, respectively, will also be discussed on the basis of our results.

In Chapter 4, the behavior of the surfactant in IL was investigated by tensiometry and pulsed-field gradient spin-echo (PGSE)-NMR. Both techniques were independently used to determine the critical micelle concentration (*CMC*) and agreed well with each other. The latter technique also demonstrated that the anion of the IL is partially incorporated into the SDS micelles, revealing a more complex aggregation behavior than in aqueous solutions. Our results, and the wide variety of available ILs, suggest new opportunities to control micellization behavior.

In Chapter 5, our study moved to the interface. The influence of charged surfactant on IL interfaces will be discussed based on the results of X-ray photoelectron spectroscopy (XPS). The roles of surfactant alkyl chain length, concentration, and information depth on interfacial properties are investigated. Depending on the chain length and concentration, the surfactants can alter the IL interface to varying extents, highlighting a simple route to manipulate interfacial properties.

In Chapter 6, conclusions of this thesis study will be presented.

1.6 References

1. Barrer, R. M., The viscosity of pure liquids. II. Polymerised ionic melts. *T Faraday Soc* **1943**, *39*, 0059-0066.

2. Walden, P., Molecular weights and electrical conductivity of several fused salts. *Bulletin de l'Academie Imperiale des Sciences de St.-Petersbourg* **1914**, 405-422.
3. Chum, H. L.; Koch, V. R.; Miller, L. L.; Osteryoung, R. A., Electrochemical Scrutiny of Organometallic Iron Complexes and Hexamethylbenzene in a Room-Temperature Molten-Salt. *J. Am. Chem. Soc.* **1975**, *97* (11), 3264-3265.
4. Wilkes, J. S.; Levisky, J. A.; Wilson, R. A.; Hussey, C. L., Dialkylimidazolium Chloroaluminate Melts - a New Class of Room-Temperature Ionic Liquids for Electrochemistry, Spectroscopy, and Synthesis. *Inorg. Chem.* **1982**, *21* (3), 1263-1264.
5. Fry, S. E.; Pienta, N. J., Effects of Molten-Salts on Reactions - Nucleophilic Aromatic-Substitution by Halide-Ions in Molten Dodecyltributylphosphonium Salts. *J. Am. Chem. Soc.* **1985**, *107* (22), 6399-6400.
6. Castner, E. W.; Wishart, J. F., Spotlight on ionic liquids. *J. Chem. Phys.* **2010**, *132* (12), -.
7. Greaves, T. L.; Drummond, C. J., Ionic liquids as amphiphile self-assembly media. *Chem. Soc. Rev.* **2008**, *37* (8), 1709--1726.
8. Rogers, R. D.; Seddon, K. R., Ionic liquids - Solvents of the future? *Science* **2003**, *302* (5646), 792-793.
9. Maier, F.; Cremer, T.; Kolbeck, C.; Lovelock, K. R. J.; Paape, N.; Schulz, P. S.; Wasserscheid, P.; Steinrueck, H.-P., Insights into the surface composition and enrichment effects of ionic liquids and ionic liquid mixtures. *Phys. Chem. Chem. Phys.* **2010**, *12* (8), 1905-1915.
10. Dobler, D.; Schmidts, T.; Klingenhofer, I.; Runkel, F., Ionic liquids as ingredients in topical drug delivery systems. *International Journal of Pharmaceutics* **2013**, *441* (1-2), 620-627.
11. He, Y. Y.; Li, Z. B.; Simone, P.; Lodge, T. P., Self-assembly of block copolymer micelles in an ionic liquid. *J. Am. Chem. Soc.* **2006**, *128* (8), 2745-2750.
12. Bai, Z. F.; He, Y. Y.; Lodge, T. P., Block copolymer micelle shuttles with tunable transfer temperatures between ionic liquids and aqueous solutions. *Langmuir* **2008**, *24* (10), 5284-5290.
13. Welton, T., Room-Temperature Ionic Liquids. Solvents for Synthesis and Catalysis. *Chemical Reviews* **1999**, *99* (8), 2071-2084.
14. Wasserscheid, P.; Keim, W., Ionic liquids - New "solutions" for transition metal catalysis. *Angew. Chem. Int. Edit.* **2000**, *39* (21), 3772--3789.
15. Yao, C.; Pitner, W. R.; Anderson, J. L., Ionic Liquids Containing the Tris(pentafluoroethyl)trifluorophosphate Anion: a New Class of Highly Selective and Ultra Hydrophobic

Solvents for the Extraction of Polycyclic Aromatic Hydrocarbons Using Single Drop Microextraction. *Anal. Chem.* **2009**, *81* (12), 5054-5063.

16. Greaves, T. L.; Drummond, C. J., Protic ionic liquids: Properties and applications. *Chem. Rev.* **2008**, *108* (1), 206-237.

17. Aliaga, C.; Santos, C. S.; Baldelli, S., Surface chemistry of room-temperature ionic liquids. *Phys. Chem. Chem. Phys.* **2007**, *9* (28), 3683-3700.

18. Marsh, K. N.; Boxall, J. A.; Lichtenthaler, R., Room temperature ionic liquids and their mixtures - a review. *Fluid Phase Equilib.* **2004**, *219* (1), 93-98.

19. Chiappe, C.; Pieraccini, D., Ionic liquids: solvent properties and organic reactivity. *J. Phys. Org. Chem.* **2005**, *18* (4), 275-297.

20. Fletcher, K. A.; Pandey, S., Surfactant aggregation within room-temperature ionic liquid 1-ethyl-3-methylimidazolium bis(trifluoromethylsulfonyl)imide. *Langmuir* **2004**, *20* (1), 33-36.

21. Zheng, L. Q.; Li, N.; Zhang, S. H.; Wu, J. P.; Li, X. W.; Yu, L., Aggregation behavior of a fluorinated surfactant in 1-butyl-3-methylimidazolium ionic liquids. *J. Phys. Chem. B* **2008**, *112* (39), 12453-12460.

22. Li, N.; Zhang, S. H.; Zheng, L. Q.; Dong, B.; Li, X. W.; Yu, L., Aggregation behavior of long-chain ionic liquids in an ionic liquid. *Phys. Chem. Chem. Phys.* **2008**, *10* (30), 4375-4377.

23. Ogino, K.; Kakihara, T.; Abe, M., Estimation of the Critical Micelle Concentrations and the Aggregation Numbers of Sodium Alkyl Sulfates by Capillary-Type Isotachopheresis. *Colloid Polym. Sci.* **1987**, *265* (7), 604-612.

24. Patrascu, C.; Gauffre, F.; Nallet, F.; Bordes, R.; Oberdisse, J.; de Lauth-Viguerie, N.; Mingotaud, C., Micelles in ionic liquids: Aggregation behavior of alkyl poly(ethyleneglycol)-ethers in 1-butyl-3-methyl-imidazolium type ionic liquids. *Chemphyschem* **2006**, *7* (1), 99-101.

25. Anderson, J. L.; Pino, V.; Hagberg, E. C.; Sheares, V. V.; Armstrong, D. W., Surfactant solvation effects and micelle formation in ionic liquids. *Chemical Communications* **2003**, (19), 2444-2445.

26. Bhattacharya, S.; Haldar, J.; Aswal, V. K.; Goyal, P. S., Molecular modulation of surfactant aggregation in water: Effect of the incorporation of multiple headgroups on micellar properties. *Angew. Chem. Int. Edit.* **2001**, *40* (7), 1228-+.

27. Sedev, R., Surface tension, interfacial tension and contact angles of ionic liquids. *Curr. Opin. Colloid In.* **2011**, *16* (4), 310-316.

28. Israelachvili, J. N., *Intermolecular and surface forces*. Academic Press: San Diego, 1992.

29. Anderson, J. L.; Pino, V.; Hagberg, E. C.; Sheares, V.; Armstrong, D. W., Surfactant solvation effects and micelle formation in ionic liquids. *Chem. Commun.* **2003**, (19), 2444-2445.
30. Li, N.; Zhang, S.; Zheng, L.; Wu, J.; Li, X.; Yu, L., Aggregation behavior of a fluorinated surfactant in 1-butyl-3-methylimidazolium ionic liquids. *J. Phys. Chem. B* **2008**, *112* (39), 12453-12460.
31. Li, N.; Zhang, S.; Zheng, L.; Inoue, T., Aggregation behavior of a fluorinated surfactant in 1-butyl-3-methylimidazolium bis(trifluoromethylsulfonyl)imide ionic liquid. *Langmuir* **2009**, *25* (18), 10473-82.
32. Santos, C. S.; Baldelli, S., Gas-liquid interface of room-temperature ionic liquids. *Chem. Soc. Rev.* **2010**, *39* (6), 2136-2145.
33. Hayes, R.; Warr, G. G.; Atkin, R., At the interface: solvation and designing ionic liquids. *Phys. Chem. Chem. Phys.* **2010**, *12* (8), 1709-1723.
34. Gannon, T. J.; Law, G.; Watson, P. R.; Carmichael, A. J.; Seddon, K. R., First observation of molecular composition and orientation at the surface of a room-temperature ionic liquid. *Langmuir* **1999**, *15* (24), 8429-8434.
35. Law, G.; Watson, P. R., Surface orientation in ionic liquids. *Chem. Phys. Lett.* **2001**, *345* (1-2), 1-4.
36. Baldelli, S., Influence of water on the orientation of cations at the surface of a room-temperature ionic liquid: A sum frequency generation vibrational spectroscopic study. *J. Phys. Chem. B* **2003**, *107* (25), 6148-6152.
37. Sloutskin, E.; Ocko, B. M.; Tamam, L.; Kuzmenko, I.; Gog, T.; Deutsch, M., Surface layering in ionic liquids: An X-ray reflectivity study (vol 127, pg 7796, 2005). *J. Am. Chem. Soc.* **2005**, *127* (51), 18333-18333.
38. Santos, C. S.; Baldelli, S., Surface orientation of 1-methyl-, 1-ethyl-, and 1-butyl-3-methylimidazolium methyl sulfate as probed by sum-frequency generation vibrational spectroscopy. *J. Phys. Chem. B* **2007**, *111* (18), 4715-4723.
39. Waring, C.; Bagot, P. A. J.; Slattery, J. M.; Costen, M. L.; McKendrick, K. G., O((3)P) Atoms as a Probe of Surface Ordering in 1-Alkyl-3-methylimidazolium-Based Ionic Liquids. *J. Phys. Chem. Lett.* **2010**, *1* (1), 429-433.
40. Niga, P.; Wakeham, D.; Nelson, A.; Warr, G. G.; Rutland, M.; Atkin, R., Structure of the Ethylammonium Nitrate Surface: An X-ray Reflectivity and Vibrational Sum Frequency Spectroscopy Study. *Langmuir* **2010**, *26* (11), 8282-8288.

41. Wang, Y. T.; Voth, G. A., Unique spatial heterogeneity in ionic liquids. *J. Am. Chem. Soc.* **2005**, *127* (35), 12192-12193.
42. Bhargava, B. L.; Balasubramanian, S., Layering at an ionic liquid-vapor interface: A molecular dynamics simulation study of [bmim][PF(6)]. *J. Am. Chem. Soc.* **2006**, *128* (31), 10073-10078.
43. Sloutskin, E.; Lynden-Bell, R. M.; Balasubramanian, S.; Deutsch, M., The surface structure of ionic liquids: Comparing simulations with x-ray measurements. *J. Chem. Phys.* **2006**, *125* (17).
44. Wang, Y.; Jiang, W.; Yan, T.; Voth, G. A., Understanding ionic liquids through atomistic and coarse-grained molecular dynamics simulations. *Accounts Chem. Res.* **2007**, *40* (11), 1193-1199.
45. Lynden-Bell, R. M.; Del Popolo, M. G.; Youngs, T. G. A.; Kohanoff, J.; Hanke, C. G.; Harper, J. B.; Pinilla, C. C., Simulations of ionic liquids, solutions, and surfaces. *Accounts Chem. Res.* **2007**, *40* (11), 1138-1145.
46. Chen, L. G.; H., S. S.; Bermudez, H., Characterization of Self-assembled Amphiphiles in Ionic Liquids. Paul, B. K., Ed. Wiley: 2014.
47. Tariq, M.; Freire, M. G.; Saramago, B.; Coutinho, J. A. P.; Lopes, J. N. C.; Rebelo, L. P. N., Surface tension of ionic liquids and ionic liquid solutions. *Chem. Soc. Rev.* **2012**, *41* (2), 829-868.
48. Inoue, T.; Higuchi, Y.; Misono, T., Differential scanning calorimetric study of nonionic surfactant mixtures with a room temperature ionic liquid, bmimBF(4). *J. Colloid. Interf. Sci.* **2009**, *338* (1), 308-311.
49. Tsujii, K.; Mino, J., Krafft Point Depression of Some Zwitterionic Surfactants by Inorganic Salts. *J. Phys. Chem.* **1978**, *82* (14), 1610-1614.
50. Rico, I.; Lattes, A., Formamide, a Water Substitute .12. Krafft Temperature and Micelle Formation of Ionic Surfactants in Formamide. *J. Phys. Chem.* **1986**, *90* (22), 5870-5872.
51. Smith, E. F.; Villar Garcia, I. J.; Briggs, D.; Licence, P., Ionic liquids in vacuo; solution-phase X-ray photoelectron spectroscopy. *Chem. Commun.* **2005**, (45), 5633-5635.
52. Smith, E. F.; Rutten, F. J. M.; Villar-Garcia, I. J.; Briggs, D.; Licence, P., Ionic liquids in vacuo: Analysis of liquid surfaces using ultra-high-vacuum techniques. *Langmuir* **2006**, *22* (22), 9386-9392.
53. Gottfried, J. M.; Maier, F.; Rossa, J.; Gerhard, D.; Schulz, P. S.; Wasserscheid, P.; Steinruck, H. P., Surface studies on the ionic liquid 1-ethyl-3-methylimidazolium ethylsulfate using X-ray photoelectron spectroscopy (XPS). *Z. Phys. Chem.* **2006**, *220* (10-11), 1439-1453.
54. Lockett, V.; Sedev, R.; Bassell, C.; Ralston, J., Angle-resolved X-ray photoelectron spectroscopy of the surface of imidazolium ionic liquids. *Phys. Chem. Chem. Phys.* **2008**, *10* (9), 1330-1335.

55. Kolbeck, C.; Cremer, T.; Lovelock, K. R. J.; Paape, N.; Schulz, P. S.; Wasserscheid, P.; Maier, F.; Steinruck, H. P., Influence of Different Anions on the Surface Composition of Ionic Liquids Studied Using ARXPS. *J. Phys. Chem. B* **2009**, *113* (25), 8682-8688.
56. Lovelock, K. R. J.; Kolbeck, C.; Cremer, T.; Paape, N.; Schulz, P. S.; Wasserscheid, P.; Maier, F.; Steinruck, H. P., Influence of Different Substituents on the Surface Composition of Ionic Liquids Studied Using ARXPS. *J. Phys. Chem. B* **2009**, *113* (9), 2854-2864.
57. Lovelock, K. R. J.; Villar-Garcia, I. J.; Maier, F.; Steinruck, H. P.; Licence, P., Photoelectron Spectroscopy of Ionic Liquid-Based Interfaces. *Chem. Rev.* **2010**, *110* (9), 5158-5190.
58. http://www.ntt-at.com/product/x-ray_focus/.
59. Chen, L. G.; Lerum, R. V.; Aranda-Espinoza, H.; Bermudez, H., Surfactant-Mediated Ion Exchange and Charge Reversal at Ionic Liquid Interfaces. *J. Phys. Chem. B* **2010**, *114* (35), 11502-11508.
60. Chen, L. G.; Bermudez, H., Probing the interface of charged surfactants in ionic liquids by XPS. In *ACS Symposium Series 1117*, Visser, A. E., Ed. American Chemical Society: Washington, DC, 2012; pp 289-302.
61. <http://mestrelab.com/resources/dosy/>.
62. Pettersson, E.; Topgaard, D.; Stilbs, P.; Soderman, O., Surfactant/nonionic polymer interaction. a NMR diffusometry and NMR electrophoretic investigation. *Langmuir* **2004**, *20* (4), 1138-1143.
63. Kunze, M.; Jeong, S.; Paillard, E.; Schonhoff, M.; Winter, M.; Passerini, S., New Insights to Self-Aggregation in Ionic Liquid Electrolytes for High-Energy Electrochemical Devices. *Advanced Energy Materials* **2011**, *1* (2), 274-281.
64. Pramanik, R.; Sarkar, S.; Ghatak, C.; Rao, V. G.; Sarkar, N., Ionic Liquid Containing Microemulsions: Probe by Conductance, Dynamic Light Scattering, Diffusion-Ordered Spectroscopy NMR Measurements, and Study of Solvent Relaxation Dynamics. *J. Phys. Chem. B* **2011**, *115* (10), 2322-2330.

CHAPTER 2

SOLUBILITY AND AGGREGATION OF CHARGED SURFACTANTS IN IONIC LIQUIDS*

* This chapter was published in [Chen, L. G.; Bermudez, H., "Solubility and aggregation of charged surfactants in ionic liquids." *Langmuir*, 28, 1157-1162, (2012)].⁶⁵

2.1 Introduction

Room-temperature ionic liquids (ILs), organic salts with a melting point below 100°C, continue to receive intense attention as a result of their unusual and diverse properties. ILs are extremely versatile; their properties can be readily adjusted by variation of the cation and anion species.⁹ As bulk solvents, ILs generally demonstrate negligible vapor pressure, high thermal stability, and a wide range of solubility for various compounds.⁷⁻⁸ For example, the bulk properties of ILs have also been exploited to achieve self-assembly of micelles and vesicles.¹¹⁻¹² The interfacial properties of ILs are also of central importance in applications such as lubrication, (heterogeneous) catalysis, and chromatography.¹³⁻¹⁶

Although they are as sometimes referred to as "designer" solvents due to their seemingly endless diversity, achieving desired properties remains largely empirical. This state of affairs motivates the synthesis and characterization of many new IL

compounds to build and validate structure-property relationships. However, simple mixing is a traditional route to bypassing the iterative procedure of synthesis and characterization. One form of such mixing (and tuning of properties) is the introduction of surfactants to an interface. Because surfactants preferentially partition to the interface, they can extend the versatility of interfacial properties, with the possibility of greater control.

It is well-established that the critical micelle concentration (CMC) for charged surfactants in aqueous solutions is reduced as the ionic strength increases.²⁸ Intuitively, the presence of salt in water screens the electrostatic repulsion between charged headgroups, facilitating aggregation between surfactants and thereby lowering the CMC. The corresponding situation in ILs is not readily apparent, and from the argument above it might be anticipated that CMCs in ILs are much lower than in aqueous solutions. In contrast to this expectation, many experiments have shown that CMCs of neutral surfactants in ILs tend to be higher than in water,^{20, 24, 29-31} a result attributed to "solvatophobicity" or "solvophobicity". We note that surveys of the literature to date are complicated by many studies where the solvent is actually a water-IL mixture. To gain further insight into solubility and aggregation behavior in ILs, here we examine a series of common charged amphiphiles (alkyl trimethylammonium bromides) in four distinct neat ionic liquids. We did not restrict ourselves to a single class of ILs (e.g., imidazolium) because our intent was to obtain information on the general behavior of surfactant-IL systems. The main factor in selecting the ILs chosen here was their

relatively high bare interfacial tensions. Our results indicate that the CMC values not only vary substantially, but also can be either higher or lower than that of water. These results suggest an ability to rationally tune the CMC for any given surfactant by the appropriate choice of ionic liquid.

2.2 Experimental Section

Ionic Liquids (ILs). 1-ethyl-3-methyl imidazolium ethylsulfate [EMIM][EtSO₄], **I**, and 1-butyl-3-methylimidazolium tetrafluoroborate [BMIM][BF₄], **III**, were obtained from Sigma (>95% and >98%, respectively) and bis(2-hydroxyethyl) dimethylammonium methylsulfonate [BHEDMA][MeSO₃], **II**, was a gift from Professor T. J. McCarthy. 1-butyl-1-methylpyrrolidinium dicyanamide [BMPyr][DCA], **IV**, was acquired from IoLiTec with mass fraction purities >98%. Their molecular weights and viscosities at room temperature are shown in Table 2.1. The structures of ILs are shown in Figure 2.1. All of the ionic liquids were dried by being heated at 70 °C under vacuum for 2 days. **IV** was purified following the procedure described in Lockett, et al.⁵⁴ The purity of the neat ionic liquids and selected surfactants was assessed by ¹H-NMR or ¹³C-NMR and did not reveal any impurities. These findings were also confirmed by X-ray photoelectron spectroscopy (XPS) control experiments (see Table 2.2).

Table 2.1 Physical Properties of Ionic Liquids and Water at Room Temperature

	I	II	III	IV	V	H ₂ O
MW (g/mol)	236.29	229.29	226.02	208.31	108.1	18.02
Viscosity (Pa·s)	0.107	2.34	0.28	0.05	0.028	0.001
surface tension (mN/m)	48.7±0.5 (N=37)	64.5±0.5 (N=28)	44.7±0.5 (N=15)	53.3±0.3 (N=7)	47.5 ⁶⁶	72.8

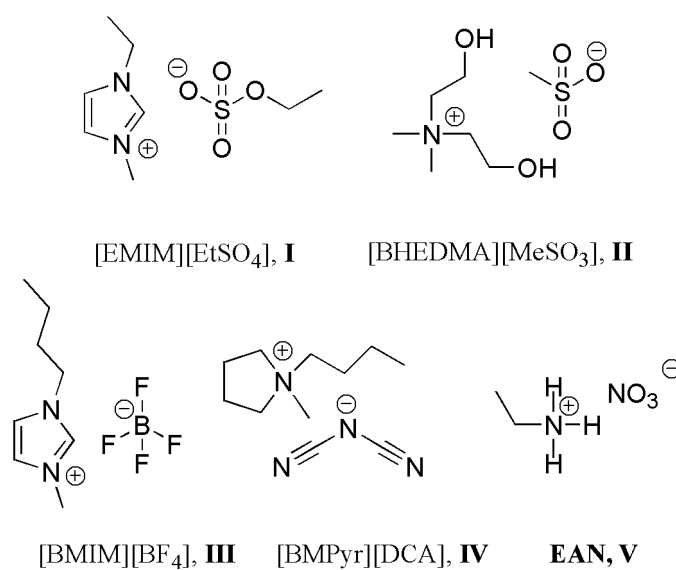


Figure 2.1 Structures of ionic liquids considered in this study.

Table 2.2 Elemental Ratio of Neat Ionic Liquids from XPS, Recorded at Takeoff Angle of 45° (Following the procedures in Chapter 5)

		C%	O%	N%	S%	F%	B%
I	theory	53.3	26.7	13.3	6.7	/	/
	expt.	52.1	28.5	13.1	6.4	/	/
II	theory	50.0	35.7	7.1	7.1	/	/
	expt.	49.5	37.0	6.9	6.6	/	/
III	theory	53.3	/	13.3	/	26.7	6.7
	expt.	51.9	/	12.3	/	28.5	7.4
IV	theory	73.3	/	26.7	/	/	/
	expt.	75.2	/	24.8	/	/	/

Surfactants. Dodecyltrimethylammonium bromide (C₁₂TAB) (99%) and hexadecyltrimethylammonium bromide (C₁₆TAB) (>99%) were purchased from Fisher. Hexyltrimethylammonium bromide (C₆TAB) (>98%), octyltrimethylammonium bromide (C₈TAB) (>98%), decyltrimethylammonium bromide (C₁₀TAB) (>98%), and tetradecyltrimethylammonium bromide (C₁₄TAB) (>99%) were purchased from Sigma. All surfactants were used as received.

Surface Characterization. Krafft temperatures were determined by visual observation of clear glass vials containing 1mL of IL and varying amounts of surfactant.⁵⁰ The IL-surfactant mixtures were slowly heated with vigorous shaking. The temperature at which surfactant was completely dissolved was recorded. This method, while not particularly accurate, has the advantage of being simple and easy to perform.

Surface tension was measured by the Wilhelmy method using a Micro Trough XS (Kibron, Inc.) and is especially suited for high-temperature experiments as compared to pendant-drop or bubble methods. At room temperature, all four ionic liquids have relatively high interfacial tensions relative to those of traditional organic solvents but much lower than that of water (Table 2.1). Our experimental values are in good agreement with those of literature, when available.^{17, 67-69}

For room temperature isotherms, in-house reverse osmosis (RO) water was passed through a 0.22 μ m filter and then used to dissolve the surfactants. After dissolution, solutions were heated to 50 °C to make stock solutions, which were

subsequently diluted to appropriate concentrations as needed. Approximately 300-500 μ L of RO water, **I**, or **II** was examined as subphase in a metal alloy plate containing Teflon-lined wells with a fixed area of 2.9 cm². To determine the effect of added surfactant, ~5-40 μ L of surfactant solutions were applied dropwise to the surface of IL. Surface tensions were measured after an equilibration time of 15 min. We note that although water is introduced into the system, it is always less than 12% by volume and does not significantly alter the bare interfacial tension.^{18, 70}

For high temperature isotherms, surfactants were dissolved directly in ILs at elevated temperature. Surfactant-IL solutions (300 μ L) with different concentrations were applied on an aluminum plate with glass wells. The temperature was controlled and monitored by using a hotplate placed underneath the multi-well plate and an Omega HH506RA multilogger thermometer probe in the well of interest.

2.3 Results and Discussion

The Krafft temperature T_k is a point of phase change below that a charged surfactant remains in solidlike form, while above which its solubility rises sharply.⁷¹ At the Krafft point there is an equilibrium among this ordered (but solvated) phase, dispersed monomers, and micellar structures. To obtain the CMC of the surfactants in the ionic liquids, measurements must be made above the Krafft temperature. Plots of surfactant solubility versus temperature (Figure 2.2, Figure 2.3 and Figure 2.4) yield the Krafft temperature T_k .⁴⁹ In the case of gradual changes in solubility, T_k is identified

from the transition between linear regimes. For example, Figure 2.2 shows the solubility behavior for C₈TAB, C₁₂TAB, C₁₄TAB, and C₁₆TAB in **III**.

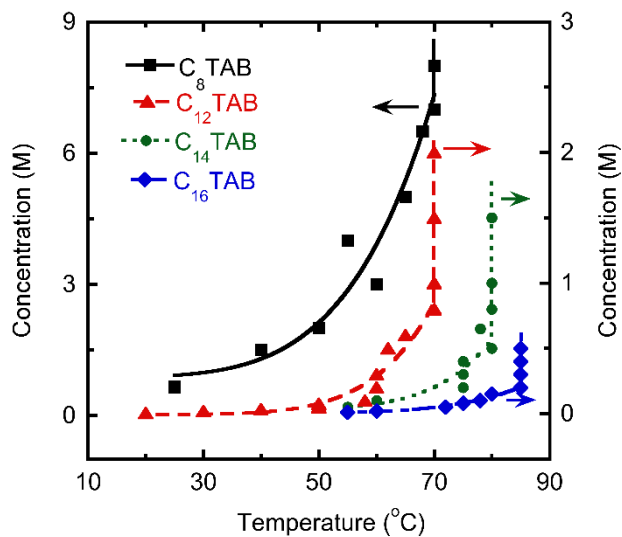


Figure 2.2 Krafft temperature measurements by solubility for octyl, dodecyl, tetradecyl, and hexadecyltrimethylammonium bromides in [BMIM][BF₄], **III**.

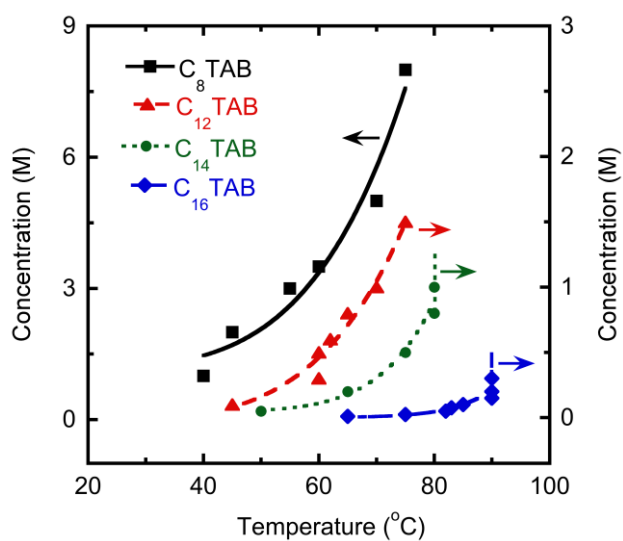


Figure 2.3 Krafft temperature measurements by solubility for octyl, dodecyl, tetradecyl, and hexadecyltrimethylammonium bromides in [EMIM][EtSO₄], **I**.

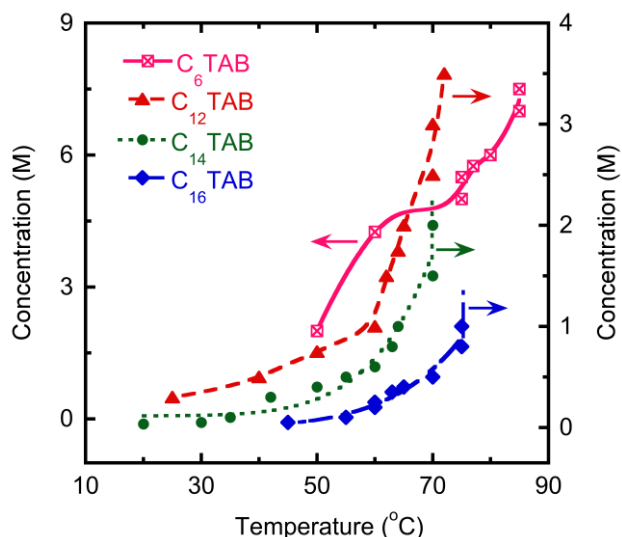


Figure 2.4 Krafft temperature for hexyl, dodecyl, tetradecyl, and hexadecyltrimethylammonium bromides in [BMPyr][DCA], **IV**.

Table 2.3 summarizes the Krafft temperature chain length dependence of C_n TAB in the ILs and water. The Krafft temperatures for C_n TAB in **II** are below room temperature for all surfactant chain lengths. **I** and **III** were found to have higher Krafft temperatures with increasing chain length of surfactant, which is the same trend as reported in the literature for V^{66} and H_2O^{72} . Interestingly, **IV** does not seem to obey this chain length trend.

Table 2.3 Krafft Temperature ($^{\circ}C$) of C_n TAB in **I**, **III**, **IV**, **V** and Water

chain length	I	III	IV	V^{66}	H_2O^{72}
6	/	/	80 ± 2.5	/	/
8	60 ± 2.5	60 ± 2.5	/	/	< 0
10	65 ± 5	65 ± 2.5	70 ± 2.5	/	< 0
12	70 ± 2.5	70 ± 1	65 ± 2	20	< 0
14	75 ± 2.5	80 ± 2	65 ± 2	34	~ 0
16	85 ± 2.5	85 ± 2	70 ± 2	48	24

Generally speaking, by increasing the length of the surfactant alkyl chain, van der Waals interactions are also increased. As a result, the Krafft temperature is shifted higher. Besides van der Waals interactions between alkyl chains, solution conditions can also affect the Krafft temperature. With increasing counterion concentration, Krafft temperatures are generally increased, irrespective of whether the counterions are introduced from the surfactant itself⁷³ or by addition of corresponding salt^{71,74}. In other words, the increased ionic strength of the solvent phase will screen repulsive electrostatic interactions between the charged surfactants, thereby favoring an ordered (solidlike) phase and increasing T_k . The result is an inhibitory “counterion effect” on solubility/micellization⁷³ because as the surfactant concentration increases, so does the counterion concentration. If we assume that the solubility of surfactants will be intrinsically lower for longer chains, then as the chain length increases there is a competition between the decreased counterion concentration (lowering T_k) and the increasing van der Waals interactions (raising T_k). It is possible that for trimethylammonium surfactants in **IV**, the counterion effect dominates and would give the observed trend in Table 2.3.

Another relevant example is the case of added alcohol, which has been shown to depress the Krafft temperature.⁷⁵ It is therefore not surprising that **II**, with its two hydroxyl-terminated chains, displays the lowest Krafft temperatures out of the four ILs studied here. It becomes apparent that the interplay of the above effects makes it a nontrivial matter to anticipate Krafft temperatures for surfactants in ILs. However, the

chemical diversity of ILs should facilitate greater control over this important interfacial property.

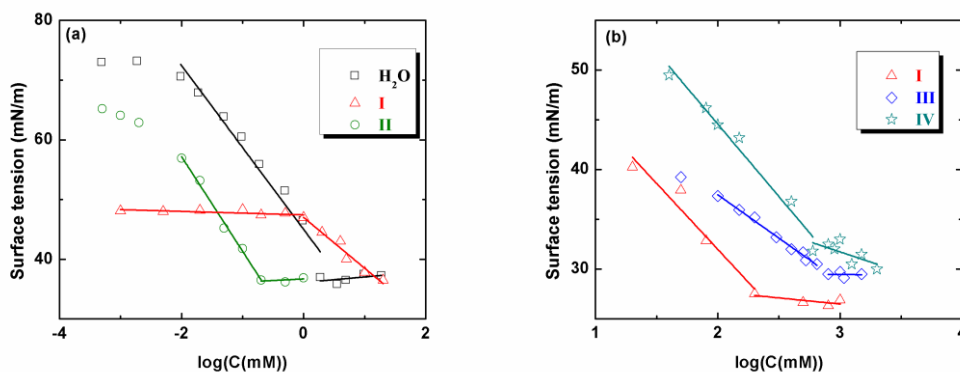


Figure 2.5 Isotherms of $C_{14}TAB$ in different subphase at $20^{\circ}C$ (a, in H_2O , **I**, and **II**) and at $90^{\circ}C$ (b, in **I**, **III**, and **IV**).

When a surface becomes saturated with surfactant monomers, it becomes favorable for micelles to form in the bulk solution. This process occurs in both water and IL systems. Plots of surface tension as a function of concentration for $C_{14}TAB$ at $20^{\circ}C$ and $90^{\circ}C$ in different subphases are given in parts a and b, respectively, of Figure 2.5. As can be seen, the surface tension decreases upon addition of surfactant from the value of pure solvent to a final value which remains more or less constant. This transition is identified as the CMC of the surfactant. Note that $C_{14}TAB$ in **I** at $20^{\circ}C$ does not show a CMC (the red open triangle in Figure 2.5a) because its Krafft temperature is much higher than room temperature. At room temperature, the viscosity of the neat IL is roughly 100 times larger than that of water (Table 2.1). Moreover, at high surfactant concentration, this particular surfactant-IL solution appeared to become

somewhat crystalline and was too viscous for its surface tension to be reliably measured. However, when the same experiment was performed for $C_{14}TAB$ in **I** at $90^\circ C$, a CMC can be clearly identified (the red open triangle in Figure 2.5b). The above effects are presented as an example of what is characteristic surfactant behavior above and below the Krafft temperature.

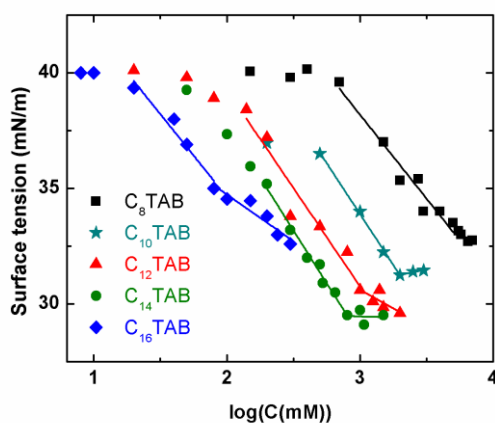


Figure 2.6 Isotherms of C_nTAB in $[BMIM][BF_4]$, **III**, at $90^\circ C$.

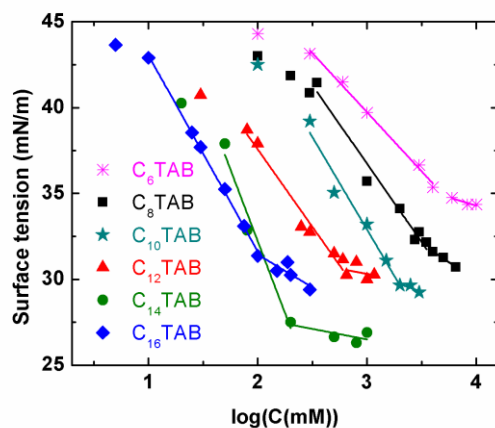


Figure 2.7 Isotherms of C_nTAB in $[EMIM][EtSO_4]$, **I** at $90^\circ C$.

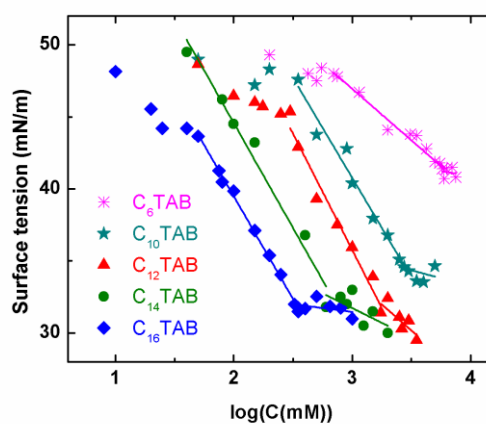


Figure 2.8 Isotherms of C_n TAB in [BMPyr][DCA], IV at 90°C.

By maintaining a fixed isotherm temperature of 90 °C, comparisons of interfacial properties are facilitated. Figure 2.6, Figures 2.7 and Figure 2.8 summarize high temperature (i.e., 90 °C) isotherms of alkyltrimethylammonium bromides in **III**, **I** and **IV**, respectively. As the alkyl chain length of surfactants increases, there is a clear shift to the left while the surface tension is lowered (Figure 2.6). It is apparent that with increasing chain length, the solution will have lower CMC and corresponding surface tension γ_{CMC} , which is similar to that of aqueous systems. From these isotherms, a series of valuable surface properties can be elucidated, such as, effectiveness of surface tension reduction Π_{CMC} , surface excess concentration at saturation Γ_1 and surface area/molecule A_1 at the air-liquid interface (Table 2.4, Table 2.5 and Table 2.6).

Table 2.4 Surface Properties of C_n TAB in [BMIM][BF₄], **III** at 90°C

chain length	CMC ^a (mM)	CMC ^b (mM)	γ_{CMC} (mN/m)	Π_{CMC} (mN/m)	Γ_1 ($\mu\text{mol}/\text{m}^2$)	A_1 (A^2)
8	4000	4450	33.5	7.1	0.65	256.5
10	2500	1990	31.3	9.7	0.78	211.7
12	1000	1060	30.5	9.8	0.76	218.9
14	800	800	29.5	10.5	0.81	204.1
16	150	90	34.9	4.7	0.64	260.0

^a Estimated from Figure 2.2. ^b Calculated from Figure 2.6.

Table 2.5 Surface Properties of C_n TAB in [EMIM][EtSO₄], **I** at 90°C

chain length	CMC(mM) estimate	CMC(mM)	γ_{CMC} (mN/m)	Π_{CMC} (mN/m)	Γ_1 ($\mu\text{mol}/\text{m}^2$)	A_1 (A^2)
6	/	5110	34.8	9.8	0.61	270.6
8	3500	3310	32.0	11.5	0.81	203.8
10	2000	1960	29.7	14.3	0.96	172.8
12	1000	590	30.6	13.2	0.80	206.6
14	500	190	27.4	17.9	1.49	111.3
16	100	106	31.4	15.0	1.02	163.0

Table 2.6 Surface Properties of C_n TAB in [BMPyr][DCA], **IV** at 90°C

chain length	CMC(mM) estimate	CMC(mM)	γ_{CMC} (mN/m)	Π_{CMC} (mN/m)	Γ_1 ($\mu\text{mol}/\text{m}^2$)	A_1 (A^2)
6	6000	6450	41.2	7.8	0.6	260.5
10	3000	2820	34.5	14.4	1.2	134.5
12	2000	1670	32.2	16.8	1.4	115.6
14	1000	720	32.1	17.3	1.3	128.1
16	500	340	32.0	16.6	1.3	131.1

The CMC can be estimated from solubility phase diagrams (e.g., Figure 2.2), by identifying the first sudden and rapid rise in solubility as a function of the temperature. The CMC can also be calculated from the intersection of two linear

regimes of the isotherms in Figure 2.6. From Table 2.4, it is evident that the CMCs obtained from either method are in good agreement with each other.

Π_{CMC} is defined by $\Pi_{CMC} = \gamma_0 - \gamma_{CMC}$, where γ_0 is the surface tension of the pure solvent and γ_{CMC} is the surface tension of the solution at the CMC. This parameter indicates the maximum reduction of surface tension for pure solvent caused by the addition of surfactant, and hence reflects the effectiveness of the surfactant. Because γ_0 values of the neat ILs are somewhat lower than that for water, and their γ_{CMC} are comparable, the calculated Π_{CMC} is found to be smaller than that of water, showing the reduced effectiveness of the same surfactant in lowering the surface tension in ionic liquids.

A typical trend is that, as chain length increases, the saturated surface tension γ_{CMC} is lowered and therefore the corresponding surface pressure at the CMC, Π_{CMC} , is higher. However, the surfactant with the longest chain length, C₁₆TAB, appears to disobey the trend because it has the largest γ_{CMC} and lowest Π_{CMC} . One possible reason is that the plateau in surface tension has not yet been reached (Figure 2.6) or that the Krafft temperature for C₁₆TAB in **III** is very near the temperature of the isotherm, resulting in a relatively unstable solution. This latter notion is supported by the good consistency with the trend for **IV** (Table 2.6, Supporting Information), where C₁₆TAB has much lower Krafft temperature (Table 2.3) than that for **I** and **III**.

The surface excess concentration Γ_1 and the interfacial area per surfactant molecule A_1 were calculated by use of the appropriate Gibbs equation.⁷⁶ Γ_1 is a useful measure of the effectiveness of adsorption of the surfactant, and A_1 provides information on the degree of packing and the orientation of the adsorbed surfactant molecule.

For solutions of singly charged ionic surfactant ($m=2$)⁷⁶⁻⁷⁷ in the absence of any other solutes, $G_1 = -\frac{1}{mRT} \left(\frac{\gamma}{\ln C} \right)_T$, and $A_1 = \frac{1}{G_1}$. From Table 2.4, we can see Γ_1 generally increases from C₈TAB to C₁₄TAB in **III** and A_1 decreases. This trend means that, with increasing chain length, more surfactant molecules are adsorbed when the surface is saturated, resulting a higher packing density and a lower γ_{CMC} . For the same reason discussed above, C₁₆TAB displays an atypical surface excess concentration and surface density.

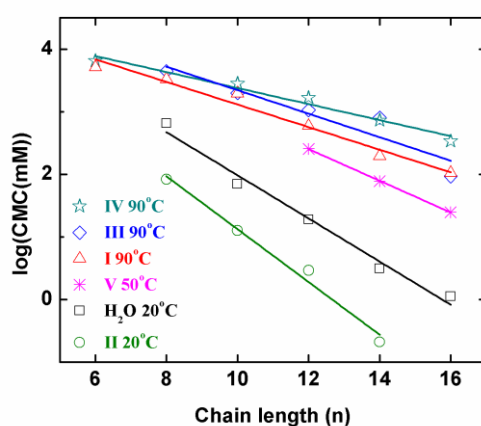


Figure 2.9 Dependence of chain length of surfactant on CMC in different solvents at temperatures higher than their Krafft temperatures.

Figure 2.9 shows the linear relationship of $\log(\text{CMC})$ versus chain length in all ILs and water. The data for ethylammonium nitrate **V** were obtained from previously published report.⁶⁶ While many studies of aqueous solution have already pointed out the relationship between $\log(\text{CMC})$ and chain length,^{22-23, 66} in IL solvents such an analysis must be reconsidered. In addition, we aimed to understand why the CMCs of charged surfactants in ILs can be both larger (e.g. **I**) or smaller (e.g. **II**) than in water, especially when it is observed that ILs generally give higher CMCs.^{24, 29, 78} It would be of great importance to understand the CMC and solubility behavior of the same surfactant in different solvents.

Part of the answers to the above questions can be found by a mean-field consideration of solubility.²⁸ Considering a two-phase system where the molecular interaction energy of a particular type of molecule or particle has different values, μ_1^i and μ_2^i , if one phase ($i = 1$) is a pure liquid ($\log X_1 = 0$), from the well-known Boltzmann distribution, we have

$$X_2 = X_1 \exp[-(\mu_2^i - \mu_1^i) / kT] = X_1 \exp(-\Delta\mu^i / kT) \quad (2.1)$$

where X_1 and X_2 are the equilibrium concentrations of the molecules in the two phases.

In general, $\Delta\mu^i$ can be any type of interaction that contributes to the chemical potential.

We assume the simplest intermolecular interaction to be

$$\Delta\mu^i \approx A\gamma_i \quad (2.2)$$

where γ_i is the interfacial energy of the surfactant-solvent interface and A is the interfacial area per surfactant. Extending this analysis to account for other intermolecular interactions (e.g., dispersion, induction, etc.) is limited to crude estimates due to a lack of detailed IL characterization data and was therefore not pursued further. Combining the above two equations gives

$$\log X_s = -\Delta\mu^i / kT = -\frac{\gamma_{12}}{kT} A \quad (2.3)$$

where, X_s , the quotient of X_2 and X_1 , is the solubility of the surfactant. Given the structure of the surfactants, we assume the area A is proportional to the chain length and therefore $\log X_s$ is also proportional to the chain length n .

Because the CMC is more or less independent of temperature above T_k , the CMC can be considered to be equal to the solubility under these conditions. Therefore, Equation 2.3 can be used to explain the linear relationship between $\log(\text{CMC})$ and chain length in Figure 2.9:

$$\log(\text{CMC}) \approx \log X_s \approx -\frac{\gamma_{12}}{kT} n \quad (2.4)$$

Here, the interfacial energy γ_{12} can be expressed⁷⁹ as:

$$\gamma_{12} = \gamma_1 + \gamma_2 - 2\Phi_{12}\sqrt{\gamma_1\gamma_2} \quad (2.5)$$

where γ_1 and γ_2 are the surface tensions of pure solvent and pure surfactant, respectively. The quantity Φ_{12} is a factor accounting for different types of interactions (dispersion, induction, etc.) across the interface. Because the pure surfactants used here are solids, γ_2 is estimated from the surface tension of liquid hydrocarbons with the similar chain lengths.

For the interface of water with hydrocarbons, it is well known that γ_{12} and γ_2 for octane-water system are 50.8mN/m and 21.8mN/m, respectively.⁸⁰ We assume γ_2 for C_n TAB series used here are close to the surface tension of pure octane. Therefore, the proportionality constant can be determined from Equation 2.4 and the Φ_{12} for octane-water system can be calculated from Equation 2.2. By using the calculated constant and the slopes in Figure 2.9, γ_{12} and Φ_{12} for all five ILs can be calculated (Table 2.7).

Table 2.7 Summary of CMC Analysis of Data from Figure 2.9

	I	II	III	IV	V	H ₂ O
γ_{12} (mN/m)	30.6	62.2	31.9	21.4	40.5	50.8 ⁷⁹⁻⁸¹
Φ_{12}	0.57	0.32	0.51	0.76	0.41	0.55

Overall, it seems that the larger the interfacial tension γ_{12} , the lower the CMC. This correlation supports the notion that interfacial energy is the major factor affecting the aggregation process for both aqueous and ionic liquid solutions. We note that such a conclusion would not be apparent from inspection of the bare interfacial tensions (Table 2.1). This view is also consistent with the observation that the CMC for C_n TAB surfactants in **II** is lower than that in water. The two hydroxyl groups in **II** result in a

much larger interfacial tension with the C_nTAB surfactants and hence show saturation at a relatively lower concentration. At first glance, the validity of our results may seem counterintuitive, since we did not include electrostatic interactions in our mean-field model. However, increasing experimental evidence⁸²⁻⁸³ suggests that the extremely high ionic concentration of ILs in an exceptionally effective screen of electrostatic interactions. We note that such behavior bears a resemblance to the “ideal” behavior of polymer melts, where excluded volume effects cancel.

The Φ_{12} values reflect the types of interactions within each phase and across the interface,⁸¹ with higher values reflecting greater similarity (and hence increased mutual solubility). Thus the lowest Φ_{12} value for trimethylammonium surfactants in **II** is consistent with the lowest observed CMC. Similarly, the largest Φ_{12} value for **IV** is consistent with the largest observed CMC. It is obvious from Equation 2.5 that Φ_{12} is intimately related to the interfacial tension, and equivalent arguments can be made from that perspective. We note while the general trend can be qualitatively described, there is no obvious reason why the CMC for C_nTAB in **I** is lower than the CMC for C_nTAB in **III**. Separate experiments by our group to determine IL polarity using Reichardt's dye⁸⁴ did not indicate substantial differences between **I** and **III** (data not shown). Given the small differences between **I** and **III** and the uncertainty in each CMC determination, it is simply possible that these CMC values are not statistically distinct. Another reason for the unusual behavior of **I** may be related to the extent of ion pairing between the specific cation and anion of the IL.⁸⁵

Equation 2.4 also suggests that directly measuring the interfacial energy between ILs and other materials (e.g., contact angle²⁷) would be very useful not only in confirming our results, but also in predicting the aggregation and solubility of surfactants in both existing and newly available ILs. As more detailed characterization of ILs becomes available, the effects of additional intermolecular interactions may also be considered.

2.4 Conclusions

In summary, the aggregation and solubility behavior of charged surfactants in ILs have been investigated and compared to those in water. Temperature is of great importance in both bulk aggregation and surface assembly of surfactants in ILs, as dictated by the solubility phase diagram. Isotherms at room temperature or high temperature are measured to give a series of useful surface properties including the chain length dependence of the CMC. These properties give us a better understanding of the surface activity of surfactants in ILs. By using a mean-field approach, we conclude that the interfacial energy is crucial in both solubility and aggregation behaviors. The role of IL chemistry is reflected in the net attractive interactions across the interface. Because interfacial energy appears to be the essential factor, our results suggest that there may be a simple method for choosing ionic liquids with desirable solvation capability and aggregation properties. Finally, we note that there is still a room for even further manipulation of interfacial properties: the combination of ILs and

water has already been shown to modify the aggregation behavior of particles and surfactants.^{83, 86-87}

2.5 References

7. Greaves, T. L.; Drummond, C. J., Ionic liquids as amphiphile self-assembly media. *Chem. Soc. Rev.* **2008**, *37* (8), 1709--1726.
8. Rogers, R. D.; Seddon, K. R., Ionic liquids - Solvents of the future? *Science* **2003**, *302* (5646), 792-793.
9. Maier, F.; Cremer, T.; Kolbeck, C.; Lovelock, K. R. J.; Paape, N.; Schulz, P. S.; Wasserscheid, P.; Steinrueck, H.-P., Insights into the surface composition and enrichment effects of ionic liquids and ionic liquid mixtures. *Phys. Chem. Chem. Phys.* **2010**, *12* (8), 1905-1915.
11. He, Y. Y.; Li, Z. B.; Simone, P.; Lodge, T. P., Self-assembly of block copolymer micelles in an ionic liquid. *J. Am. Chem. Soc.* **2006**, *128* (8), 2745-2750.
12. Bai, Z. F.; He, Y. Y.; Lodge, T. P., Block copolymer micelle shuttles with tunable transfer temperatures between ionic liquids and aqueous solutions. *Langmuir* **2008**, *24* (10), 5284-5290.
13. Welton, T., Room-Temperature Ionic Liquids. Solvents for Synthesis and Catalysis. *Chemical Reviews* **1999**, *99* (8), 2071-2084.
14. Wasserscheid, P.; Keim, W., Ionic liquids - New "solutions" for transition metal catalysis. *Angew. Chem. Int. Edit.* **2000**, *39* (21), 3772--3789.
15. Yao, C.; Pitner, W. R.; Anderson, J. L., Ionic Liquids Containing the Tris(pentafluoroethyl)trifluorophosphate Anion: a New Class of Highly Selective and Ultra Hydrophobic Solvents for the Extraction of Polycyclic Aromatic Hydrocarbons Using Single Drop Microextraction. *Anal. Chem.* **2009**, *81* (12), 5054-5063.
16. Greaves, T. L.; Drummond, C. J., Protic ionic liquids: Properties and applications. *Chem. Rev.* **2008**, *108* (1), 206-237.
17. Aliaga, C.; Santos, C. S.; Baldelli, S., Surface chemistry of room-temperature ionic liquids. *Phys. Chem. Chem. Phys.* **2007**, *9* (28), 3683-3700.
18. Marsh, K. N.; Boxall, J. A.; Lichtenthaler, R., Room temperature ionic liquids and their mixtures - a review. *Fluid Phase Equilib.* **2004**, *219* (1), 93-98.

20. Fletcher, K. A.; Pandey, S., Surfactant aggregation within room-temperature ionic liquid 1-ethyl-3-methylimidazolium bis(trifluoromethylsulfonyl)imide. *Langmuir* **2004**, *20* (1), 33-36.
22. Li, N.; Zhang, S. H.; Zheng, L. Q.; Dong, B.; Li, X. W.; Yu, L., Aggregation behavior of long-chain ionic liquids in an ionic liquid. *Phys. Chem. Chem. Phys.* **2008**, *10* (30), 4375-4377.
23. Ogino, K.; Kakihara, T.; Abe, M., Estimation of the Critical Micelle Concentrations and the Aggregation Numbers of Sodium Alkyl Sulfates by Capillary-Type Isotachopheresis. *Colloid Polym. Sci.* **1987**, *265* (7), 604-612.
24. Patrascu, C.; Gauffre, F.; Nallet, F.; Bordes, R.; Oberdisse, J.; de Lauth-Viguerie, N.; Mingotaud, C., Micelles in ionic liquids: Aggregation behavior of alkyl poly(ethyleneglycol)-ethers in 1-butyl-3-methyl-imidazolium type ionic liquids. *Chemphyschem* **2006**, *7* (1), 99-101.
27. Sedev, R., Surface tension, interfacial tension and contact angles of ionic liquids. *Curr. Opin. Colloid In.* **2011**, *16* (4), 310-316.
28. Israelachvili, J. N., *Intermolecular and surface forces*. Academic Press: San Diego, 1992.
29. Anderson, J. L.; Pino, V.; Hagberg, E. C.; Sheares, V.; Armstrong, D. W., Surfactant solvation effects and micelle formation in ionic liquids. *Chem. Commun.* **2003**, (19), 2444-2445.
30. Li, N.; Zhang, S.; Zheng, L.; Wu, J.; Li, X.; Yu, L., Aggregation behavior of a fluorinated surfactant in 1-butyl-3-methylimidazolium ionic liquids. *J. Phys. Chem. B* **2008**, *112* (39), 12453-12460.
31. Li, N.; Zhang, S.; Zheng, L.; Inoue, T., Aggregation behavior of a fluorinated surfactant in 1-butyl-3-methylimidazolium bis(trifluoromethylsulfonyl)imide ionic liquid. *Langmuir* **2009**, *25* (18), 10473-82.
49. Tsujii, K.; Mino, J., Krafft Point Depression of Some Zwitterionic Surfactants by Inorganic Salts. *J. Phys. Chem.* **1978**, *82* (14), 1610-1614.
50. Rico, I.; Lattes, A., Formamide, a Water Substitute .12. Krafft Temperature and Micelle Formation of Ionic Surfactants in Formamide. *J. Phys. Chem.* **1986**, *90* (22), 5870-5872.
54. Lockett, V.; Sedev, R.; Bassell, C.; Ralston, J., Angle-resolved X-ray photoelectron spectroscopy of the surface of imidazolium ionic liquids. *Phys. Chem. Chem. Phys.* **2008**, *10* (9), 1330-1335.
65. Chen, L. G.; Bermudez, H., Solubility and Aggregation of Charged Surfactants in Ionic Liquids. *Langmuir* **2012**, *28* (2), 1157-1162.
66. Evans, D. F.; Yamauchi, A.; Roman, R.; Casassa, E. Z., Micelle Formation in Ethylammonium Nitrate, a Low-Melting Fused Salt. *J. Colloid. Interf. Sci.* **1982**, *88* (1), 89-96.

67. Gao, L. C.; McCarthy, T. J., Ionic liquids are useful contact angle probe fluids. *J. Am. Chem. Soc.* **2007**, *129* (13), 3804-+.
68. Gao, L. C.; McCarthy, T. J., Ionic liquid marbles. *Langmuir* **2007**, *23* (21), 10445-10447.
69. Sanchez, L. G.; Espel, J. R.; Onink, F.; Meindersma, G. W.; de Haan, A. B., Density, Viscosity, and Surface Tension of Synthesis Grade Imidazolium, Pyridinium, and Pyrrolidinium Based Room Temperature Ionic Liquids. *J. Chem. Eng. Data* **2009**, *54* (10), 2803-2812.
70. Huddleston, J. G.; Visser, A. E.; Reichert, W. M.; Willauer, H. D.; Broker, G. A.; Rogers, R. D., Characterization and comparison of hydrophilic and hydrophobic room temperature ionic liquids incorporating the imidazolium cation. *Green Chem.* **2001**, *3* (4), 156-164.
71. Nakayama, H.; Shinoda, K., Effect of Added Salts on Solubilities and Krafft Points of Sodium Dodecyl Sulfate and Potassium Perfluoro-Octanoate. *B. Chem. Soc. Jpn.* **1967**, *40* (8), 1797-&.
72. Luczak, J.; Jungnickel, C.; Joskowska, M.; Thoming, J.; Hupka, J., Thermodynamics of micellization of imidazolium ionic liquids in aqueous solutions. *J. Colloid. Interf. Sci.* **2009**, *336* (1), 111-116.
73. Shinoda, K.; Hutchinson, E., Pseudo-Phase Separation Model for Thermodynamic Calculations on Micellar Solutions. *J. Phys. Chem.* **1962**, *66* (4), 577-&.
74. Bales, B. L.; Benraou, M.; Zana, R., Krafft temperature and micelle ionization of aqueous solutions of cesium dodecyl sulfate. *J. Phys. Chem. B* **2002**, *106* (35), 9033-9035.
75. Nakayama, H.; Shinoda, K.; Hutchins, E., Effect of Added Alcohols on Solubility and Krafft Point of Sodium Dodecyl Sulfate. *J. Phys. Chem.* **1966**, *70* (11), 3502-&.
76. Rosen, M. J., *Surfactants and interfacial phenomena*. Wiley-interscience: New York, 1989.
77. Bae, S.; Haage, K.; Wantke, K.; Motschmann, H., On the factor in Gibbs equation for ionic surfactants. *J. Phys. Chem. B* **1999**, *103* (7), 1045-1050.
78. Gao, Y. N.; Li, N.; Li, X. W.; Zhang, S. H.; Zheng, L. Q.; Bai, X. T.; Yu, L., Microstructures of Micellar Aggregations Formed within 1-Butyl-3-methylimidazolium Type Ionic Liquids. *J. Phys. Chem. B* **2009**, *113* (1), 123-130.
79. Good, R. J.; Elbing, E., Generalization of Theory for Estimation of Interfacial Energies. *Ind. Eng. Chem.* **1970**, *62* (3), 54-&.
80. Fowkes, F. M., Attractive Forces at Interfaces. *Ind. Eng. Chem.* **1964**, *56* (12), 40-&.

81. Girifalco, L. A.; Good, R. J., A Theory for the Estimation of Surface and Interfacial Energies .1. Derivation and Application to Interfacial Tension. *J. Phys. Chem.* **1957**, *61* (7), 904-909.
82. Ueno, K.; Inaba, A.; Kondoh, M.; Watanabe, M., Colloidal stability of bare and polymer-grafted silica nanoparticles in ionic liquids. *Langmuir* **2008**, *24* (10), 5253-5259.
83. Smith, J. A.; Werzer, O.; Webber, G. B.; Warr, G. G.; Atkin, R., Surprising Particle Stability and Rapid Sedimentation Rates in an Ionic Liquid. *J. Phys. Chem. Lett.* **2010**, *1* (1), 64-68.
84. Reichardt, C., Pyridinium N-phenoxide betaine dyes and their application to the determination of solvent polarities part 29 - Polarity of ionic liquids determined empirically by means of solvatochromic pyridinium N-phenolate betaine dyes. *Green Chem.* **2005**, *7* (5), 339-351.
85. Ueno, K.; Tokuda, H.; Watanabe, M., Ionicity in ionic liquids: correlation with ionic structure and physicochemical properties (vol 8, pg 1649, 2010). *Phys. Chem. Chem. Phys.* **2010**, *12* (45), 15133-15134.
86. Behera, K.; Om, H.; Pandey, S., Modifying Properties of Aqueous Cetyltrimethylammonium Bromide with External Additives: Ionic Liquid 1-Hexyl-3-methylimidazolium Bromide versus Cosurfactant n-Hexyltrimethylammonium Bromide. *J. Phys. Chem. B* **2009**, *113* (3), 786-793.
87. Behera, K.; Pandey, S., Concentration-dependent dual behavior of hydrophilic ionic liquid in changing properties of aqueous sodium dodecyl sulfate. *J. Phys. Chem. B* **2007**, *111* (46), 13307-13315.

CHAPTER 3

CHARGE SCREENING BETWEEN ANIONIC AND CATIONIC SURFACTANTS IN IONIC LIQUIDS*

* This chapter was published in [Chen, L. G.; Bermudez, H., Charge Screening between Anionic and Cationic Surfactants in Ionic Liquids. *Langmuir* **2013**, 29 (9), 2805-2808.]⁸⁸

3.1 Introduction

Mixed surfactant systems, including their mixed micelles, exhibit striking changes in their physical properties as compared to single component surfactants and hence are of great theoretical and practical interests. These systems are encountered in numerous applications for the purpose of separation, foam-generation, dispersion, and detergency.⁸⁹⁻⁹⁰ Based on the type of head groups in surfactants, various combinations of nonionic/cationic/anionic surfactants have been studied by a number of workers,^{89,91-92} and several models have been proposed to rationalize their behavior.⁹³⁻⁹⁷ Among them, two widely used models are those of Clint⁹³ and Rubingh⁹⁴. The former describes ideal surfactant mixtures, while the latter uses regular solution theory to describe non-ideal surfactant mixtures. Among all the possibilities, binary mixtures of oppositely charged surfactants (i.e., cationic

and anionic) are of special interest because of their strong electrostatic interaction in water and thus enhanced surface activity.

It is known that aqueous solutions of surfactant mixtures can have critical micelle concentrations (*CMC*) either lower⁹⁴ or higher⁹⁸ than that of each individual surfactant due to specific interactions (synergistic or antagonistic) between surfactants within micelles. These interactions as well as the surfactant composition strongly affect the phase behavior of anionic/cationic surfactant mixtures. Therefore, a better understanding of the specific interactions and the resulting micellar composition and interfacial behavior is of central importance.

Most of the previous work on mixed surfactant systems has been concerned with the aqueous solution. However, over the last few years, amphiphiles in ionic liquids (ILs) have received increasing attention.^{7, 20, 29} Ionic liquids are extraordinary solvents with potential opportunities for numerous applications, for example, ionic liquids could be useful for contact angle probe fluids or catalysis.^{67,}⁹⁹ To our knowledge, excluding one study on nonionic surfactant mixtures in ILs,¹⁰⁰ the aggregation and phase behavior of *ionic surfactant mixtures* in ionic liquids has not been reported. Our previous work from Chapter 2⁶⁵ as well as other reports⁸² has suggested that in ionic liquids, the electrostatic interactions between single component charged surfactants are negligible due to strong charge screening. Here we use the ionic liquid 1-ethyl-3-methyl imidazolium ethylsulfate [EMIM][EtSO₄]

to explore its influence on anionic/cationic surfactant mixtures. [EMIM][EtSO₄] was chosen as a model ionic liquid because it has been extensively studied. A direct comparison between aqueous and ionic liquid solutions would not only help us better understand the specific interactions between surfactants, but also could broaden the application range for both mixed surfactants and ionic liquids.

3.2 Experimental Section

Materials and Methods. 1-ethyl-3-methyl imidazolium ethylsulfate [EMIM][EtSO₄] was obtained from Sigma (>95%). This ionic liquid was dried by heating at 70°C under vacuum for 2 days. The purity of the neat ionic liquid and selected surfactants was assessed by ¹H-NMR or ¹³C-NMR and did not reveal any impurities. These findings were also confirmed by XPS control experiments.⁵⁹ Dodecyltrimethylammonium bromide (DTAB) (99%), and sodium dodecylsulfate (SDS) (98+%) were purchased from Fisher. DTAB was purified by recrystallization from an acetone/ethanol mixture¹⁰¹ and SDS was used as received. The structures of the ionic liquid and two surfactants are shown in Figure 3.1. 3,3'-Dioctadecyloxycarbocyanine Perchlorate (DiO) was obtained from Invitrogen. deuterium oxide, (99.98 atom%) was obtained from sigma. All reagents and solvents were used as received. Fluorescence spectra were recorded using a JASCO FP-6500 spectrofluorimeter. ¹H NMR spectra were recorded on a 400 MHz Bruker NMR spectrometer.

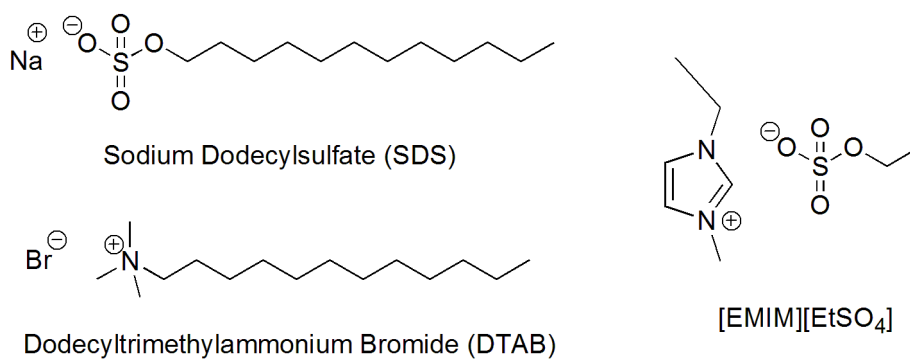


Figure 3.1 Structures of SDS, DTAB and [EMIM][EtSO₄].

Surface Characterization. Surface tension was measured by means of the Wilhelmy method using a Micro Trough XS (Kibron, Inc.). For room temperature isotherms in water, in-house reverse osmosis (RO) water was passed through a 0.22 μ m filter and then used to dissolve the surfactants. For surfactant mixtures, stock solutions of cationic and anionic surfactants were mixed at certain molar ratios and kept at room temperature for over 48h until the solution became completely clear. For high temperature isotherms in [EMIM][EtSO₄], surfactants or surfactant mixtures were dissolved directly in [EMIM][EtSO₄] at elevated temperature. After dissolution, solutions were subsequently diluted to appropriate concentrations as needed. Surfactant solutions (300 μ L) with different concentrations were applied on an aluminum plate with glass wells. Surface tensions were measured after an equilibration time of 30 min. Temperature was controlled and monitored by using a hotplate placed underneath the multi-well plate and an Omega HH506RA multilogger thermometer probe in the well of interest. All concentrations here are presented as millimoles of surfactant per liter of solvent

(mmol/L). In the case of surfactant mixtures, the concentration is based on moles of the total surfactant alkyl chain to facilitate comparison.

CMC Measurement by Fluorescence Spectroscopy. 0.1 mg DiO was dissolved in 1 mL acetone and then 50 μ L of DiO solution was added into a glass vial and the solvent was evaporated by using a heat gun. 1 mL of surfactant mixture-[EMIM][EtSO₄] stock solution was predissolved and added into the glass vial. DiO was partially dissolved in the solution with vigorous shaking. Then the solution was filtered with a 1 μ m syringe filter to remove residual DiO. The Fluorescence Spectroscopy was recorded at 90°C. For CMC measurement, solutions with encapsulated DiO were successively diluted by neat [EMIM][EtSO₄]. The maximum intensity of the peak was plotted against the surfactant total concentration and the transition point was reported as the CMC.

CMC Measurement by ¹H NMR. For ionic liquid solution, No-D ¹H NMR was measured at 90°C with D₂O as a shimming reference solvent. And the peak position was adjusted and compared by the spectrum of a neat [EMIM][EtSO₄].

3.3 Results and Discussion

To obtain the *CMC* of the surfactants in solutions, measurements must be above the Krafft temperature T_k .^{50, 73} T_k values were determined by visual observation as describe in Chapter 2,⁶⁵ and the summary of T_k are listed in the Table

3.1. In general, the T_k for surfactant-water solutions are below room temperature. However, all the T_k of our surfactant-IL solutions determined by solubility measurements are above room temperature but below 90°C. Therefore, isotherms were measured at 20°C in water and at 90°C in [EMIM][EtSO₄]. Because Shinoda⁷³ and Schick¹⁰² have pointed out that *CMC* is a weak function to the change of temperature, a comparison of the two systems at different temperatures is reasonable. All the isotherms are shown in Figures 3.2 and 3.3 and these were used to determine *CMC* values from the intersection of linear fits. For each isotherm, we constructed several pairs of linear fits (generally 3) by using varying numbers of isotherm data points. This approach allowed us to calculate the mean value for the *CMC* and its standard error, and these are shown in Figure 3.3. We emphasize that the gradual nature of the transition in ILs (Figure 3.4) does not reflect surface activity behavior that is different from that of water. Probe fluorescence (Figure 3.5) and ¹H-NMR (Figure 3.6 and 3.7) were used as independent *CMC* measures of selected samples, and all of the data are in good agreement.

Table 3.1 Krafft Temperatures of SDS/DTAB Mixtures in [EMIM][EtSO₄]

SDS mole fraction	T_k (°C)
0.0	65 ± 5
0.25	70 ± 5
0.5	70 ± 5
0.75	65 ± 5
1.0	40 ± 5

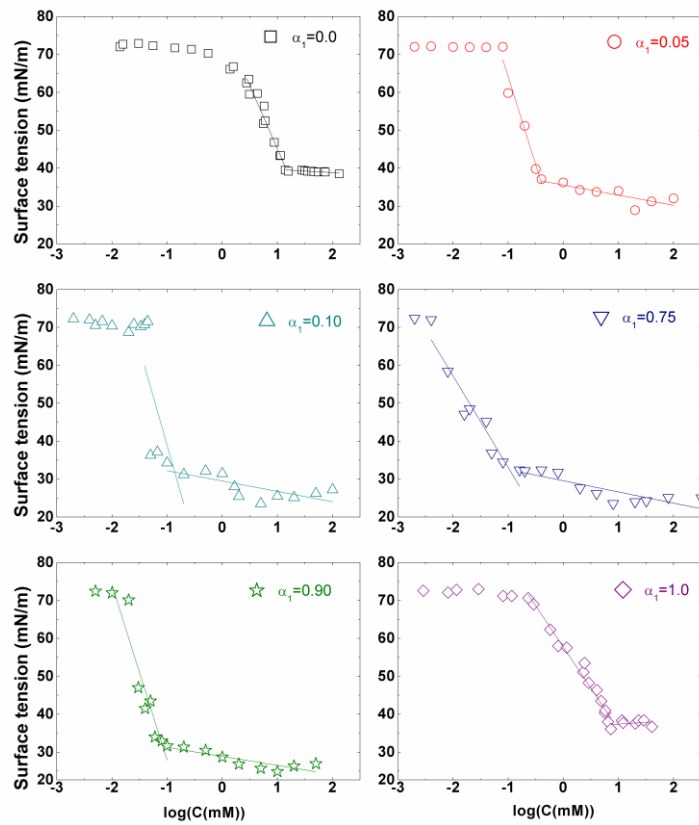


Figure 3.2 Isotherms of SDS/DTAB Mixtures with different mole fraction of a component in the mixture, α_1 , in water at 20°C.

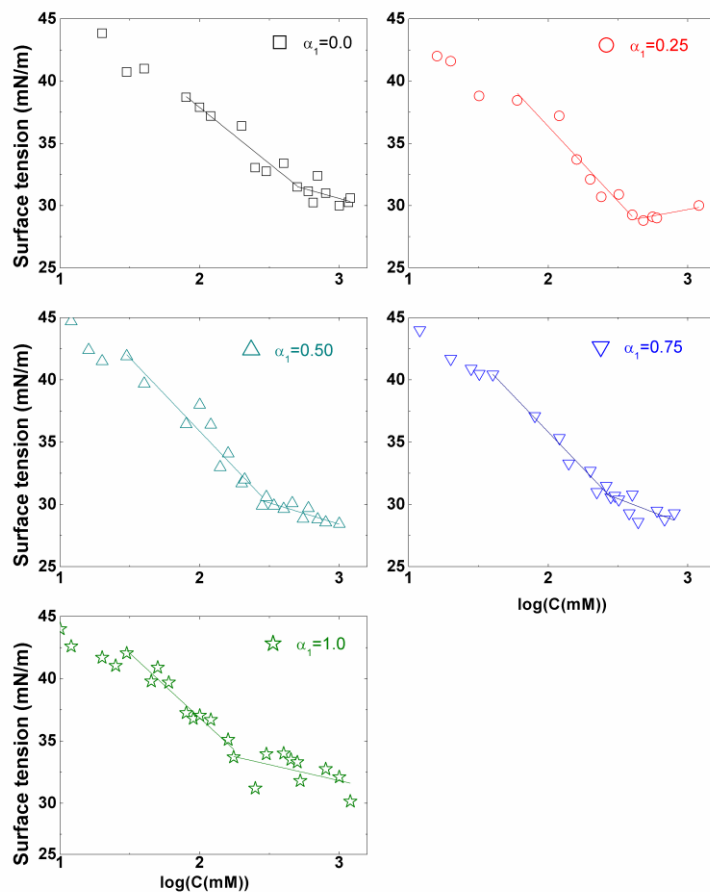


Figure 3.3 Isotherms of SDS/DTAB Mixtures with different mole fraction of a component in the mixture, α_1 , in $[EMIM][EtSO_4]$ at $90^\circ C$.

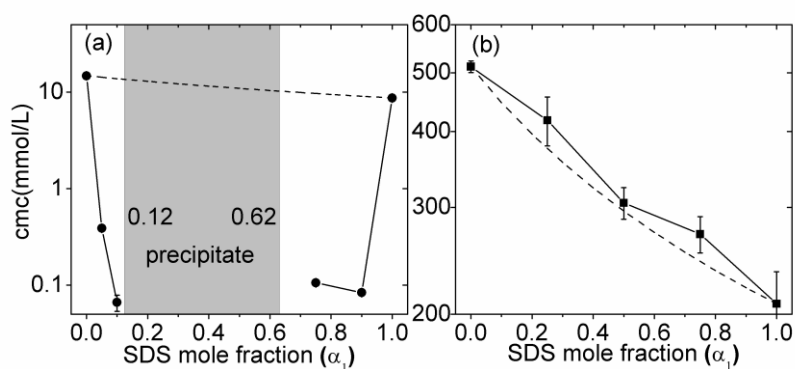


Figure 3.4 Critical micelle concentrations (CMC_{12}) for SDS/DTAB mixtures in (a) water (solid circles) at $20^\circ C$ and (b) $[EMIM][EtSO_4]$ (solid squares) at $90^\circ C$. The dashed lines represent cmc_{12}^{id} from Equation (3.1).

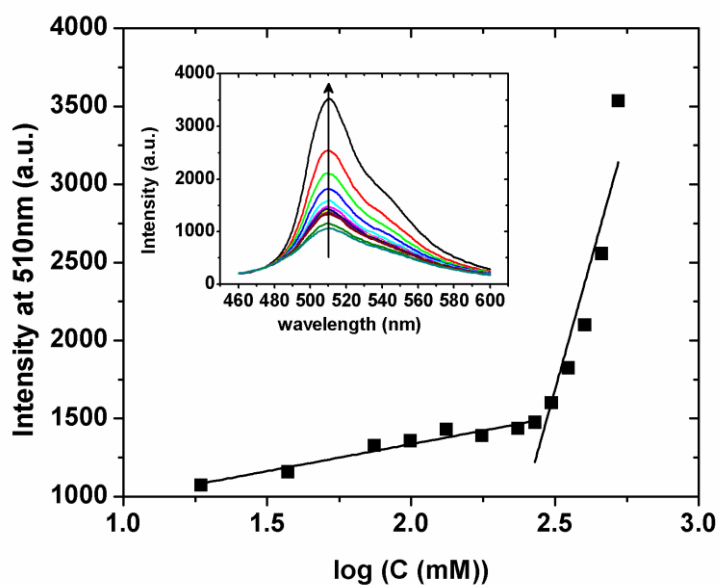


Figure 3.5 CMC calculation of SDS/DTAB mixtures ($\alpha_1 = 0.75$) in $[EMIM][EtSO_4]$ by fluorescence spectroscopy. Inset is fluorescence of DiO in the surfactant-IL solutions with different concentrations (the arrow indicates increasing concentrations). The CMC was determined to be 208mM.

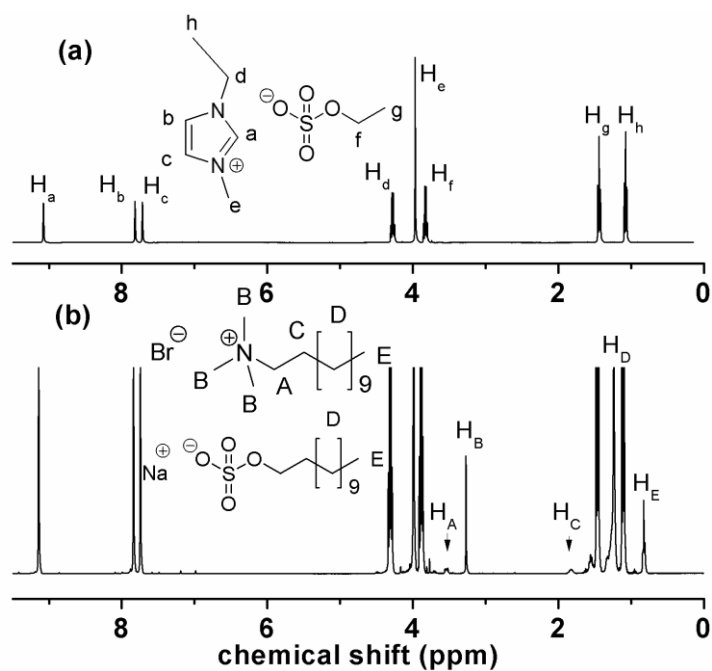


Figure 3.6 1H NMR spectrum at $90^\circ C$ obtained for (a) $[EMIM][EtSO_4]$ and (b) SDS/DTAB mixtures ($\alpha_1 = 0.75$) in $[EMIM][EtSO_4]$. The total surfactant concentration is 800mM.

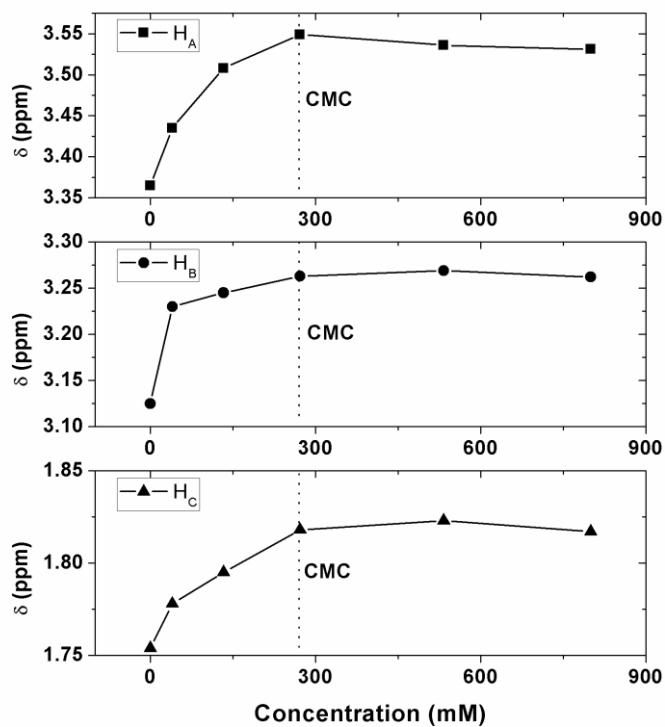


Figure 3.7 Plots of δ for surfactants protons as a function of SDS/DTAB mixtures ($\alpha_1 = 0.75$) concentration in $[EMIM][EtSO_4]$.

Clint⁹³ has shown that for an ideal binary surfactant mixture, the critical micelle concentration cmc_{12}^{id} can be calculated from the single component values, CMC_1 and CMC_2 , and the mole fraction of a component in the mixture, α_1 , as described by Equation 3.1. Herein we denote SDS as component 1 and DTAB as component 2.

$$\frac{1}{cmc_{12}^{id}} = \frac{\alpha_1}{cmc_1} + \frac{(1-\alpha_1)}{cmc_2} \quad (3.1)$$

When cmc_{12}^{id} and the experimentally determined CMC for the mixture (CMC_{12}) are different, a non-zero interaction between the two components exists. From Equation 3.1, ideal mixtures are predicted to have a CMC intermediate between the two single component CMC values.

Figure 3.4 plots CMC_{12} and cmc_{12}^{id} of SDS/DTAB mixtures in both water and [EMIM][EtSO₄]. We have to note that in water, the range $0.12 < \alpha_1 < 0.62$ corresponds to a multiphase region,¹⁰³ and therefore in this concentration range, CMC_{12} is not applicable. In sharp contrast to ideal mixing behavior (Figure 3.4 (a) dashed line), the CMC_{12} in water are much lower than those of the single components due to the *strong attractive electrostatic interaction* between the oppositely charged head groups. This so-called synergistic effect¹⁰⁴ is also observed for the surface activity of mixtures in water. If we exclude the single component data ($\alpha_1 = 0$, $\alpha_1 = 1$) in water, the trend in CMC_{12} is decreasing slightly with increasing SDS mole fraction (Figure 3.4 (a)). This gradual decrease might be due to the fact that $CMC_1 < CMC_2$; that is, pure SDS has a lower CMC than pure DTAB in water.

In contrast to the U-shaped CMC_{12} behavior of the SDS/DTAB mixtures in water, CMC_{12} values for the same mixtures in [EMIM][EtSO₄] are intermediate between the two single component CMC values (Figure 3.4 (b)). The CMC_{12} values in [EMIM][EtSO₄] are also clearly much higher than those in water because of

lower solvophobic interaction between the alkyl chain and IL as compared to the hydrophobic interaction between the alkyl chain and water.^{7, 78} Furthermore, the CMC_{12} curve in [EMIM][EtSO₄] is only slightly above the ideal cmc_{12}^{id} curve (dashed line) calculated from Equation 3.1, which is due to *weak repulsive interactions* between the components in the mixed micelle.¹⁰⁵⁻¹⁰⁶ In addition, there is no multiphase composition gap in [EMIM][EtSO₄], which broadens the application of anionic/cationic surfactant mixtures. As compared to water, the different CMC behavior indicates a dramatic change in the interactions between surfactant molecules in ILs. We believe this behavior is due to the cations and anions from both the IL and the surfactant creating a “sea of ions” which screens electrostatic interactions between them.⁸² This charge screening, at a much lower degree, is a well-known salt effect in aqueous solution.²⁸

The Debye screening length, the distance beyond which Coulomb interactions can be essentially ignored,²⁸ lends support to highly effective charge screening in IL systems. In the case of neat [EMIM][EtSO₄], the Debye length is about 0.16 nm, which is even shorter than the radius of surfactant alkyl chain (0.2 nm). In contrast, the Debye length of a 1mM NaCl aqueous solution is about 10 nm. Even if we recognize the limits of applicability of Debye theory,¹⁰⁷ this comparison argues that the electrostatic interaction in IL is much weaker than in water and can be largely ignored. Such a strong charge screening effect would result in the surfactant-IL solution being close to ideal, as is observed in Figure 3.4 (b).

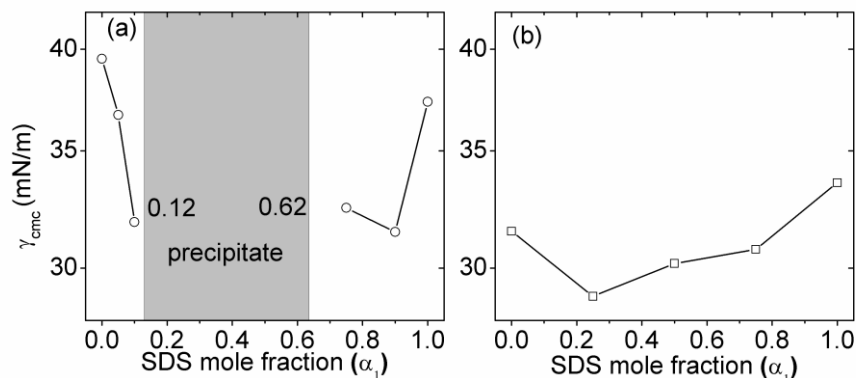


Figure 3.8 Surface tensions at CMC (γ_{CMC}) for SDS/DTAB mixtures in (a) water (open circles) at 20°C and (b) [EMIM][EtSO₄] (open squares) at 90°C.

In Figure 3.8, the surface tension at CMC (γ_{CMC}) of SDS/DTAB mixtures in water (20°C) and [EMIM][EtSO₄] (90°C) is plotted against the SDS mole fraction in the surfactant mixture α_1 . In both water and [EMIM][EtSO₄], mixtures always show higher surface activity than the single components as seen by the lower γ_{CMC} of the mixtures (Figure 3.8). We note that for [EMIM][EtSO₄], γ_{CMC} is not monotonic with α_1 as is CMC_{12} . This trend indicates different behavior at the air-liquid interface and the bulk solution. The mixed monolayers at the interface have better packing than single component surfactants, as determined by the maximum surface excess concentration (Γ_m) (Table 3.2), and hence have lower γ_{CMC} . Comparing the two solvents (Figure 3.8), the lower γ_{CMC} in [EMIM][EtSO₄] than in water is probably due to the higher measurement temperature.

Table 3.2 Maximum Surface Excess Concentration (Γ_m) of SDS/DTAB Mixtures in [EMIM][EtSO₄]. The values of Γ_m are calculated from the Gibbs Adsorption Equation⁷⁶

SDS mole fraction	Γ_m ($\mu\text{mol}/\text{m}^2$)
0.0	0.65
0.25	0.86
0.50	0.85
0.75	0.84
1.0	0.75

To obtain more information on the micellar level, compositions in mixed micelles were calculated and compared to the two models for both solvents. From the Clint ideal mixing model,⁹³ the SDS fraction in the mixed micelles at the *CMC* (x_1^{id}) can be obtained after calculating cmc_{12}^{id} :

$$x_1^{id} = \frac{\alpha_1 cmc_{12}^{id}}{cmc_1} \quad (3.2)$$

Rubingh^{94, 105} extended the ideal mixing model by using regular solution theory, and this approach also permits calculation of SDS fraction in the mixed micelles at the *CMC* (x_1) by numerically solving eq 3.3:

$$x_1^2 \ln\left[\frac{\alpha_1 cmc_{12}}{x_1 cmc_1}\right] = (1-x_1)^2 \ln\left[\frac{(1-\alpha_1) cmc_{12}}{(1-x_1) cmc_2}\right] \quad (3.3)$$

The characteristic of this nonideal model is the net interaction parameter β for surfactants within mixed micelles:

$$\beta = \frac{\ln(\alpha_1 cmc_{12} / x_1 cmc_1)}{(1-x_1)^2} \quad (3.4)$$

Values of the interaction parameter β were calculated using Equation 3.4 for both water and [EMIM][EtSO₄] solvents. The sign and magnitude of β for water and [EMIM][EtSO₄] (Table 3.3), indicate *strong attractive* and *weak repulsive* interactions between surfactant molecules, respectively. The difference in the interactions is consistent with the different aggregation and surface activity behavior in water versus IL.

Table 3.3 Interaction Parameter (β) of SDS/DTAB Mixtures in Water and [EMIM][EtSO₄]

SDS mole fraction	Solvent	
	water	[EMIM][EtSO ₄]
0.05	-16	n.d.
0.1	-20	n.d.
0.25	n.a.	0.43
0.5	n.a.	0.15
0.75	-19	1.2
0.9	-21	n.d.

Note: n.a. represents not applicable in water due to the two-phase gap, and n.d. represents not determined in [EMIM][EtSO₄].

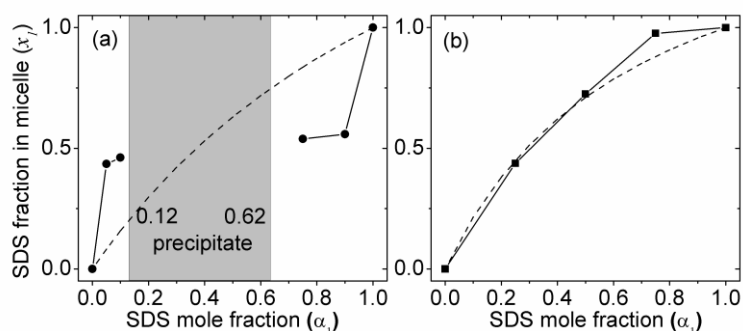


Figure 3.9 SDS mole fraction in micelles (x_1) from Equation 3.3 for SDS/DTAB mixtures in (a) water (solid circles) and (b) [EMIM][EtSO₄] (solid squares),

evaluated from Equation 3.3 at the CMC. The dashed lines represent x_1^{id} from Equation 3.2.

The calculated x_1^{id} and x_I in water and [EMIM][EtSO₄] are plotted against α_1 in Figure 3.9. In water, irrespective of the SDS mole fraction in the mixture, the SDS mole fraction in the mixed micelles is always close to 0.5, with a slight ascending trend (Figure 3.9 (a)). This tendency to a 1:1 ratio in the mixed micelles is presumably due to the strong electrostatic attraction between cationic and anionic head groups in water. On the contrary, in [EMIM][EtSO₄] x_I is always quite close to x_1^{id} (Figure 3.9 (b)). This result again agrees the nearly ideal behavior of mixed surfactants in [EMIM][EtSO₄] and suggests that this system is not strongly driven by electrostatic attractions. Moreover, x_I is always higher than α_1 , which means SDS is more prone to form micelle than DTAB in [EMIM][EtSO₄]. This difference in micellization ability can be confirmed by the lower *CMC* value of pure SDS ($\alpha_1 = 1$) as compared to pure DTAB ($\alpha_1 = 0$) in [EMIM][EtSO₄] (see Figure 3.4 (b)). Cui and coworkers¹⁰⁸ recently suggested that mixed surfactants do not aggregate simultaneously; rather, the component with lower *CMC* aggregates first, and the second component joins these existing micelles upon reaching its own *CMC*, which results in the mixed micells having a composition which differs from the bulk.

3.4 Conclusions

In summary, the effect of SDS/DTAB mixture composition on aggregation and interfacial behavior in [EMIM][EtSO₄] has been investigated and compared to water. In both water and [EMIM][EtSO₄], the mixtures always show higher surface activity than that of the single component due to better interfacial packing. But they have very different micellar behavior in the two solvents. In [EMIM][EtSO₄], nearly ideal mixing of the two oppositely charged surfactants was observed over the entire composition range. The behavior in [EMIM][EtSO₄] is in sharp contrast with water, where the strong electrostatic attraction between the two oppositely charged surfactants dominates their aggregation behavior, resulting a composition gap because of precipitation. Our experiments suggest that charge screening in [EMIM][EtSO₄] is quite strong, due to its high charge density. A small deviation of CMC_{12} from the ideal values indicates weak repulsion between the surfactant molecules within micelles, supported by the models of Rubingh. This study could significantly broaden the potential application of mixed micelles in ILs where specific conditions are demanding (e.g., high temperature, low pressure, broad composition range).

3.5 References

7. Greaves, T. L.; Drummond, C. J., Ionic liquids as amphiphile self-assembly media. *Chem. Soc. Rev.* **2008**, *37* (8), 1709--1726.

20. Fletcher, K. A.; Pandey, S., Surfactant aggregation within room-temperature ionic liquid 1-ethyl-3-methylimidazolium bis(trifluoromethylsulfonyl)imide. *Langmuir* **2004**, *20* (1), 33-36.
28. Israelachvili, J. N., *Intermolecular and surface forces*. Academic Press: San Diego, 1992.
29. Anderson, J. L.; Pino, V.; Hagberg, E. C.; Sheares, V.; Armstrong, D. W., Surfactant solvation effects and micelle formation in ionic liquids. *Chem. Commun.* **2003**, (19), 2444-2445.
50. Rico, I.; Lattes, A., Formamide, a Water Substitute .12. Krafft Temperature and Micelle Formation of Ionic Surfactants in Formamide. *J. Phys. Chem.* **1986**, *90* (22), 5870-5872.
59. Chen, L. G.; Lerum, R. V.; Aranda-Espinoza, H.; Bermudez, H., Surfactant-Mediated Ion Exchange and Charge Reversal at Ionic Liquid Interfaces. *J. Phys. Chem. B* **2010**, *114* (35), 11502-11508.
65. Chen, L. G.; Bermudez, H., Solubility and Aggregation of Charged Surfactants in Ionic Liquids. *Langmuir* **2012**, *28* (2), 1157-1162.
67. Gao, L. C.; McCarthy, T. J., Ionic liquids are useful contact angle probe fluids. *J. Am. Chem. Soc.* **2007**, *129* (13), 3804-+.
73. Shinoda, K.; Hutchinson, E., Pseudo-Phase Separation Model for Thermodynamic Calculations on Micellar Solutions. *J. Phys. Chem.* **1962**, *66* (4), 577-&.
76. Rosen, M. J., *Surfactants and interfacial phenomena*. Wiley-interscience: New York, 1989.
78. Gao, Y. N.; Li, N.; Li, X. W.; Zhang, S. H.; Zheng, L. Q.; Bai, X. T.; Yu, L., Microstructures of Micellar Aggregations Formed within 1-Butyl-3-methylimidazolium Type Ionic Liquids. *J. Phys. Chem. B* **2009**, *113* (1), 123-130.
82. Ueno, K.; Inaba, A.; Kondoh, M.; Watanabe, M., Colloidal stability of bare and polymer-grafted silica nanoparticles in ionic liquids. *Langmuir* **2008**, *24* (10), 5253-5259.
88. Chen, L. G.; Bermudez, H., Charge Screening between Anionic and Cationic Surfactants in Ionic Liquids. *Langmuir* **2013**, *29* (9), 2805-2808.
89. Holland, P. M.; Rubingh, D. N., Mixed Surfactant Systems - an Overview. *Acc Symposium Series* **1992**, *501*, 2-30.
90. Ong, C. P.; Ng, C. L.; Lee, H. K.; Li, S. F. Y., The Use of Mixed Surfactants in Micellar Electrokinetic Chromatography. *Electrophoresis* **1994**, *15* (10), 1273-1275.
91. Shiloach, A.; Blankschtein, D., Measurement and prediction of ionic/nonionic mixed micelle formation and growth. *Langmuir* **1998**, *14* (25), 7166-7182.

92. Kume, G.; Gallotti, M.; Nunes, G., Review on anionic/cationic surfactant mixtures. *Journal of Surfactants and Detergents* **2008**, *11* (1), 1-11.
93. Clint, J. H., Micellization of Mixed Nonionic Surface-Active Agents. *Journal of the Chemical Society-Faraday Transactions I* **1975**, *71* (6), 1327-1334.
94. Holland, P. M.; Rubingh, D. N., Nonideal Multicomponent Mixed Micelle Model. *J. Phys. Chem.* **1983**, *87* (11), 1984-1990.
95. Motomura, K.; Yamanaka, M.; Aratono, M., Thermodynamic Consideration of the Mixed Micelle of Surfactants. *Colloid Polym. Sci.* **1984**, *262* (12), 948-955.
96. Puvvada, S.; Blankschtein, D., Thermodynamic Description of Micellization, Phase-Behavior, and Phase-Separation of Aqueous-Solutions of Surfactant Mixtures. *J. Phys. Chem.* **1992**, *96* (13), 5567-5579.
97. Shiloach, A.; Blankschtein, D., Predicting micellar solution properties of binary surfactant mixtures. *Langmuir* **1998**, *14* (7), 1618-1636.
98. Bakshi, M. S.; Sachar, S.; Mahajan, N.; Kaur, I.; Kaur, G.; Singh, N.; Sehgal, P.; Doe, H., Mixed-micelle formation by strongly interacting surfactant binary mixtures: effect of head-group modification. *Colloid Polym. Sci.* **2002**, *280* (11), 990-1000.
99. Wasserscheid, P.; Keim, W., Ionic liquids - New "solutions" for transition metal catalysis. *Angew. Chem. Int. Edit.* **2000**, *39* (21), 3772-3789.
100. Sakai, H.; Saitoh, T.; Misono, T.; Tsuchiya, K.; Sakai, K.; Abe, M., Nonionic Surfactant Mixtures in an Imidazolium-Type Room-Temperature Ionic Liquid. *Journal of Oleo Science* **2011**, *60* (11), 563-567.
101. Jiang, L. X.; Bin Huang, J.; Bahramian, A.; Li, P. X.; Thomas, R. K.; Penfold, J., Surface Behavior, Aggregation and Phase Separation of Aqueous Mixtures of Dodecyl Trimethylammonium Bromide and Sodium Oligoarene Sulfonates: the Transition to Polyelectrolyte/Surfactant Behavior. *Langmuir* **2012**, *28* (1), 327-338.
102. Schick, M. J., Effect of Temperature on Critical Micelle Concentration of Nonionic Detergents - Thermodynamics of Micelle Formation. *J. Phys. Chem.* **1963**, *67* (9), 1796-&.
103. Kamenka, N.; Chorro, M.; Talmon, Y.; Zana, R., Study of Mixed Aggregates in Aqueous-Solutions of Sodium Dodecyl-Sulfate and Dodecyltrimethylammonium Bromide. *Colloids and Surfaces* **1992**, *67*, 213-222.

104. Rosen, M. J.; Murphy, D. S., Synergism in Binary-Mixtures of Surfactants .5. 2-Phase Liquid Liquid-Systems at Low Surfactant Concentrations. *J. Colloid. Interf. Sci.* **1986**, *110* (1), 224-236.
105. Rubingh, D. N., Mixed Micelle Solutions. In *Solution Chemistry of Surfactants*, Mittal, K. L., Ed. Plenum Press: New York, 1979; Vol. 1, pp 337-354.
106. Lopez-Fontan, J. L.; Suarez, M. J.; Mosquera, V.; Sarmiento, F., Micellar behavior of n-alkyl sulfates in binary mixed systems. *J. Colloid. Interf. Sci.* **2000**, *223* (2), 185-189.
107. Frank, H. S.; Thompson, P. T., Fluctuations and the Limit of Validity of the Debye-Huckel Theory. *J. Chem. Phys.* **1959**, *31* (4), 1086-1095.
108. Cui, X. H.; Jiang, Y.; Yang, C. S.; Lu, X. Y.; Chen, H.; Mao, S. Z.; Liu, M. L.; Yuan, H. Z.; Luo, P. Y.; Du, Y. R., Mechanism of the Mixed Surfactant Micelle Formation. *J. Phys. Chem. B* **2010**, *114* (23), 7808-7816.

CHAPTER 4

SHORT IONIC LIQUIDS PLAY ROLES AS BOTH SOLVENT AND CO- SURFACTANT IN MICELLIZATION*

* This chapter was submitted to *Journal of Physical Chemistry Letter*.

4.1 Introduction

Aggregation of surfactants in ionic liquids (ILs) is receiving increased attention; these systems have many potential applications such as solubilization¹⁰⁹, separation¹¹⁰, dispersion¹¹¹⁻¹¹², catalysis¹⁴, drug delivery¹⁰, etc. The advantages of ionic liquids as solvents are due to their unique physical and chemical properties (e.g., negligible vapor pressure and thermostability) and these properties can be readily adjusted by variation of cation, anion, or the cation substituents. Prior works have shown that ionic liquids can act not only as a solvent, but also as a surfactant.^{22, 113} Self-assembly of surfactants in ionic liquids is thus potentially more complicated than in aqueous solutions. Different aggregation structures have been reported in these systems, such as micelles, microemulsions, liquid crystals, vesicles, and gel.⁷⁸ Our group (Chapter 2, 3, and 5),^{59-60, 65, 88} and others^{7, 20, 30, 66, 114} have studied both the interfacial and micellar aggregation of charged surfactants in ionic liquids. However, the size and shape of surfactant micelles in ionic liquids is still not clear. In this chapter, we report on sodium dodecyl

sulfate (SDS) behavior in the ionic liquid 1-ethyl-3-methyl imidazolium ethylsulfate [EMIM][EtSO₄]. Firstly, tensiometry is used to measure the critical micelle concentration (*cmc*) of the solution. Pulsed-field gradient spin-echo (PGSE)-NMR technique is then used independently verify the *cmc* and to characterize the diffusion coefficient as a function of SDS concentration. The advantage of using PGSE-NMR is that all the ionic species in the system ([EMIM], [EtSO₄], and SDS) are characterized in a label-free manner. This type of direct comparison between surfactant behavior in aqueous and ionic liquid solvents gives insights which could broaden the range of applications range for such surfactant/ionic liquid systems.

4.2 Experimental Section

Materials and Methods. 1-ethyl-3-methyl imidazolium ethylsulfate [EMIM][EtSO₄], were obtained from Sigma (> 95%). This ionic liquid was dried by heating at 70 °C under vacuum for 2 days. The purity of the neat ionic liquid and selected surfactants was assessed by ¹H-NMR or ¹³C-NMR and did not reveal any impurities. These findings were also confirmed by XPS control experiments (see Chapter 5, Chen et al.⁵⁹). Sodium dodecylsulfate (SDS) (98+%) were purchased from Fisher and were used as received.

Surface Characterization. Surface tension was measured by means of the Wilhelmy method using a Micro Trough XS (Kibron, Inc.). At room temperature, the surface tension for neat [EMIM][EtSO₄] at room temperature is 48.7 ± 0.5 which is

relatively higher than that of traditional organic solvents but much lower than that of water. Our experimental value is in good agreement with that of literature.⁶⁸

For room temperature isotherms in water, in-house reverse osmosis (RO) water was passed through a 0.22 μm filter and then used to dissolve SDS. For high temperature isotherms in [EMIM][EtSO₄], SDS was dissolved directly in [EMIM][EtSO₄] at elevated temperature. After dissolution, solutions were subsequently diluted to appropriate concentrations as needed. All concentrations here are presented as millimoles of surfactant per liter of solvent (mmol/L). Surfactant solutions (300 μL) with different concentrations were applied on an aluminum plate with glass wells. Surface tensions were measured after an equilibration time of 30 min. Temperature was controlled and monitored by using a hotplate placed underneath the multi-well plate and an Omega HH506RA multilogger thermometer probe in the well of interest.

Pulsed-field gradient spin-echo (PGSE-NMR). All solutions were prepared by directly dissolving certain amount of SDS in [EMIM][EtSO₄] or D₂O. PGSE-NMR diffusion measurements were carried out on a 400 MHz Bruker NMR spectrometer equipped with a temperature controller. The self-diffusion measurements were performed with a Gaussian-shape pulsed field gradient stimulated echo, whose magnitude is 5.35 Gauss/mm. The diffusion time, Δ , between the two pulses was set between 200-500 ms, and the gradient pulse duration, δ , was set between 2 and 6 ms,

depending on the diffusion coefficient of the mobile species. The diffusion coefficient value was determined from the intensity change equation:

$$I = I_0 e^{-D\gamma^2 g^2 \delta^2 (\Delta - \frac{\delta}{3})}$$

Here, I and I_0 are the areas of the signal obtained with or without gradient pulses respectively, D is the diffusion coefficient, γ is the gyromagnetic ratio of proton, whose value is given by $2.675 \cdot 10^8 \text{ T}^{-1} \text{ s}^{-1}$, g is the magnitude of the two gradient pulses.

The ^1H -NMR spectra example of SDS in $[\text{EMIM}][\text{EtSO}_4]$ is shown below in Figure 4.1. The diffusion coefficient value of proton peaks from the same ion species are consistent with each other. Due to the overlap of some peaks, the diffusion coefficient of $[\text{EMIM}]$ is the average value of H_a , H_b , H_c , H_d , and H_e ; Diffusion coefficient of $[\text{EtSO}_4]$ is from H_h ; Diffusion coefficient of SDS is the average of H_c and H_d .

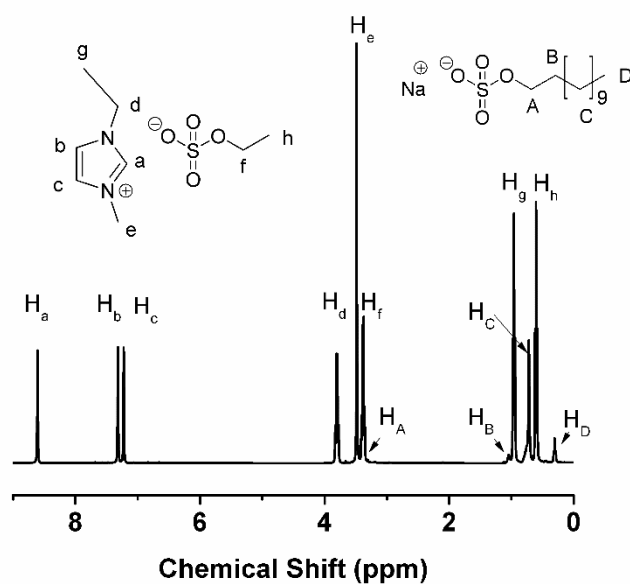


Figure 4.1 $^1\text{H-NMR}$ spectra of SDS in $[\text{EMIM}][\text{EtSO}_4]$ at SDS concentration of 575 mM.

Viscosity. Viscosity measurements were conducted on a stress-controlled TA Advantage 2000 rheometer using a 40 mm aluminum parallel-plate geometry¹¹⁵ at a constant temperature of 90 °C for $[\text{EMIM}][\text{EtSO}_4]$ and 20 °C for D_2O . A solvent trap was used to prevent sample evaporation (for D_2O solution) during measurements. The geometry was rotational mapped before conducting measurements to erase any history. In the mode of steady state flow, the shear rate was chosen in the range of 0.5-500 s^{-1} to obtain a plateau region of viscosity value. Viscosity was obtained from the average value of the plateau. Both forward and backward cycles were conducted and they showed little to no hysteresis. The viscosity of neat solvent D_2O (1.25 mPa·s at 20 °C) and $[\text{EMIM}][\text{EtSO}_4]$ (11.8 mPa·s at 90 °C) were consistent with literature values.

4.3 Results and Discussion

We first obtain the *cmc* of SDS in [EMIM][EtSO₄] by tensiometry, noting that such measurements must be conducted above the Krafft temperature T_k .⁵⁰ The T_k of SDS in water is below 20 °C¹¹⁶ and in [EMIM][EtSO₄] is below 50 °C (by solubility measurements, data not shown). Therefore, we measure surface tension at 20 °C for aqueous solutions and at 90 °C for IL solutions.

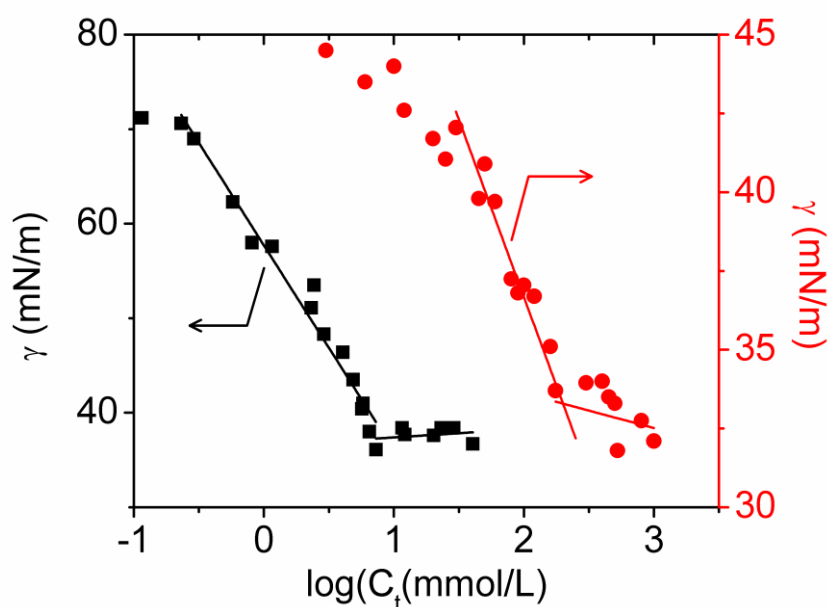


Figure 4.2 Isotherms of SDS in water at 20 °C (solid square) and in [EMIM][EtSO₄] at 90 °C (solid circle).

As shown in Figure 4.2, the surface tension of SDS in water (20 °C) and [EMIM][EtSO₄] (90 °C) are plotted against SDS concentration. The *cmc* of SDS in water is 8.7 mmol/L, which is consistent with literature.²⁸ [EMIM][EtSO₄] shows higher solvation ability than water as seen from the much higher *cmc* (208 mmol/L),

attributed to the difference in solvophobicity. That is, the organic character of the [EMIM] cation and the amphiphilic nature of the [EtSO₄] anion of make the IL more alike to the SDS surfactant than water. The lower γ_{cmc} (i.e., surface tension at cmc) in [EMIM][EtSO₄] as compared to water is most likely due to the difference in temperature. Surface properties in addition to the cmc and γ_{cmc} are summarized in Table 4.1.

Table 4.1 cmc , γ_{cmc} and Surface Properties (Surface Pressure at cmc (Π_{cmc}), Surface Excess Concentration (Γ_1) and the Interfacial Area per Molecule (A_1)) of SDS in Water (20°C) and [EMIM][EtSO₄] (90°C) Obtained by Tensiometry

SDS	water	[EMIM][EtSO ₄]
cmc (mmol/L)	8.7	208
γ_{cmc} (mN/m)	37.3	33.6
Π_{cmc} (mN/m)	35	10.6
Γ_1 ($\mu\text{mol}/\text{m}^2$)	1.9	0.75
A_1 (Å^2)	86	222.9

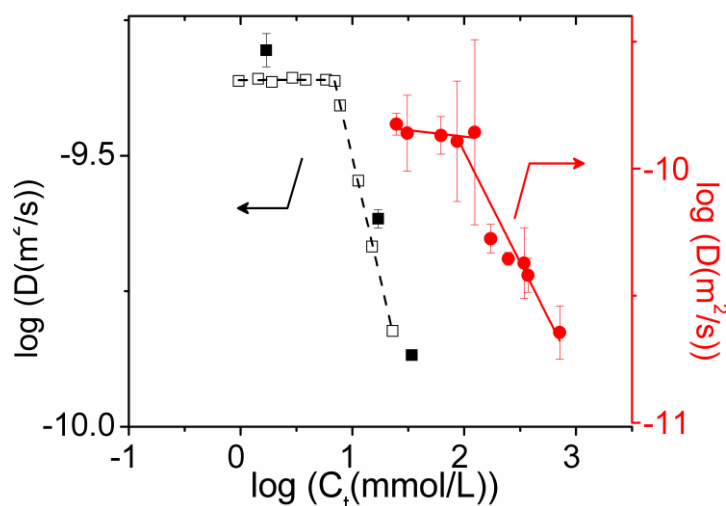


Figure 4.3 Diffusion coefficient of SDS in D₂O at 20 °C (empty squares, data taken from Pettersson et al.⁶²) and [EMIM][EtSO₄] at 90 °C (solid circles) as a function of

SDS concentration. Note: SDS in D₂O at 20 °C data from our own PGSE-NMR measurements are depicted by solid squares.

Figure 4.3 plots the diffusion coefficient of SDS in D₂O and [EMIM][EtSO₄] as a function of SDS concentration. Diffusion coefficient measurements are repeated at least 3 times as shown in Table 4.2, Supporting Information. The diffusion coefficients remain constant up to the *cmc*, and they decrease steadily thereafter. The *cmc* values obtained by PGSE-NMR are about 7 and 200 mmol/L for SDS in D₂O and [EMIM][EtSO₄], respectively, and agree well with the values from tensiometry in Figure 4.2.

Table 4.2 Diffusion Coefficient Value ($\times 10^{-10}$ m²/s) of SDS in [EMIM][EtSO₄] at Various Concentrations

Concentration (mmol/L)	[EMIM]	[EtSO ₄]	SDS	Number of measurements
0	2.25±0.10	1.77±0.09	/	9
41.6	2.43±0.16	1.94±0.14	1.50±0.06	3
52	2.29±0.14	1.81±0.15	1.38±0.21	4
104	2.22±0.24	1.76±0.23	1.35±0.10	3
145	1.98±0.24	1.54±0.26	1.28±0.30	3
208	2.15±0.52	1.70±0.52	1.39±0.51	3
290	1.30±0.05	0.84±0.04	0.53±0.03	4
416	1.18±0.03	0.72±0.01	0.44±0.01	4
575	1.13±0.09	0.70±0.08	0.42±0.06	5
624	1.06±0.07	0.63±0.04	0.38±0.03	6
1200	0.76±0.07	0.39±0.04	0.23±0.02	4

Because micelles are self-assembled structures, the diffusion coefficients measured by PGSE-NMR are a mean value of the free monomer and micelle. Thus, a molar-weighted average⁶² gives

$$D = \frac{C_f}{C_t} D_f + \frac{C_M}{C_t} D_M \quad (0.1)$$

where $D_{f,M}$ are the diffusion coefficients of free monomer and micelle surfactant, respectively. $C_{f,M,t}$ are the concentrations of free monomer, micelle and total surfactant, respectively and are related by mass balance: $C_t = C_f + C_M$. For SDS concentrations below the cmc , the free monomer concentration equals the total SDS concentration and thus $D = D_f$ for $C_t < cmc$. For SDS concentrations above the cmc , we assume that the concentration of free monomer SDS is constant and equal to the cmc . Thus we have

$$D = \frac{cmc}{C_t} D_f + \frac{(C_t - cmc)}{C_t} D_M \quad \text{for } C_t > cmc \quad (0.2)$$

Multiplying Equation 4.1 by the solution viscosity η and rearranging gives

$$D\eta C_t = D_f \eta C_f + D_M \eta C_M \quad (0.3)$$

From Equation 4.3 we see that when $C_t < cmc$, $D\eta C_t = D_f \eta C_t$ (4.3 a) and

when $C_t > cmc$, from Equation 4.2 we see that

$$D\eta C_t = D_f \eta cmc + D_M \eta (C_t - cmc) = (D_f \eta - D_M \eta) cmc + D_M \eta C_t \quad (4.3b).$$

According to the Stokes-Einstein equation¹¹⁷, $D = \frac{k_B T}{F \eta R_H}$ (0.4), where F is a

correction factor accounting for both the shape and size of the solute particle, and R_H is the hydrodynamic radius of the particle. By inspection R_H is inversely proportional to $D\eta$. For both free monomer and micelle species, the product $D\eta$ (i.e., $D_f \eta$ or $D_M \eta$)

is constant by using the assumption that the hydrodynamic radius of both species is independent of the SDS concentration. Therefore, the product $D\eta C_t$ is linearly related with the total SDS concentration C_t by Equations 4.3 (a) and 4.3 (b), with slopes $D_f\eta$ and $D_M\eta$ for C_t below and above cmc , respectively.

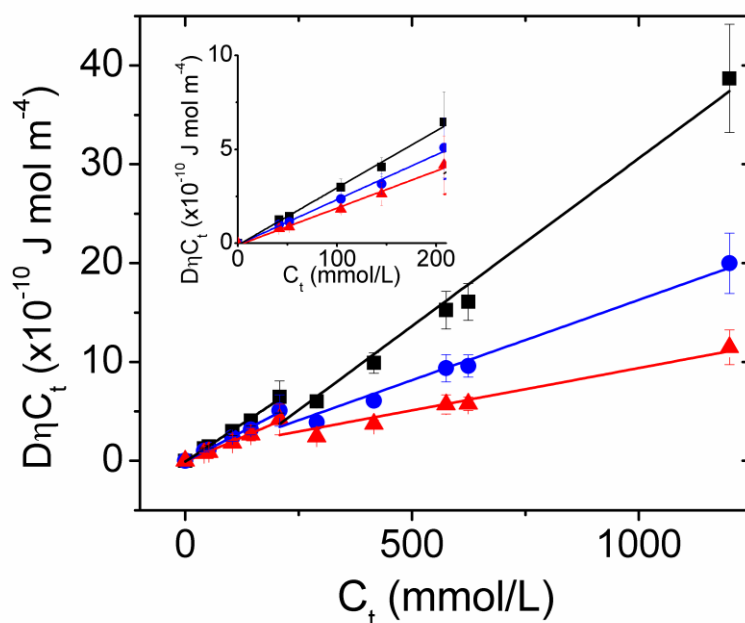


Figure 4.4 The product of diffusion coefficient, viscosity, and total SDS concentration ($D\eta C_t$) for [EMIM] (solid squares), [EtSO₄] (solid circles) and SDS (solid triangles) as function of total SDS concentration. The solid lines are best fits corresponding to Equations 4.3 (a) and 4.3 (b).

Figure 4.4 shows the relationship between $D\eta C_t$ and C_t for the three ionic species in SDS-IL system, where we can see there are two linear regions with a break at cmc . The slopes of the two linear regions are summarized in Table 4.3. As already mentioned, the slopes are inversely proportional to the size of ionic species in the solution. At all concentrations, the slopes for the three ionic species are always in this

order: [EMIM] > [EtSO₄] > SDS. Thus the size of the three species are always in the reverse order: SDS > [EtSO₄] > [EMIM], and confirm our expectations from their known chemical structures. Depending on the concentration being below or above the *cmc*, we expect different effects for the solvent ([EMIM][EtSO₄]) and the solute (SDS) due to the formation of micelles.

Table 4.3 Slopes from Figure 3 (i.e., $D_f\eta$ or $D_M\eta$) and their Ratio α

	$D_f\eta$ ($\times 10^{-12}$ J/m) ^a	$D_M\eta$ ($\times 10^{-12}$ J/m) ^b	$\alpha = D_M\eta / D_f\eta$
[EMIM]	3.0±0.11	3.4±0.24	0.88
[EtSO ₄]	2.4±0.09	1.6±0.14	1.5
SDS	2.0±0.08	0.86±0.13	2.3

^a Values for $C_t < cmc$

^b Values for $C_t > cmc$

From Table 4.3, we see that even though the three species experience a transition at the *cmc*, the changes in size on either side of the transition are different. The ratios of the two slopes, $D_M\eta / D_f\eta$, defined here as α , reflect the change of size due to the onset of aggregation. The larger the ratio α , the larger the size increase. For an ideal species with concentration-independent size, we expect $\alpha=1$. We first observe that α values for the IL [EMIM] cation and [EtSO₄] anion are relatively small (0.88 and 1.5, respectively), while for the α value SDS is much larger (2.3). This larger α value for SDS indicates its aggregation in solution upon concentrations exceeding the *cmc*, and indeed the change in slope is statistically significant ($p < 0.001$, by Student's t-test). Secondly, the relative increase of α for [EtSO₄] (1.5) suggests that [EtSO₄] is partially

involved in the micelle formation. Thus [EtSO₄] can be considered as a co-surfactant with a short hydrocarbon chain, in agreement with previous studies demonstrating a co-surfactant role for certain IL ions.^{22, 113} Indeed, the incorporation of [EtSO₄] into SDS micelles has been recently observed by MD simulations. (McCutchen, M.; Chen, L. G.; Bermudez, H.; Matysiak, S., The interplay of dynamical properties between ionic liquids and ionic surfactants: mechanism and aggregation. *Phys. Chem. Chem. Phys.*, submitted for publication, **2014**.) Thirdly, the minor increase of the slope for [EMIM] is not statistically significant ($p > 0.05$, by Student's t-test) and reflects the negligible presence of [EMIM] within the micelles.

Analogous $D\eta C_i$ data for SDS in D₂O are shown in Figure 4.5. Note that the viscosity of SDS/D₂O solutions are generally assumed to be constant with total SDS concentration, which is in contrast to SDS/[EMIM][EtSO₄] solutions (Table 4.4, Supporting Information). From Figure 4.5, the calculated ratio α for SDS in D₂O is 17, much larger than that in [EMIM][EtSO₄]. The larger size increase in D₂O is probably due to the larger solvophobicity of water as explained above, indicating a stronger driving force for micelle formation in aqueous solution compared to ILs.

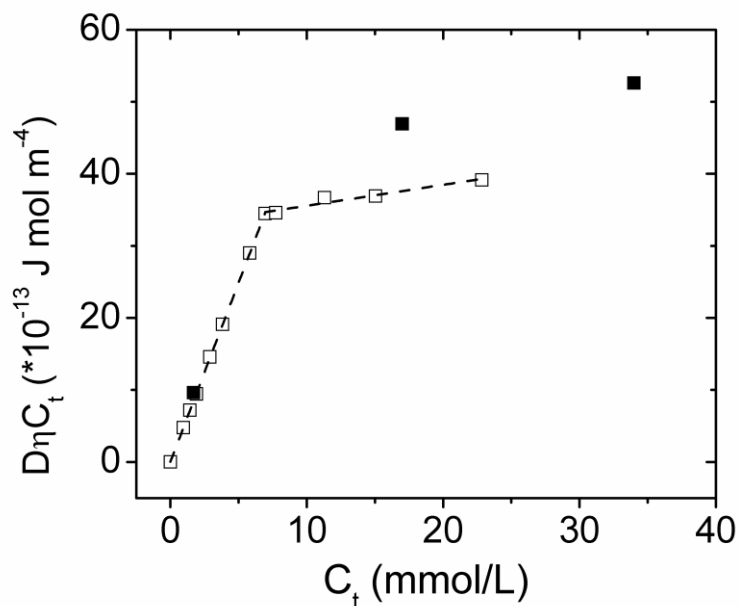


Figure 4.5 The product of diffusion coefficient, viscosity, and total SDS concentration ($D\eta C_t$) for SDS as function of total SDS concentration in D_2O . The dash lines are best fits corresponding to Equations 4.3 (a) and 4.3 (b). Taken from Pettersson et al..⁶² Note: the solid square data are from our own PGSE-NMR measurements.

Table 4.4 Viscosity η (mPa·s) of SDS in [EMIM][EtSO₄] at Various Concentrations

Concentration (mmol/L)	Viscosity (η) (mPa·s)	Number of Measurements (N)
0	11.8±0.5	5
41.6	12.4±0.3	5
52	12.1±0.6	5
104	12.9±1.3	3
145	14.2±0.2	3
208	14.4±1.0	3
290	16.0±0.7	5
416	20.2±2.1	5
575	23.4±2.3	6
624	24.3±2.4	5
1200	42.3±4.7	5

In principle, one could calculate the hydrodynamic radius, R_H , of the ionic species based on Equation 4.4. However, we have not performed such a calculation on

account of (i) the uncertainty regarding the F factor in Equation 4.4, (ii) the difficulty in decoupling D_f and D_M , and (iii) the assumptions made to arrive at Equations 4.3 (a) and 4.3 (b).

4.4 Conclusions

In summary, the effect of surfactant concentration on aggregation behavior in ILs has been investigated by tensiometry and PGSE-NMR and compared to water. Both techniques are used to measure the cmc of SDS and yield consistent results. By applying the conventional analysis for the equilibrium between monomer and micelle, we derive an expression showing the linear relationship between the product $D\eta C_t$ and C_t , with the slopes reflecting the size of each species in the solution. Our data show evidence that the IL anion [EtSO₄] partially incorporates into SDS micelles, resulting in slower diffusion when the surfactant concentration is above the cmc . These findings highlight the importance of IL chemistry to influence aggregation processes, and suggests future opportunities to tailor micelle properties (e.g., composition, size, and dynamics) through the suitable choice of IL.

4.5 References

7. Greaves, T. L.; Drummond, C. J., Ionic liquids as amphiphile self-assembly media. *Chem. Soc. Rev.* 2008, 37 (8), 1709--1726.
10. Dobler, D.; Schmidts, T.; Klingenhofer, I.; Runkel, F., Ionic liquids as ingredients in topical drug delivery systems. *International Journal of Pharmaceutics* 2013, 441 (1-2), 620-627.

14. Wasserscheid, P.; Keim, W., Ionic liquids - New "solutions" for transition metal catalysis. *Angew. Chem. Int. Edit.* 2000, 39 (21), 3772--3789.
20. Fletcher, K. A.; Pandey, S., Surfactant aggregation within room-temperature ionic liquid 1-ethyl-3-methylimidazolium bis(trifluoromethylsulfonyl)imide. *Langmuir* 2004, 20 (1), 33-36.
22. Li, N.; Zhang, S. H.; Zheng, L. Q.; Dong, B.; Li, X. W.; Yu, L., Aggregation behavior of long-chain ionic liquids in an ionic liquid. *Phys. Chem. Chem. Phys.* 2008, 10 (30), 4375-4377.
28. Israelachvili, J. N., *Intermolecular and surface forces*. Academic Press: San Diego, 1992.
30. Li, N.; Zhang, S.; Zheng, L.; Wu, J.; Li, X.; Yu, L., Aggregation behavior of a fluorinated surfactant in 1-butyl-3-methylimidazolium ionic liquids. *J. Phys. Chem. B* 2008, 112 (39), 12453-12460.
50. Rico, I.; Lattes, A., Formamide, a Water Substitute .12. Krafft Temperature and Micelle Formation of Ionic Surfactants in Formamide. *J. Phys. Chem.* 1986, 90 (22), 5870-5872.
59. Chen, L. G.; Lerum, R. V.; Aranda-Espinoza, H.; Bermudez, H., Surfactant-Mediated Ion Exchange and Charge Reversal at Ionic Liquid Interfaces. *J. Phys. Chem. B* 2010, 114 (35), 11502-11508.
60. Chen, L. G.; Bermudez, H., Probing the interface of charged surfactants in ionic liquids by XPS. In *ACS Symposium Series 1117*, Visser, A. E., Ed. American Chemical Society: Washington, DC, 2012; pp 289-302.
62. Pettersson, E.; Topgaard, D.; Stilbs, P.; Soderman, O., Surfactant/nonionic polymer interaction. a NMR diffusometry and NMR electrophoretic investigation. *Langmuir* 2004, 20 (4), 1138-1143.
65. Chen, L. G.; Bermudez, H., Solubility and Aggregation of Charged Surfactants in Ionic Liquids. *Langmuir* 2012, 28 (2), 1157-1162.
66. Evans, D. F.; Yamauchi, A.; Roman, R.; Casassa, E. Z., Micelle Formation in Ethylammonium Nitrate, a Low-Melting Fused Salt. *J. Colloid. Interf. Sci.* 1982, 88 (1), 89-96.
68. Gao, L. C.; McCarthy, T. J., Ionic liquid marbles. *Langmuir* 2007, 23 (21), 10445-10447.
78. Gao, Y. N.; Li, N.; Li, X. W.; Zhang, S. H.; Zheng, L. Q.; Bai, X. T.; Yu, L., Microstructures of Micellar Aggregations Formed within 1-Butyl-3-methylimidazolium Type Ionic Liquids. *J. Phys. Chem. B* 2009, 113 (1), 123-130.
88. Chen, L. G.; Bermudez, H., Charge Screening between Anionic and Cationic Surfactants in Ionic Liquids. *Langmuir* 2013, 29 (9), 2805-2808.

109. Singh, S.; Simmons, B. A.; Vogel, K. P., Visualization of Biomass Solubilization and Cellulose Regeneration During Ionic Liquid Pretreatment of Switchgrass. *Biotechnology and Bioengineering* 2009, *104* (1), 68-75.
110. Han, X.; Armstrong, D. W., Ionic liquids in separations. *Accounts Chem. Res.* 2007, *40* (11), 1079-1086.
111. Ueno, K.; Watanabe, M., From Colloidal Stability in Ionic Liquids to Advanced Soft Materials Using Unique Media. *Langmuir* 2011, *27* (15), 9105-9115.
112. Fileti, E. E.; Chaban, V. V., Imidazolium Ionic Liquid Helps to Disperse Fullerenes in Water. *J. Phys. Chem. Lett.* 2014, *5* (11), 1795-1800.
113. Comelles, F.; Ribosa, I.; Gonzalez, J. J.; Garcia, M. T., Interaction of Nonionic Surfactants and Hydrophilic Ionic Liquids in Aqueous Solutions: Can Short Ionic Liquids Be More Than a Solvent? *Langmuir* 2012, *28* (41), 14522-14530.
114. Hao, J. C.; Song, A. X.; Wang, J. Z.; Chen, X.; Zhuang, W. C.; Shi, F.; Zhou, F.; Liu, W. M., Self-assembled structure in room-temperature ionic liquids. *Chemistry-a European Journal* 2005, *11* (13), 3936-3940.
115. Khandavalli, S.; Rothstein, J. P., Extensional rheology of shear-thickening fumed silica nanoparticles dispersed in an aqueous polyethylene oxide solution. *Journal of Rheology* 2014, *58* (2), 411-431.
116. Bakshi, M. S.; Kaura, A.; Miller, J. D.; Paruchuri, V. K., Sodium dodecyl sulfate-poly(amidoamine) interactions studied by AFM imaging, conductivity, and Krafft temperature measurements. *J. Colloid. Interf. Sci.* 2004, *278* (2), 472-477.
117. Macchioni, A.; Ciancaleoni, G.; Zuccaccia, C.; Zuccaccia, D., Determining accurate molecular sizes in solution through NMR diffusion spectroscopy. *Chem. Soc. Rev.* 2008, *37* (3), 479-489.

CHAPTER 5

PROBING THE INTERFACE OF CHARGED SURFACTANTS IN IONIC LIQUIDS BY XPS*

*This chapter was published in [Chen, L. G.; Bermudez, H., Probing the interface of charged surfactants in ionic liquids by XPS. In *ACS Symposium Series 1117*, Visser, A. E., Ed. American Chemical Society: Washington, DC, 2012; pp 289-302.]⁶⁰ and [Chen, L. G.; Lerum, R. V.; Aranda-Espinoza, H.; Bermudez, H., Surfactant-Mediated Ion Exchange and Charge Reversal at Ionic Liquid Interfaces. *J. Phys. Chem. B* **2010**, *114* (35), 11502-11508.]⁵⁹

5.1 Introduction

Room-temperature ionic liquids (ILs), organic salts with a melting point below 100 °C, continue to receive intense attention because of their unusual and diverse properties. The nature of the IL interface is of central importance in applications such as catalysis, chromatography, and fuel cells.¹³⁻¹⁷ The self-assembly of amphiphilic molecules such as surfactants in ILs is also of fundamental interest to the field of colloid and interface science.²⁰⁻²⁴

Because of the negligible vapor pressure of ILs, ultrahigh vacuum (UHV) techniques can be used to interrogate IL surface and bulk properties.^{9, 51-56, 118} The application of UHV based techniques including X-ray photoelectron spectroscopy

(XPS), secondary ion mass spectrometry (SIMS),⁵² metastable impact electron spectroscopy (MIES),¹¹⁹ direct recoil spectroscopy,¹²⁰ and low-energy ion scattering (LEIS),¹²¹ provides insight into both chemistry and surface properties at molecular length scales. Other surface-sensitive methods without UHV conditions include sum frequency generation (SFG),¹²²⁻¹²³ X-ray reflectivity,¹²³⁻¹²⁴ and surface tension measurements.¹²⁵⁻¹²⁷ Among all of these techniques, XPS is arguably the most common and prominent UHV-based tool to provide unique information on chemical composition, chemical state identification and even composition depth profiles of the near-surface region. A comprehensive review article was recently published by Lovelock et al.⁵⁷ on photoelectron spectroscopy applied to IL interfaces. Since the first work on XPS of ILs at the IL-air interface reported by Smith et al.⁵¹ and Caporali et al.¹²¹ in 2005, there have been many XPS studies on the influence of anions⁵⁵ and substituents⁵⁶ on the surface composition of neat ILs. Other XPS studies have sought to reveal the orientation of ions at the interface,⁵⁴ to monitor organic reactions in ILs¹²⁸ and to characterize novel IL materials such as amino acid based ionic liquids.¹²⁹ XPS has also been used to investigate surface enhancement and solubility of salts dissolved in ILs.^{118, 130} However, few studies have examined more complex systems such as surfactant-IL mixtures. Through the introduction of (charged) surfactants, the interfacial properties such as surface tension, composition, and charge can be tuned and controlled. More importantly, these properties can be quantitatively characterized by XPS.

This chapter intends to highlight opportunities in colloid and interface science made possible by the unique properties of ionic liquids and the strengths of XPS. While the ability of ILs to solubilize a wide variety of compounds is of clear interest and continues to be studied,^{99, 131-136} mixtures that include ILs have complex phase behavior that is relevant to many potential applications. For example, the formation of microemulsions or other dispersed phases can be facilitated and controlled through the use of amphiphilic molecules.¹³⁷ At a more basic level, ionic liquids provide a window to re-examine our understanding of solubility and aggregation phenomena, which is most often based on our experiences with water, a unique solvent itself. To begin addressing some of these questions, we have used two model hydrophilic ionic liquids, 1-ethyl-3-methylimidazolium ethyl sulfate, **I**, and bis(2-hydroxyethyl) dimethylammonium methylsulfonate, **II** (see Figure 5.1). These ionic liquids are commonly referred to as [EMIM][EtSO₄] and [BHEDMA][MeSO₃], respectively. These ionic liquids have been widely studied^{52-53, 59, 65, 138-139} and are miscible with water in all proportions. Sodium alkyl sulfate and alkyltrimethylammonium bromides with different alkyl chain lengths were deliberately chosen as model ionic surfactants, so as to resemble moieties in the ILs and thereby promote more complex surface interactions. With these components, we find that ion exchange and charge reversal can occur at the interface, depending on the natures of the IL and surfactant.

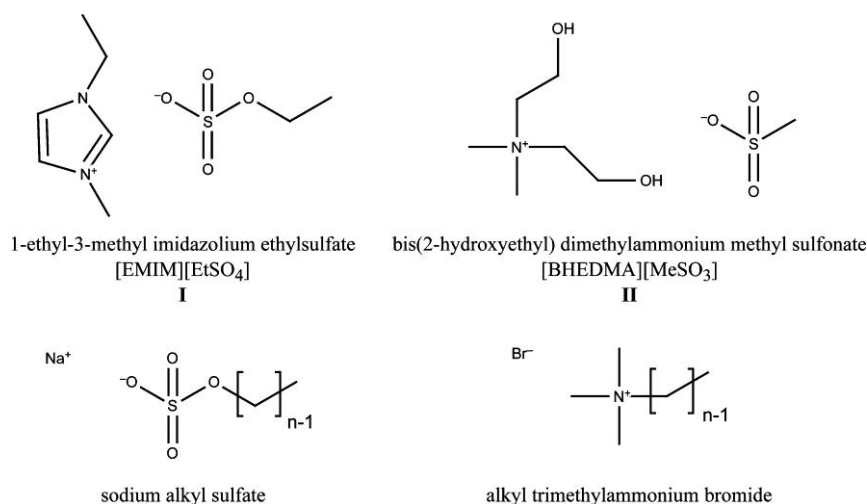


Figure 5.1 Structures of the ionic liquids and surfactants in this study.

5.2 Experimental

Materials. [EMIM][EtSO₄], **I**, was obtained from Sigma (>95%), and [BHEDMA][MeSO₃], **II**, was a gift from T. J. McCarthy.⁶⁷ Both of the ionic liquids were dried by heating at 70°C under vacuum for 2 days. The purity of the neat ionic liquids, and selected surfactants, were assessed by ¹H-NMR and did not reveal any impurities. These findings were confirmed by subsequent XPS control experiments (Figure 5.2).⁵⁹

Sodium hexadecylsulfate (SC₁₆S), sodium dodecylsulfate (SC₁₂S), sodium hexylsulfate (SC₆S), Tween 20, cetyl trimethylammonium bromide (C₁₆TAB) and Dodecyltrimethylammonium bromide (C₁₂TAB) (99%) were purchased from Fisher. Sodium octylsulfate, polyoxyethylene(4) lauryl ether (Brij 30), hexyltrimethylammonium bromide (C₆TAB) (>98%), octyltrimethylammonium bromide (C₈TAB) (>98%), decyltrimethylammonium bromide (C₁₀TAB) (>98%), and

tetradecyltrimethylammonium bromide (C₁₄TAB) (>99%) were purchased from Sigma. All surfactants were used as received. The water used to dissolve the surfactants was treated with in-house reverse osmosis (RO) and additionally passed through a 0.22 μm filter. After dissolution in RO water, solutions were heated to 50 °C to make stock solutions, which were subsequently diluted to the appropriate concentrations as needed. All samples were optically transparent by visual inspection.

Tensiometry. Surface tension was measured by the Wilhelmy method using a Micro Trough XS (Kibron, Finland). At room temperature, both of the ILs have relative high interfacial tensions with air, $\gamma_{\text{I}} = 48.3 \pm 0.8$ mN/m (N=30) and $\gamma_{\text{II}} = 64.5 \pm 0.5$ mN/m (N=26). These values are in good agreement with interfacial tensions obtained by independent laboratories using other methods.⁶⁷ Subphase volumes were 300-500 μL of either RO water, **I**, or **II**. Each subphase was palced in Teflon-lined wells with a fixed area, in a metal alloy plate. To determine the effect of added surfactant, between 5 and 40μL of surfactant aqueous solutions were applied to each well. We note that although water is introduced in the application of surfactant, it is always less than 12% by volume and does not significantly alter the bare surface tension ($\Delta\gamma < 3\%$), which was also found by Marsh et al.¹⁸ Surface tensions were measured after an equilibration time of 15 min. Finally, small amounts of water in imidazolium-based ILs have been shown both by experiment¹⁴⁰ and simulation¹⁴¹ to be molecularly dispersed and not phase separated.

X-ray Photoelectron Spectroscopy. Five microliters of aqueous surfactant solutions were applied onto the surface of 5 μ L of IL droplets using (oxygen-plasma-cleaned) silicon wafers as substrates. Samples were dried in a flowing nitrogen environment for 3 days at room temperature prior to conducting XPS measurement. XPS data were recorded using a Physical Electronics Quantum 2000 Microprobe instrument with monochromatic Al X-rays at 50 W, and a 200 μ m spot area. The analyzing surface area was neutralized by an ion gun. Survey scans (3 min) were followed by regional scans (20 min) for each atomic element of interest. Regional scans were adjusted by a two-point linear background subtraction⁵⁵ and normalized with respect to the relevant peak position for illustrative purpose only. Atomic compositions were obtained by using known sensitivity factors for the instrument and setup (See Appendix C). To determine molecular compositions, atomic mass balances were performed using the chemical formulas of each species (see Results and Discussion). Importantly, the purity of the neat IL and the negligible influence of water and nitrogen introduced during preparation were confirmed by several different XPS control experiments.

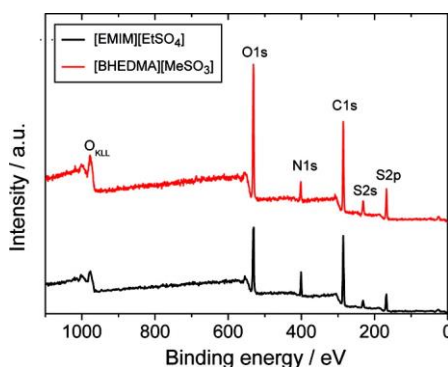


Figure 5.2 XPS spectra of neat [EMIM][EtSO₄] (black, down) and [BHEDMA][MeSO₃] (red, up), recorded at $\theta=45^\circ$ takeoff angle.

At a given takeoff angle θ , the exponential decay of the photoelectron intensity is given by $\frac{I}{I_0} = \exp\left(-\frac{z}{\lambda \sin\theta}\right)$, where z points along the inward surface normal.¹⁴² Manipulation of the above expression leads to the fractional intensity $\frac{I}{I_{tot}} = 1 - \exp\left(-\frac{z}{\lambda \sin\theta}\right)$, where I_{tot} is the total intensity. The depth corresponding to 95% of the signal (i.e., z at $I/I_{tot} = 0.95$) is denoted by d , and we find $d \approx 3\lambda \sin\theta$. We note that XPS results for both neat ILs match the expected atomic ratios, consistent with minimal impurities (Figure 5.2). Furthermore, treatment of neat [EMIM][EtSO₄] with Ar⁺ bombardment reveals negligible change in C1s and N1s signals. Most importantly, the Si2p signal is always at the noise level, eliminating the possibility of Si contamination (Figure 5.3). As still another control, experiments demonstrate that the water used to introduce the surfactant does not contain measurable contaminants because the expected atomic ratios are obtained. This control consisted of adding the appropriate volume of water, followed by nitrogen drying, as above.

Due to the numerous species present, decoupling the peaks into contributions from particular elemental types is somewhat complicated. Therefore, rather than attempting to fit multiple Gaussian functions to our spectra, we analyzed the compositional data by means of atomic mass balances. Atomic mass balances can be found in standard chemical engineering textbooks¹⁴³⁻¹⁴⁴ and rely on the presence of one or more unique atomic species (e.g., nitrogen or sulfur). As an example, we present this analysis in detail for SDS on [EMIM][EtSO₄]. The four ionic species present are C₁₂SO₄⁻, Na⁺, C₆N₂⁺, and C₂SO₄⁻, corresponding in this example to an index $i = 1-4$. Note that hydrogens are omitted in the above formulas because they are not detectable by XPS. Simply counting gives the total number of molecules $n_{tot} = \sum_i n_i$. The total number of atoms is then $w_{tot} = \sum_i w_i n_i$ where w_i is the number of atoms in the i th species. We can immediately write a balance for each element as $\sum_i w_i^E n_i = y^E w_{tot}$, where E denotes an element and y^E denotes the atomic fraction of element E. For the example above, we obtain a set of four linearly independent equations:

$$\sum_i w_i^C n_i = y^C w_{tot} = 12n_1 + 6n_3 + 2n_4$$

$$\sum_i w_i^N n_i = y^N w_{tot} = 2n_3$$

$$\sum_i w_i^S n_i = y^S w_{tot} = n_1 + n_4$$

$$\sum_i w_i^{Na} n_i = y^{Na} w_{tot} = n_2$$

The above system is readily solved for all the n_i , since the y^E are known directly from the XPS measurement.

$$\begin{aligned} n_1 &= (y^C - 2y^S - 3y^N)w_{tot}/10 \\ n_2 &= y^{Na}w_{tot} \\ n_3 &= y^Nw_{tot}/2 \\ n_4 &= y^Sw_{tot} - n_1 = (12y^S - y^C + 3y^N)w_{tot}/10 \end{aligned}$$

The mole fractions are then $x_i = \frac{n_i}{n_{tot}}$, and because these concentrations are obtained by XPS, they are hereafter denoted as x_i^{surf} . Note that the x_i^{surf} are spatial averages over the length scale $d \approx 3$ nm, which is greater than the molecular lengths of the ions and surfactants.^{28, 145} Using larger XPS takeoff angles is undesirable because the resultant sampling depths would be less than the size of the surfactants.

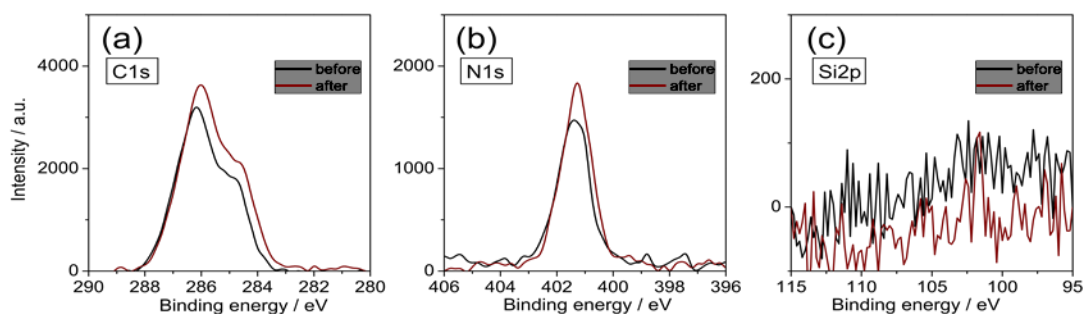


Figure 5.3 XPS regional spectra (a) C1s, (b) N1s, and (c) Si2p, for neat [EMIM][EtSO₄] after 7.5 min of Ar⁺ ion bombardment. Note that silicon content is minimal, reflective of minimal impurities.

5.3 Results and Discussion

The phase behavior of ionic surfactants is complex and depends on the solvent, concentration, and temperature. For example, micellization only occurs above a critical concentration and critical temperature, referred to as the critical micelle concentration

(CMC) and Krafft temperature (T_k), respectively. In Chapter 2, we have shown that Krafft temperatures for ionic surfactants in ILs are generally much higher than room temperature.⁶⁵ As a consequence, surface tension measurements at room temperature do not entirely reflect the phase behavior of surfactants, in particular at high concentrations (Figure 5.4). Because our XPS measurements were conducted at room temperature, these results are not complicated by the potential appearance of micelles. Of course, at sufficiently high surfactant concentrations, a separate solid phase will appear in equilibrium with the liquid phase. At low surfactant concentrations, interfacial properties will not be substantially altered – at least until a surface monolayer has been established. Indeed, as was first noted by Rayleigh,¹⁴⁶ the first break in plots of surface tension vs. concentration (i.e., isotherms) marks the onset of this condensed phase (Figure 5.4). Here we denote this transition concentration as C_a , and it furthermore provides a useful reference point. For example, using a relative concentration $C^* \approx 10C_a$ allows us to compare surfactants of different chain lengths in a more meaningful way than on an absolute basis (e.g., Figure 5.5).

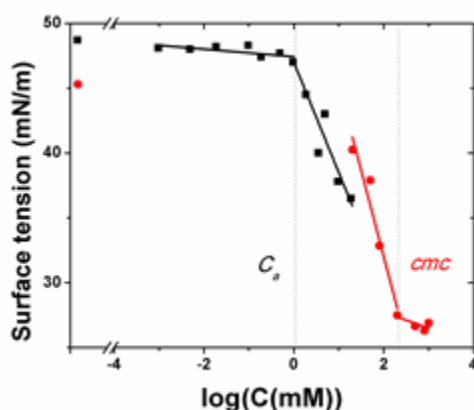


Figure 5.4 Isotherms of $C_{14}TAB$ in $[EMIM][EtSO_4]$ at different temperatures: $20^\circ C$ (black squares) and $90^\circ C$ (red circles). The surface tensions of neat IL at different temperatures are shown as the first points before the break. The Krafft temperature for this system is $T_k = 75^\circ C$.⁶⁵

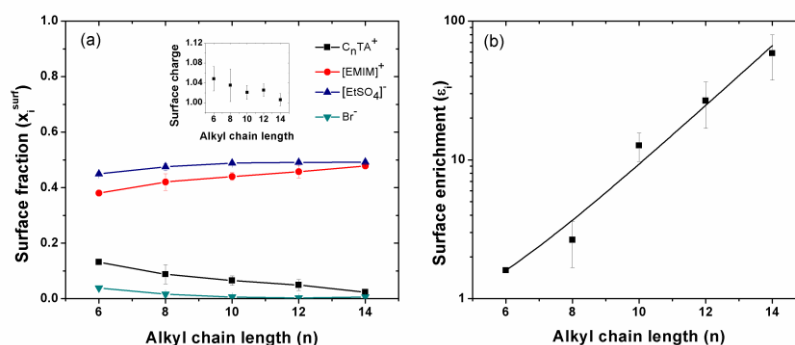


Figure 5.5 (a) Surface fractions, x_i^{surf} , (C_nTA^+ (black squares), $[EMIM]^+$ (red circles), $[EtSO_4]^-$ (blue triangles), and Br^- (dark cyan triangles) and overall surface charge ratios (inset) and (b) surface enrichment of C_nTAB on $[EMIM][EtSO_4]$. Overall surface charge is defined as the ratio of total surface cations to total surface anions. Surface enrichment is defined as the ratio $\epsilon_i = x_i^{surf} / x_i^{bulk}$, where x_i^{surf} are taken over the XPS information depth $d \approx 3.2$ nm.

Table 5.1 lists both the transition concentrations (C_a) and critical micelle concentrations (CMC) of C_nTAB in $[EMIM][EtSO_4]$ and in water. As noted earlier, the CMC can only be attained above the Krafft temperature. Although the C_a is a function

of temperature, the values reported here are at room temperature to facilitate interpretation of the XPS measurements. Our own CMC determinations in water are consistent with literature values,¹⁴⁷⁻¹⁴⁸ and these CMC are generally lower than those in ionic liquids, indicating the well-known behavior of greater solubility in ionic liquids. These results and others indicate that CMC values with respect to ionic liquids are determined by several interactions, including electrostatic forces and interfacial energy. (Actually, we have shown that interfacial energy between surfactant and ionic liquid is the key factor according to our study in Chapter 2 and 3). Furthermore, because the same CMC trend is observed for the neutral surfactants such as Brij-30 and Tween 20 (data not shown), it becomes apparent that IL is playing an essential role in determining the interfacial behavior. To avoid the complexity of discussing multiple species in surfactants and ionic liquids, in our following discussion, we will only focus on alkyltrimethylammonium bromide in [EMIM][EtSO₄].

Table 5.1 Alkyltrimethylammonium Bromide Transition Concentrations, in mM, Determined by Tensiometry at room temperature

chain length	[EMIM][EtSO ₄]		water		
	C_a (90°C)	CMC_{exp} (90°C)	C_a (20°C)	CMC_{exp} (20°C)	CMC_{ref} (25°C)
6	70	5100	/	/	990 ¹⁴⁷
8	33	3300	43	380	261 ¹⁴⁷
10	6.0	2000	4.3	69	64.6 ¹⁴⁸
12	1.4	510	2.2	14.8	14.2 ¹⁴⁸
14	0.6	190	0.03	3.1	3.6 ¹⁴⁸

5.3.1 Chain Length Effect

Analysis of XPS data typically involves decoupling signal peaks into contributions from particular elemental types based on their respective binding energies.⁵²⁻⁵⁵ However, this process is complicated in our systems due to the increased number of species: two ions from the IL and two ions from the surfactant. We therefore analyzed the elemental composition data by means of atomic mass balances,¹⁴³⁻¹⁴⁴ which only rely on the presence of one or more unique atomic species (e.g., nitrogen or sulfur). In essence, this approach simply accounts for the relative amounts of a given element within each molecular species (See the experimental part of this Chapter).⁵⁹ Once the compositions of all molecular species are determined, numerous additional quantities may be calculated. The mole fractions of each species x_i^{surf} gives an effective surface concentration averaged over the information depth $d \approx 3.2$ nm (based on an emission angle of 45°) which is greater than the molecular lengths of the ions and surfactants.^{28, 145} Figure 5.5 (a) shows the surface fractions of each species in the C_n TAB / [EMIM][EtSO₄] mixtures. It can be seen that the IL components always remain the major surface species, which is likely due to the relatively low overall concentration of surfactants. As mentioned earlier, the *bulk* concentration for each mixture is fixed at $C^* \approx 10C_a$. In spite of this normalized concentration, the shorter chain length surfactants are more abundant near the surface than their longer counterparts are.

To more carefully consider the effect of surfactant chain length, we define "surface enrichment" as the ratio of surface fraction to bulk fraction, $\varepsilon_i = x_i^{surf} / x_i^{bulk}$, which provides a measure of the relative tendency of a species to segregate to the interface (i.e., for an ideal mixture $\varepsilon_i = 1$). We find that all C_nTA^+ surfactants exhibit surface enrichments $\varepsilon \gg 1$, confirming their surface activity at the IL interface (Figure 5.5 (b)). Therefore, XPS can be used as a direct measure of surface activity even in mixtures, which may prove advantageous in situations where tensiometry is either not possible or inconvenient. Furthermore, ε increases exponentially with chain length, which we presume to be due to IL solvatophobicity, analogous to the hydrophobic effect in water.²⁸ A key result of Figure 5.5 is that while the surface fraction of longer surfactants (e.g., $C_{14}TA^+$) is not particularly large, they are partitioning to the interface much more efficiently than shorter surfactants. We also note that the surfactant Br^- counterions are undetectable (below 0.1 atomic %) at the interface for longer surfactants, suggestive of nearly complete dissociation. This situation is in stark contrast to C_nTAB behavior in water, where a significant fraction of Br^- counterions remains bound to the surfactant (or micelle).¹⁴⁹ Our observation of Br^- dissociation is consistent with earlier studies reporting the dissociation of halides in ILs (e.g., Cl^- from $[Pt(NH_3)_4]Cl_2$ in $[EMIM][EtSO_4]$).^{118, 120} The surface enrichment of C_nTA^+ and simultaneous dissociation of Br^- indicate a complex interplay among the various charged species. Previous work from our group⁵⁹ (data not shown) with anionic surfactants shows similar surface fraction and enrichment effects which suggest that

this behavior does not depend on the specific chemical identity of the ionic surfactant. We are currently exploring the importance of counterions more carefully through the examination of zwitterionic and catanionic surfactants.

Another quantity that is directly determined from the XPS compositional data is the overall surface charge, defined here as the ratio of total cations to total anions. We again emphasize that this property is defined over the information depth $d \approx 3$ nm. This ratio is expected to be unity due to the condition of electroneutrality and we find that the surface charge ratio is 1.01 ± 0.03 for neat [EMIM][EtSO₄] ($N = 27$), which implies a slight net positive charge of the IL. However, considering the relative error of the XPS experiments, the overall surface charge is indeed close to electroneutrality. As shown in the inset of Figure 5.5 (a), the surface charge ratio shows significant overlap with that of the neat [EMIM][EtSO₄] for all surfactant chain lengths. If we recall that $C^* \approx 10C_a$, it seems plausible to interpret this effect to be a result of both IL ions being the majority species at the interface.

5.3.2 Concentration Effect

To further examine the influence of surfactants on IL interfacial properties, we varied the surfactant concentration for two specific chain lengths: $n=8$ and $n=14$. With increasing C₈TAB surfactant concentration, the fractions of [EMIM]⁺ and [EtSO₄]⁻ both decrease, while the fractions of C₈TA⁺ and its counterion Br⁻ both increase (Figure 5.6 (a)). This trend reflects a dynamic ion exchange process near the interface, where one

cation type progressively exchanges with the other. A similar trend is observed for the anions. This exchange of ions does not continue indefinitely, since the C_8TA^+ and Br^- fractions appear to reach a plateau at high concentrations. Such behavior suggests that even below the Krafft temperature, the interface achieves complete saturation with C_8TA^+ at a concentration near the CMC. This scenario would be consistent with surface tension-concentration isotherms carried out *above* the Krafft temperature, where the CMC can be clearly identified. However, since the XPS experiments were conducted at room temperature, a second solid phase must appear at high surfactant concentrations, and certainly before the CMC. We are led to conclude that the solid phase of C_8TA^+ is minimally surface-active in $[EMIM][EtSO_4]$.

For the longer $C_{14}TAB$ surfactant, the fraction of $C_{14}TA^+$ increases with concentration and appears to cross a transition point, beyond which it increases more steeply (Figure 5.6 (b)). In this second regime the ion exchange of the two cations ($C_{14}TA^+$ and $[EMIM]^+$) reaches completeness, that is, their fractions become equal. Curiously, this point of equality coincides almost exactly with the CMC, even though once again the system is below the Krafft temperature. The fractions of both anions (Br^- and $[EtSO_4]^-$) remain more or less constant irrespective of the surfactant concentration. Therefore, in contrast to the situation with C_8TAB , for $C_{14}TAB$ there are fewer species are participating in the ion exchange process. The concentration-dependent differences in behavior for C_8TAB and $C_{14}TAB$ might due to several reasons, possibly including that $C_{14}TA^+$ is substantially more surface active than C_8TA^+ (Figure 5.5 (b)).

Furthermore, at high $C_{14}TAB$ concentrations we observed the formation of semi-solid surface layer, which is suggestive of a multilayer film (the open symbols in Figure 5.6 (b) are used in this case). This type of film would be possible if $C_{14}TA^+$ retains significant surface activity below its Krafft temperature, but further investigation is needed to clarify the nature of this interface.

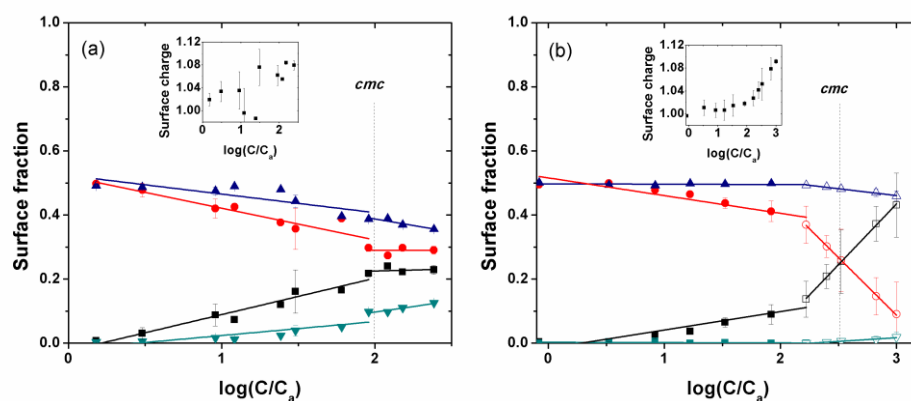


Figure 5.6 Surface fractions (C_nTA^+ (black squares), $[EMIM]^+$ (red circles), $[EtSO_4]^-$ (blue triangles), and Br^- (dark cyan triangles) and surface charge ratios (inset) of (a) C_8TAB and (b) $C_{14}TAB$ in $[EMIM][EtSO_4]$. The open symbols represent samples that exhibit a semi-solid surface film.

Even at high $C_{14}TAB$ concentrations, the Br^- counterion is minimally present while the $[EtSO_4]^-$ anion is about half of the total surface fraction. A possible reason for this behavior is that the intermolecular attraction between $C_{14}TA^+$ and $[EtSO_4]^-$ is stronger than that between $C_{14}TA^+$ and Br^- . The former interaction would clearly contain a van der Waals contribution whereas the latter would be primarily of an electrostatic nature. Results from our own previous work (Chapter 2) and that of others have indicated the possibility of highly effective charge screening within ILs,^{82, 85, 150}

which would support an interaction between C_nTA^+ and $[EtSO_4]^-$ that increases with chain length due to van der Waals attraction. While the low polarizability of halides could also explain the low Br^- surface fraction,¹¹⁸ this effect would be independent of the surfactant.

At low surfactant concentrations, the surface charge remains close to that of the neat IL (insets in Figure 5.6). However, for both surfactants there is an increasing trend with concentration, ultimately crossing into the positive charge regime. In the case of $C_{14}TAB$, this elevated positive surface charge may reflect the presumed formation of a multilayer at the interface. We note that other effects, such as the strength of ion-pairing between the IL ions,^{85, 150-151} or local heterogeneities within the IL,^{41, 44-45, 152} may be important factors in determining whether surface charge can be altered by surfactants. Indeed, angle-resolved studies have revealed surface layering of ions, which leads to a composition profile that oscillates with depth.^{124, 153}

In Figure 5.7, selected X-ray photoelectron spectra of C1s, N1s, and S2p are presented to illustrate the effects of chain length and concentration. For both C_8TAB and $C_{14}TAB$ surfactants, the C1s peak intensity increases with concentration (Figure 5.7 (a) and 5.7 (d)), suggesting the adsorption of surfactant molecules at the interface. Furthermore, the C1s peaks can be deconvoluted into two distinct peaks with binding energies of approximately 286 eV and 284 eV. These two contributions represent carbon atoms bonded to heteroatoms (nitrogen or oxygen, 286 eV) denoted by C_{hetero} ,

and carbon atoms only bonded to other carbons and hydrogen, denoted by C_{alkyl} .⁵⁶ Even without performing peak-fitting calculations (for a detailed discussion of this procedure and its assumptions, see Lovelock et al.⁵⁷), the intensity ratio of $C_{\text{alkyl}}/C_{\text{hetero}}$ increases with concentration for both surfactants, confirming that adsorption at the interface is due to the surfactant. The changes in C1s peak intensity and $C_{\text{alkyl}}/C_{\text{hetero}}$ ratio with concentration are more obvious for C₁₄TAB, which is probably due to the high surface activity of this longer chain surfactant. Consequently, the decreases in peak intensity for N1s and S2p signals (Figure 5.7 (b), (c), (e), (f)) are also more pronounced for C₁₄TAB, with the latter decrease clearly attributable to the surfactant. These qualitative results that are obtained directly from the X-ray photoelectron spectra further support our above discussions.

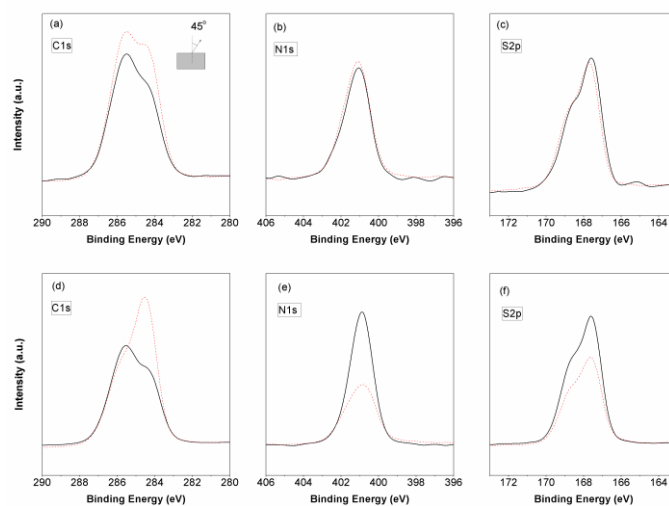


Figure 5.7 Detailed X-ray photoelectron spectra of (a, b, c) C₈TAB and (d, e, f) C₁₄TAB in [EMIM][EtSO₄] at two different surfactant concentrations. The black solid lines represent $C \approx 30C_a < CMC$, while the red dashed lines represent $C > CMC$. The spectra were taken with an emission angle of 45° (information depth $d \approx 3.2$ nm).

5.3.3 Information Depth Effect

As mentioned previously, the various quantities calculated from the XPS data are spatial averages over an information depth that is determined by the emission angle. Here we define this angle to be between the detector and the surface normal, but we note that other conventions are sometimes used. The relationship between the emission angle θ and the information depth d is given by the expression $d \approx 3\lambda \cos \theta$,⁵⁹ where λ is the electron mean free path. Since λ varies with the element being considered, we take an average over C1s, N1s, and S2p to arrive at $\lambda = 1.50$ nm. By using a larger XPS emission angle, the information depth is reduced and hence we expect to observe a larger surface fraction of surfactant. However, using *too small an information depth is undesirable* because the resultant length scales would be less than the size of the surfactants and rule out the use of both atomic mass balance analysis *and* peak-fitting deconvolution. Therefore, we examined emission angles of 75° , 45° , and 30° , which correspond to information depths of 1.2 nm, 3.2 nm, and 3.9 nm, respectively. We note that the unit length of surfactant alkyl chain is 0.126 nm,²⁸ so the fully extended surfactant chain length is between 0.63 nm ($n=6$) and 1.64 nm ($n=14$). The true chain dimensions will be somewhat smaller than the full extensions due to chain conformational flexibility and hence are expected to be within our information depths. In this regard, we emphasize once more that emission angles greater than 75° are not used since the information depth would be smaller than the thickness of surfactant monolayer at the interface.

In Figure 5.8, we use the difference in cation surface fractions $\Delta x^+ = C_n\text{TA}^+ - [\text{EMIM}]^+$ to summarize changes with concentration at various information depths. Both smaller and larger d show that with increasing surfactant concentration, the cation surface fraction difference Δx^+ is also increasing. This increase in Δx^+ is due to the fraction of $C_n\text{TA}^+$ increasing while the surface fraction of $[\text{EMIM}]^+$ is decreasing (see Figure 5.6). The value $\Delta x^+ = 0$ indicates the concentration corresponding to complete cation exchange. Clearly, this concentration shifts higher when larger d are used. On the other hand, at the smallest d studied, the larger surface fraction differences confirm that the surfactants are prone to stay close to the liquid-vapor interface.

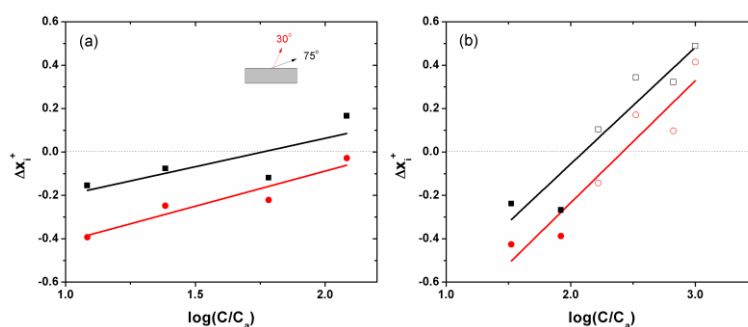


Figure 5.8 Surface fraction difference of cations $\Delta x^+ = C_n\text{TA}^+ - [\text{EMIM}]^+$, for (a) $C_8\text{TAB}$ and (b) $C_{14}\text{TAB}$ in $[\text{EMIM}][\text{EtSO}_4]$. The emission angles of 75° (black squares) and 30° (red circles) correspond to information depths d of 1.2 nm and 3.9 nm, respectively. The open symbols represent samples that exhibit a semi-solid surface film.

5.4 Conclusions

In this work we examined the influence of charged surfactants in ionic liquids by XPS. Interfacial properties such as surface composition, charge, and enrichment were studied in terms of the surfactant alkyl chain length, concentration, and XPS

information depth. Consistent with conventional tensiometry, our XPS results directly establish the surface activity of the surfactants and show that this quantity increases with alkyl chain length. We also find that an ion exchange process between like-charged surfactant and IL ions occurs at the interface, progressively increasing with surfactant concentration. Thus, surfactants can appreciably alter the interfacial properties of IL systems. By varying the XPS information depth d , we find that the effective surface activity increases inversely with d , confirming the tendency of the surfactant to remain close to the interface. Finally, we note that many opportunities remain to be explored with surfactant-IL mixtures, such as the role of counterions, nanoscale clustering in the bulk phase, and influences on layering near the interface. Although we have not done so here, careful angle-resolved XPS studies may show evidence of surfactant-induced surface layering that is distinct from the neat IL.

5.5 References

9. Maier, F.; Cremer, T.; Kolbeck, C.; Lovelock, K. R. J.; Paape, N.; Schulz, P. S.; Wasserscheid, P.; Steinrueck, H.-P., Insights into the surface composition and enrichment effects of ionic liquids and ionic liquid mixtures. *Phys. Chem. Chem. Phys.* **2010**, *12* (8), 1905-1915.
13. Welton, T., Room-Temperature Ionic Liquids. Solvents for Synthesis and Catalysis. *Chemical Reviews* **1999**, *99* (8), 2071-2084.
14. Wasserscheid, P.; Keim, W., Ionic liquids - New "solutions" for transition metal catalysis. *Angew. Chem. Int. Edit.* **2000**, *39* (21), 3772--3789.
15. Yao, C.; Pitner, W. R.; Anderson, J. L., Ionic Liquids Containing the Tris(pentafluoroethyl)trifluorophosphate Anion: a New Class of Highly Selective and Ultra Hydrophobic Solvents for the Extraction of Polycyclic Aromatic Hydrocarbons Using Single Drop Microextraction. *Anal. Chem.* **2009**, *81* (12), 5054-5063.

16. Greaves, T. L.; Drummond, C. J., Protic ionic liquids: Properties and applications. *Chem. Rev.* **2008**, *108* (1), 206-237.
17. Aliaga, C.; Santos, C. S.; Baldelli, S., Surface chemistry of room-temperature ionic liquids. *Phys. Chem. Chem. Phys.* **2007**, *9* (28), 3683-3700.
18. Marsh, K. N.; Boxall, J. A.; Lichtenthaler, R., Room temperature ionic liquids and their mixtures - a review. *Fluid Phase Equilibr.* **2004**, *219* (1), 93-98.
20. Fletcher, K. A.; Pandey, S., Surfactant aggregation within room-temperature ionic liquid 1-ethyl-3-methylimidazolium bis(trifluoromethylsulfonyl)imide. *Langmuir* **2004**, *20* (1), 33-36.
21. Zheng, L. Q.; Li, N.; Zhang, S. H.; Wu, J. P.; Li, X. W.; Yu, L., Aggregation behavior of a fluorinated surfactant in 1-butyl-3-methylimidazolium ionic liquids. *J. Phys. Chem. B* **2008**, *112* (39), 12453-12460.
22. Li, N.; Zhang, S. H.; Zheng, L. Q.; Dong, B.; Li, X. W.; Yu, L., Aggregation behavior of long-chain ionic liquids in an ionic liquid. *Phys. Chem. Chem. Phys.* **2008**, *10* (30), 4375-4377.
23. Ogino, K.; Kakihara, T.; Abe, M., Estimation of the Critical Micelle Concentrations and the Aggregation Numbers of Sodium Alkyl Sulfates by Capillary-Type Isotachopheresis. *Colloid Polym. Sci.* **1987**, *265* (7), 604-612.
24. Patrascu, C.; Gauffre, F.; Nallet, F.; Bordes, R.; Oberdisse, J.; de Lauth-Viguerie, N.; Mingotaud, C., Micelles in ionic liquids: Aggregation behavior of alkyl poly(ethyleneglycol)-ethers in 1-butyl-3-methyl-imidazolium type ionic liquids. *Chemphyschem* **2006**, *7* (1), 99-101.
28. Israelachvili, J. N., *Intermolecular and surface forces*. Academic Press: San Diego, 1992.
41. Wang, Y. T.; Voth, G. A., Unique spatial heterogeneity in ionic liquids. *J. Am. Chem. Soc.* **2005**, *127* (35), 12192-12193.
44. Wang, Y.; Jiang, W.; Yan, T.; Voth, G. A., Understanding ionic liquids through atomistic and coarse-grained molecular dynamics simulations. *Accounts Chem. Res.* **2007**, *40* (11), 1193-1199.
45. Lynden-Bell, R. M.; Del Popolo, M. G.; Youngs, T. G. A.; Kohanoff, J.; Hanke, C. G.; Harper, J. B.; Pinilla, C. C., Simulations of ionic liquids, solutions, and surfaces. *Accounts Chem. Res.* **2007**, *40* (11), 1138-1145.
51. Smith, E. F.; Villar Garcia, I. J.; Briggs, D.; Licence, P., Ionic liquids in vacuo; solution-phase X-ray photoelectron spectroscopy. *Chem. Commun.* **2005**, (45), 5633-5635.
52. Smith, E. F.; Rutten, F. J. M.; Villar-Garcia, I. J.; Briggs, D.; Licence, P., Ionic liquids in vacuo: Analysis of liquid surfaces using ultra-high-vacuum techniques. *Langmuir* **2006**, *22* (22), 9386-9392.

53. Gottfried, J. M.; Maier, F.; Rossa, J.; Gerhard, D.; Schulz, P. S.; Wasserscheid, P.; Steinruck, H. P., Surface studies on the ionic liquid 1-ethyl-3-methylimidazolium ethylsulfate using X-ray photoelectron spectroscopy (XPS). *Z. Phys. Chem.* **2006**, *220* (10-11), 1439-1453.
54. Lockett, V.; Sedev, R.; Bassell, C.; Ralston, J., Angle-resolved X-ray photoelectron spectroscopy of the surface of imidazolium ionic liquids. *Phys. Chem. Chem. Phys.* **2008**, *10* (9), 1330-1335.
55. Kolbeck, C.; Cremer, T.; Lovelock, K. R. J.; Paape, N.; Schulz, P. S.; Wasserscheid, P.; Maier, F.; Steinruck, H. P., Influence of Different Anions on the Surface Composition of Ionic Liquids Studied Using ARXPS. *J. Phys. Chem. B* **2009**, *113* (25), 8682-8688.
56. Lovelock, K. R. J.; Kolbeck, C.; Cremer, T.; Paape, N.; Schulz, P. S.; Wasserscheid, P.; Maier, F.; Steinruck, H. P., Influence of Different Substituents on the Surface Composition of Ionic Liquids Studied Using ARXPS. *J. Phys. Chem. B* **2009**, *113* (9), 2854-2864.
57. Lovelock, K. R. J.; Villar-Garcia, I. J.; Maier, F.; Steinruck, H. P.; Licence, P., Photoelectron Spectroscopy of Ionic Liquid-Based Interfaces. *Chem. Rev.* **2010**, *110* (9), 5158-5190.
59. Chen, L. G.; Lerum, R. V.; Aranda-Espinoza, H.; Bermudez, H., Surfactant-Mediated Ion Exchange and Charge Reversal at Ionic Liquid Interfaces. *J. Phys. Chem. B* **2010**, *114* (35), 11502-11508.
60. Chen, L. G.; Bermudez, H., Probing the interface of charged surfactants in ionic liquids by XPS. In *ACS Symposium Series 1117*, Visser, A. E., Ed. American Chemical Society: Washington, DC, 2012; pp 289-302.
65. Chen, L. G.; Bermudez, H., Solubility and Aggregation of Charged Surfactants in Ionic Liquids. *Langmuir* **2012**, *28* (2), 1157-1162.
67. Gao, L. C.; McCarthy, T. J., Ionic liquids are useful contact angle probe fluids. *J. Am. Chem. Soc.* **2007**, *129* (13), 3804-+.
82. Ueno, K.; Inaba, A.; Kondoh, M.; Watanabe, M., Colloidal stability of bare and polymer-grafted silica nanoparticles in ionic liquids. *Langmuir* **2008**, *24* (10), 5253-5259.
85. Ueno, K.; Tokuda, H.; Watanabe, M., Ionicity in ionic liquids: correlation with ionic structure and physicochemical properties (vol 8, pg 1649, 2010). *Phys. Chem. Chem. Phys.* **2010**, *12* (45), 15133-15134.
99. Wasserscheid, P.; Keim, W., Ionic liquids - New "solutions" for transition metal catalysis. *Angew. Chem. Int. Edit.* **2000**, *39* (21), 3772-3789.

118. Maier, F.; Gottfried, J. M.; Rossa, J.; Gerhard, D.; Schulz, P. S.; Schwieger, W.; Wasserscheid, P.; Steinruck, H. P., Surface enrichment and depletion effects of ions dissolved in an ionic liquid: an X-ray photoelectron spectroscopy study. *Angew. Chem. Int. Edit.* **2006**, *45* (46), 7778-7780.
119. Hofft, O.; Bahr, S.; Himmerlich, M.; Krischok, S.; Schaefer, J. A.; Kempster, V., Electronic structure of the surface of the ionic liquid [EMIM][Tf2N] studied by metastable impact electron spectroscopy (MIES), UPS, and XPS. *Langmuir* **2006**, *22* (17), 7120-7123.
120. Law, G.; Watson, P. R.; Carmichael, A. J.; Seddon, K. R.; Seddon, B., Molecular composition and orientation at the surface of room-temperature ionic liquids: Effect of molecular structure. *Phys. Chem. Chem. Phys.* **2001**, *3* (14), 2879-2885.
121. Caporali, S.; Bardi, U.; Lavacchi, A., X-ray photoelectron spectroscopy and low energy ion scattering studies on 1-butyl-3-methyl-imidazolium bis(trifluoromethane) sulfonimide. *J Electron Spectrosc* **2006**, *151* (1), 4-8.
122. Romero, C.; Baldelli, S., Sum frequency generation study of the room-temperature ionic liquids/quartz interface. *J. Phys. Chem. B* **2006**, *110* (12), 6213-6223.
123. Jeon, Y.; Sung, J.; Bu, W.; Vaknin, D.; Ouchi, Y.; Kim, D., Interfacial Restructuring of Ionic Liquids Determined by Sum-Frequency Generation Spectroscopy and X-Ray Reflectivity. *J Phys Chem C* **2008**, *112* (49), 19649-19654.
124. Sloutskin, E.; Ocko, B. M.; Taman, L.; Kuzmenko, I.; Gog, T.; Deutsch, M., Surface, layering in ionic liquids: An X-ray reflectivity study. *J. Am. Chem. Soc.* **2005**, *127* (21), 7796-7804.
125. Law, G.; Watson, P. R., Surface tension measurements of N-alkylimidazolium ionic liquids. *Langmuir* **2001**, *17* (20), 6138-6141.
126. Carvalho, P. J.; Freire, M. G.; Marrucho, I. M.; Queimada, A. J.; Coutinho, J. A. P., Surface tensions for the 1-alkyl-3-methylimidazolium bis(trifluoromethylsulfonyl)imide ionic liquids. *J. Chem. Eng. Data* **2008**, *53* (6), 1346-1350.
127. Ghatee, M. H.; Zolghadr, A. R., Surface tension measurements of imidazolium-based ionic liquids at liquid-vapor equilibrium. *Fluid Phase Equilibr.* **2008**, *263* (2), 168-175.
128. Niedermaier, I.; Kolbeck, C.; Taccardi, N.; Schulz, P. S.; Li, J.; Drewello, T.; Wasserscheid, P.; Steinruck, H. P.; Maier, F., Organic Reactions in Ionic Liquids Studied by in Situ XPS. *Chemphyschem* **2012**, *13* (7), 1725-1735.
129. Hurisso, B. B.; Lovelock, K. R. J.; Licence, P., Amino acid-based ionic liquids: using XPS to probe the electronic environment via binding energies. *Phys. Chem. Chem. Phys.* **2011**, *13* (39), 17737-17748.

130. Silvester, D. S.; Broder, T. L.; Aldous, L.; Hardacre, C.; Crossley, A.; Compton, R. G., Using XPS to determine solute solubility in room temperature ionic liquids. *Analyst* **2007**, *132* (3), 196-198.
131. Liu, Q. B.; Janssen, M. H. A.; van Rantwijk, F.; Sheldon, R. A., Room-temperature ionic liquids that dissolve carbohydrates in high concentrations. *Green Chem.* **2005**, *7* (1), 39-42.
132. Jacquemin, J.; Husson, P.; Majer, V.; Padua, A. A. H.; Gomes, M. F. C., Thermophysical properties, low pressure solubilities and thermodynamics of solvation of carbon dioxide and hydrogen in two ionic liquids based on the alkylsulfate anion. *Green Chem.* **2008**, *10* (9), 944-950.
133. Domanska, U., Solubilities and thermophysical properties of ionic liquids. *Pure Appl Chem* **2005**, *77* (3), 543-557.
134. Swatloski, R. P.; Spear, S. K.; Holbrey, J. D.; Rogers, R. D., Dissolution of cellulose with ionic liquids. *J. Am. Chem. Soc.* **2002**, *124* (18), 4974-4975.
135. Blesic, M.; Lopes, J. N. C.; Gomes, M. F. C.; Rebelo, L. P. N., Solubility of alkanes, alkanols and their fluorinated counterparts in tetraalkylphosphonium ionic liquids. *Phys. Chem. Chem. Phys.* **2010**, *12* (33), 9685-9692.
136. Roscioli, J. R.; Nesbitt, D. J., State-Resolved Scattering at Room-Temperature Ionic Liquid-Vacuum Interfaces: Anion Dependence and the Role of Dynamic versus Equilibrium Effects. *J. Phys. Chem. Lett.* **2010**, *1* (4), 674-678.
137. Jones, R. A. L., *Soft condensed matter*. Oxford University Press: Oxford, 2002.
138. Fernandez, A.; Torrecilla, J. S.; Garcia, J.; Rodriguez, F., Thermophysical properties of 1-ethyl-3-methylimidazolium ethylsulfate and 1-butyl-3-methylimidazolium methylsulfate ionic liquids. *J. Chem. Eng. Data* **2007**, *52* (5), 1979-1983.
139. Sarkar, S.; Pramanik, R.; Ghatak, C.; Setua, P.; Sarkar, N., Probing the Interaction of 1-Ethyl-3-methylimidazolium Ethyl Sulfate ([Emim][EtSO₄]) with Alcohols and Water by Solvent and Rotational Relaxation. *J. Phys. Chem. B* **2010**, *114* (8), 2779-2789.
140. Kazarian, S. G.; Cammarata, L.; Salter, P. A.; Welton, T., Molecular states of water in room temperature ionic liquids. *Phys. Chem. Chem. Phys.* **2001**, *3* (23), 5192-5200.
141. Hanke, C. G.; Lynden-Bell, R. M., A simulation study of water-dialkylimidazolium ionic liquid mixtures. *J. Phys. Chem. B* **2003**, *107* (39), 10873-10878.
142. Su, Z. H.; Wu, D. C.; Hsu, S. L.; McCarthy, T. J., Adsorption of end-functionalized poly(ethylene oxide)s to the poly(ethylene oxide)-air interface. *Macromolecules* **1997**, *30* (4), 840-845.
143. Hougen, O. A., *Chemical Process Principles*. Wiley: New York, 1954.

144. Felder, R. M.; Rousseau, R. W., *Elementary Principles of Chemical Processes*. John Wiley: New York, 1999.
145. Rebelo, L. P. N.; Lopes, J. N. C.; Esperanca, J. M. S. S.; Guedes, H. J. R.; Lachwa, J.; Najdanovic-Visak, V.; Visak, Z. P., Accounting for the unique, doubly dual nature of ionic liquids from a molecular thermodynamic, and modeling standpoint. *Accounts Chem. Res.* **2007**, *40* (11), 1114-1121.
146. Strutt, J. W., *Philos. Mag.* **1899**, (48), 321-337.
147. Gomez-Diaz, D.; Navaza, J. M.; Sanjurjo, B., Density, kinematic viscosity, speed of sound, and surface tension of hexyl, octyl, and decyl trimethyl ammonium bromide aqueous solutions. *J. Chem. Eng. Data* **2007**, *52* (3), 889-891.
148. Mukerjee P, M. K., *Critical micellar concentration of aqueous surfactant systems*. National Bureau of Standards: Washington, 1971.
149. Mosquera, V.; del Rio, J. M.; Attwood, D.; Garcia, M.; Jones, M. N.; Prieto, G.; Suarez, M. J.; Sarmiento, F., A study of the aggregation behavior of hexyltrimethylammonium bromide in aqueous solution. *J. Colloid. Interf. Sci.* **1998**, *206* (1), 66-76.
150. Lynden-Bell, R. M., Screening of pairs of ions dissolved in ionic liquids. *Phys. Chem. Chem. Phys.* **2010**, *12* (8), 1733-1740.
151. Angell, C. A.; Byrne, N.; Belieres, J. P., Parallel developments in aprotic and protic ionic liquids: Physical chemistry and applications. *Accounts Chem. Res.* **2007**, *40* (11), 1228-1236.
152. Triolo, A.; Russina, O.; Bleif, H. J.; Di Cola, E., Nanoscale segregation in room temperature ionic liquids. *J. Phys. Chem. B* **2007**, *111* (18), 4641-4644.
153. Bhargava, B. L.; Balasubramanian, S., Layering at an ionic liquid-vapor interface: A molecular dynamics simulation study of [bmim][PF₆]. *J. Am. Chem. Soc.* **2006**, *128* (31), 10073-10078.

CHAPTER 6

CONCLUSIONS AND OUTLOOK

In conclusion, we have investigated both aggregation and interfacial behavior of charged surfactants in ionic liquids. This thesis reports the unusual behavior and phenomenon in ionic liquids such as strong charge screening, ideal mixing, ion-exchange and charge reversal. From here, we have addressed the following four questions: 1) what is the major factor affecting the aggregation process and can we predict the solubility in different ILs? 2) What is the influence of the composition of the mixed surfactants? 3) How to measure the size of micelles in the IL solution? 4) How to characterize the air/IL interface? Each question corresponds to the major objective of one chapter above, respectively.

A number of experiments were presented to address challenges in further modifying the surfactant-IL systems and better understanding the nature of self-assembly of surfactants at IL interfaces and the interaction between solutes and IL solvents in the bulk. Our results suggest that the interfacial energy is crucial in both solubility and aggregation of surfactants in ILs. The role of IL chemistry is reflected in the net attractive interactions across the interface. Nearly ideal mixing of anionic and cationic surfactants is found over the entire composition range. PGSE-NMR reveals that ILs can play roles as both solvent and surfactant in micellization. XPS confirms

the surface activity of charged surfactants at IL interfaces and the interfacial behavior can be tuned through the judicious combination of ILs and surface-active molecules.

Presented work is not exhaustive but rather an initial investigation of surfactants in ILs which serves as a valuable role in identifying project pitfalls. Based on those findings as well as an extensive pool of literature resources we could also formulate a series of experiments demonstrating the application value of this knowledge.

The mixtures of two oppositely charged surfactants in the same IL system have been studied, showing ideal mixing behavior which is in sharp contrast to that of aqueous solution. Similar surfactants with small modifications such as non-counterions or zwitterionic surfactant may give us a better understanding of the effect of surfactant charge presentation on interfacial and aggregation behavior in ILs. (See Appendix A)

In development of the interfacial and aggregation behavior of charged surfactants with ionic liquids, the nature of ionic liquids could be further investigated by modification of ionic liquids (e.g., various anions, hydrophobicity of ILs, etc.). Natural polyelectrolyte or charged macromolecular materials such as protein and DNA would be a promising study material in the storage or manipulation process by taking advantage of unique characteristics of ionic liquids, especially for those pH sensitive materials in a pH controlled non-water ILs system. (See Appendix B)

APPENDIX A

PRELIMINARY RESULTS FOR EFFECT OF CHARGE PRESENTATION AND COUNTERIONS

A.1 Abstract: This unfinished study in the complex surfactants with different charge presentation indicates that in ILs, the surfactant efficacy is in this order: DTADS \approx 1:1 DTAB/SDS > Zwitterionic (SB-12). The effect of counterions is negligible due to the extremely strong ionic strength in ILs.

A.2 Introduction: Surfactants with different charge presentations in their head groups (i.e., zwitterionic, cationic surfactants, and equal molar ratio of mixtures of cationic and anionic surfactants, Figure A.1) were studied in both water and [EMIM][EtSO₄] to determine relative surface activities and to illustrate the role of counterions. Although zwitterionic surfactants are electrically neutral, their functional groups possess the greatest polarity within the class of nonionic surfactants. Catanionic surfactants are formed by pairing two ionic surfactant chains of opposite charge after removing their original counterions. And these two complex surfactants were both found to be vital interesting due to their special structures.^{49, 154-157} For the purpose of comparison, all of these surfactants have identical alkyl chain length. Thus, one can directly monitor the influence of head group chemistry and charge presentation on aggregation and phase behavior.

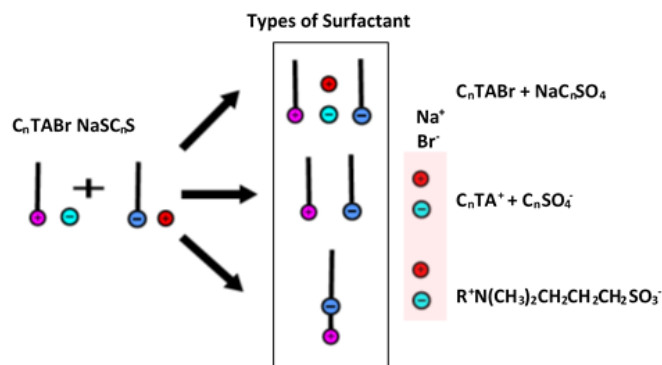


Figure A.1 Surfactants with different charge presentation.

A.3 Experimental Section

A.3.1. Materials and Methods. 1-ethyl-3-methyl imidazolium ethylsulfate [EMIM][EtSO₄], were obtained from Sigma (>95%). This ionic liquid was dried by heating at 70°C under vacuum for 2 days. The purity of the neat ionic liquid and selected surfactants was assessed by ¹H-NMR or ¹³C-NMR and did not reveal any impurities. These findings were also confirmed by XPS control experiments (see Chen et al.⁵⁹). Dodecyltrimethylammonium bromide (DTAB) (99%), and sodium dodecylsulfate (SDS) (98+%) were purchased from Fisher. N-Dodecyl-N, N-dimethyl-3-ammonio-1-propanesulfonate (SB-12) was obtained from Sigma. DTAB was purified by recrystallization from an acetone/ethanol mixture.¹⁰¹ All other surfactants were used as received.

Dodecyltrimethylammonium dodecylsulfate (DTADS) was obtained by ion exchange reaction of DTAB and SDS.^{156, 158} A 1:1 molar ratio of DTAB and SDS was stirred in dichloromethane at room temperature overnight. The impurities in organic

phase were washed by distilled water until bromide ions could not be detected by AgNO_3 solution. The structure and purity were ascertained by $^1\text{H-NMR}$, and elemental analysis. Elemental analysis (Complete Analysis Laboratories, Inc.): C, 65.63 (65.66); H, 12.18 (12.04); N, 2.74 (2.84); S, 6.39 (6.49); Br, <0.01 (0.00); Na, 0.009 (0.00). The data above in parentheses are calculated from the formula of the final product. $^1\text{H-NMR}$ (300 MHz, CDCl_3): δ 0.8 (6H, $-\text{CH}_3$, t), 1.2 (36H, $-(\text{CH}_2)_9-$, m), 1.6 (4H, $\text{CH}_2-\text{CH}_2-\text{O}$ and $\text{CH}_2-\text{CH}_2-\text{N}$, m), 3.3 (9H, $\text{N}(\text{CH}_3)_3$, s), 3.4 (2H, CH_2-N , m), 3.9 (2H, CH_2-O , t). Yield: 72%.

A.3.2. Surface Characterization. Surface tension was measured by means of the Wilhelmy method using a Micro Trough XS (Kibron, Inc.). At room temperature, the surface tension for neat $[\text{EMIM}][\text{EtSO}_4]$ at room temperature is 48.7 ± 0.5 which is relatively higher than that of traditional organic solvents but much lower than that of water. Our experimental value is in good agreement with that of literature.⁶⁸

For room temperature isotherms in water, in-house reverse osmosis (RO) water was passed through a $0.22\mu\text{m}$ filter and then used to dissolve the surfactants. For surfactant mixtures, stock solutions of cationic and anionic surfactants were mixed at certain molar ratios and kept at RT for over 48h till the solution became complete clear. For high temperature isotherms in $[\text{EMIM}][\text{EtSO}_4]$, surfactants or surfactant mixtures were dissolved directly in $[\text{EMIM}][\text{EtSO}_4]$ at elevated temperature. After dissolution, solutions were subsequently diluted to appropriate concentrations as needed. All

concentrations here are presented as millimoles of surfactant per liter of solvent (mmol/L). In the case of surfactant mixtures or catanionic surfactant, the concentration is based on moles of the total surfactant alkyl chain to facilitate comparison. Surfactant solutions (300 μ L) with different concentrations were applied on an aluminum plate with glass wells. Surface tensions were measured after an equilibration time of 30 min. Temperature was controlled and monitored by using a hotplate placed underneath the multi-well plate and an Omega HH506RA multilogger thermometer probe in the well of interest.

A.4 Results and Discussion:

The stoichiometric 1:1 mixture of DTAB/SDS provides a starting point for further comparison of charge presentation. In Figure A.2, we present the surface tension isotherms in both [EMIM][EtSO₄] (a) and water (b) for the zwitterionic surfactant SB-12, the 1:1 DTAB/SDS mixture, and the catanionic surfactant DTADS. These three types of surfactant systems have the same 12-carbon alkyl tail but different charge presentations in their headgroups. In both [EMIM][EtSO₄] and water, the zwitterionic surfactant SB-12 has the largest cmc and highest γ_{cmc} , which can be attributed to the lowest headgroup polarity. Zwitterionic surfactants are formally nonionic compounds consisting of a single molecule that is electrically neutral.¹⁵⁹ In SB-12, the two opposite charges are separated by a propylene group, which is short enough to presumably minimize the polarity of the headgroup. Comparing to zwitterionic surfactants, ionic surfactants are true salts¹⁵⁹ and they are expected to be more surface active in terms of

head group polarity. All ionic surfactants and even their cationic-anionic mixtures have lower cmc and corresponding surface tension γ_{cmc} than those of SB-12 in both [EMIM][EtSO₄] and water (Figure A.2 and Figure A.3).

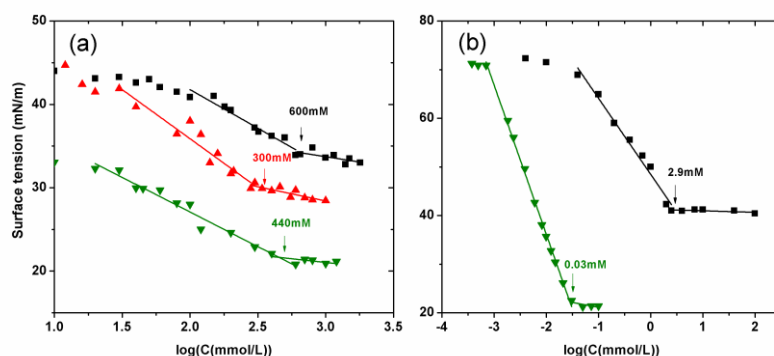


Figure A.2 Isotherms of (a) zwitterionic surfactant SB-12 (black squares), 1:1 DTAB/SDS mixture (red upward triangles), and DTADS (with Si impurity) in [EMIM][EtSO₄] (green downward triangles) at 90°C and (b) zwitterionic surfactant SB-12 (black squares) at 20°C, and DTADS in water (green downward triangles, data from reference¹⁵⁶, at 25°C). The isotherm for the 1:1 DTAB/SDS mixture in water is not available because of its multiphase character. Please note that the DTADS in this Figure has residual amount of Si.

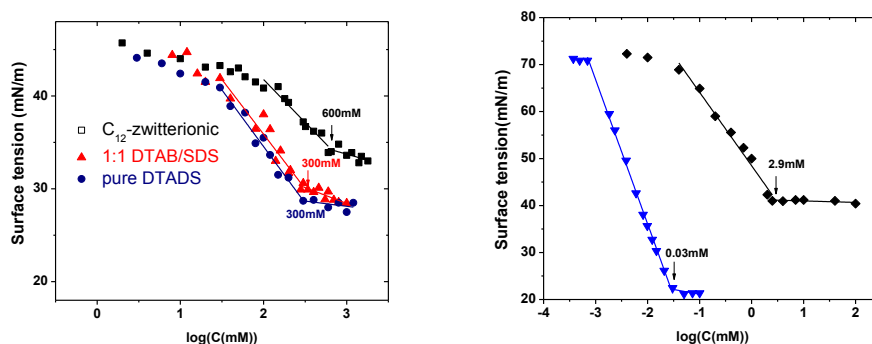


Figure A.3 Isotherms of (a) zwitterionic surfactant SB-12 (black squares), 1:1 DTAB/SDS mixture (red upward triangles), and DTADS (without Si impurity) in [EMIM][EtSO₄] (blue circles) at 90°C and (b) zwitterionic surfactant SB-12 (black squares) at 20°C, and DTADS in water (blue downward triangles, data from reference¹⁵⁶, at 25°C). The isotherm for the 1:1 DTAB/SDS mixture in water is not

available because of its multiphase character. Please note no residual Si is found in DTADS of this Figure.

Please note that the DTADS we synthesized could potentially have some residual amount of Si. The actual amount is so small that even elemental analysis could not detect. Instead, we have to use XPS to test the sample surface as the Si impurity is surface active. The surface active residual Si could have a significant effect on the surface tension measurements. Figure A.2 and Figure A.3 showed the isotherm with and without residual Si, respectively. Here we will only discuss Figure A.3.

In Figure A.3 (a), the 1:1 DTAB/SDS mixture has almost the same isotherm as that of the catanionic DTADS in [EMIM][EtSO₄], thus resulting in the same aggregation behavior (i.e., CMC and γ_{CMC}). Since the only difference between these two systems is that the former has counterions (i.e. Br⁻ and Na⁺) while the latter does not, we conclude that the counterions in [EMIM][EtSO₄] do not have any strong effect for the aggregation in ionic liquids, which is mainly due to strong charge screening in ionic liquids. For the 1:1 DTAB/SDS mixtures, the concentration of counterions (i.e., Na⁺, Br⁻) at the *cmc* is below the NaBr solubility limit in [EMIM][EtSO₄] of approximately 320 mmol/L.¹⁶⁰ However, at the highest surfactant concentrations, the corresponding NaBr concentration is beyond the solubility limit mentioned above. Because we do not observe any precipitation for even this highly concentrated system, it suggests that surfactant improves the solubility of counterions. Interestingly, such a solubility enhancement of inorganic ions has been observed in other salt-surfactant systems.¹⁶¹

Table A.1 summarizes selected surface properties of the three surfactant systems in both water and [EMIM][EtSO₄]. The surface excess concentration at saturation Γ_{max} was calculated by use of the appropriate Gibbs equation.⁷⁶⁻⁷⁷

$$\Gamma_{max} = -\frac{1}{mRT} \frac{d\gamma}{d \ln C}$$

In the aqueous solution, the value of m (the number of species at the interface whose surface concentration changes with a change in surfactant concentration) is taken as 1 for zwitterionic surfactant SB-12 because the surfactant has a net zero charge and carries no counterions.¹⁶² While for DTADS, this prefactor is taken as 2 instead. In the case of ionic liquids, the dominating “sea of ions” screens any surface excess of counterions which determines the prefactor m to be 1 no matter what surfactant systems used inside.⁷⁶

C_{10} is the bulk concentration of surfactant required to depress the surface tension of the solvent by 10 mN/m. The reason to apply C_{10} instead of more commonly used C_{20} is because neat [EMIM][EtSO₄] has lower surface tension than water, and hence the surface tension reductions are smaller in magnitude. Both Γ_{max} and C_{10} are useful measures of the effectiveness of adsorption of the surfactant. We also suggest to define and use a parameter $(cmc * C_{10})^{0.5}$, which provides an integrated view of micellization and adsorption efficiency. A small value of this parameter indicates that micellization is favored as well as adsorption of the surfactant. It is clear from the isotherms in water that DTADS is superior over SB-12 as an efficient surfactant (Figure A.3 (b)), in agreement with the $(cmc * C_{10})^{0.5}$ values. However, the isotherms in [EMIM][EtSO₄]

do not make a clear distinction in superiority between DTADS and 1:1 DTAB/SDS (Figure 3(a)). Based on the $(cmc * C_{10})^{0.5}$ values, we can conclude that the order of the overall efficiency is DTADS \approx 1:1 DTAB/SDS $>$ SB-12.

Table A.1 Surface Properties of SB-12, 1:1 DTAB/SDS, and DTADS in Water (20°C) and [EMIM][EtSO₄] (90°C) (For the 1:1 DTAB/SDS system, cmc_{12} is used)

	H ₂ O		IL	
	Γ_{\max} ($\mu\text{mol}/\text{m}^2$)	$(cmc * C_{10})^{0.5}$ (mmol/L)	Γ_{\max} ($\mu\text{mol}/\text{m}^2$)	$(cmc * C_{10})^{0.5}$ (mmol/L)
SB-12	1.4	0.6	1.5	590
1:1 DTAB/SDS	/	/	1.7	200
DTADS	2.7 ¹⁵⁶	0.006 ¹⁵⁶	1.7	200

A.5 Conclusions:

In summary, the effect of charge presentation of surfactants on aggregation and interfacial behavior in ILs have been investigated and compared to water. In the case of the three types of surfactants, they have the same alkyl apolar chain but different charge presentation in their head group. The overall surfactant efficiency order is: DTADS \approx 1:1 DTAB/SDS $>$ SB-12. From the comparison of the first two surfactant systems, we conclude that the counterions in IL has negligible effect in surfactant aggregation. Because the different behavior between DTADS (with Si impurity) and 1:1 DTAB/SDS we saw above is mainly due to the existence of residual Si in DTADS. Here we are proposing some other techniques to characterize the two surfactants. XPS should be able to detect the interfacial composition of counterions, while the PGSE-NMR would tell us the counterions effect on the aggregation size in the same IL.

A.6 References

49. Tsujii, K.; Mino, J., Krafft Point Depression of Some Zwitterionic Surfactants by Inorganic Salts. *J. Phys. Chem.* **1978**, *82* (14), 1610-1614.
59. Chen, L. G.; Lerum, R. V.; Aranda-Espinoza, H.; Bermudez, H., Surfactant-Mediated Ion Exchange and Charge Reversal at Ionic Liquid Interfaces. *J. Phys. Chem. B* **2010**, *114* (35), 11502-11508.
68. Gao, L. C.; McCarthy, T. J., Ionic liquid marbles. *Langmuir* **2007**, *23* (21), 10445-10447.
76. Rosen, M. J., *Surfactants and interfacial phenomena*. Wiley-interscience: New York, 1989.
77. Bae, S.; Haage, K.; Wantke, K.; Motschmann, H., On the factor in Gibbs equation for ionic surfactants. *J. Phys. Chem. B* **1999**, *103* (7), 1045-1050.
101. Jiang, L. X.; Bin Huang, J.; Bahramian, A.; Li, P. X.; Thomas, R. K.; Penfold, J., Surface Behavior, Aggregation and Phase Separation of Aqueous Mixtures of Dodecyl Trimethylammonium Bromide and Sodium Oligoarene Sulfonates: the Transition to Polyelectrolyte/Surfactant Behavior. *Langmuir* **2012**, *28* (1), 327-338.
154. Hoyer, H. W.; Zoellner, M.; Marmo, A., Some Colloidal Properties of Decyl-and Dodecyltrimethylammonium Dodecyl Sulfate. *J. Phys. Chem.* **1961**, *65* (10), 1804-&.
155. Fernandes, R. M. F.; Marques, E. F.; Silva, B. F. B.; Wang, Y. J., Micellization behavior of a cationic surfactant with high solubility mismatch Composition, temperature, and salt effects. *Journal of Molecular Liquids* **2010**, *157* (2-3), 113-118.
156. Gilanyi, T.; Meszaros, R.; Varga, I., Phase transition in the adsorbed layer of cationic surfactants at the air/solution interface. *Langmuir* **2000**, *16* (7), 3200-3205.
157. Behera, K.; Pandey, S., Ionic liquid induced changes in the properties of aqueous zwitterionic surfactant solution. *Langmuir* **2008**, *24* (13), 6462-6469.
158. Jiao, J. J.; Dong, B.; Zhang, H. N.; Zhao, Y. Y.; Wang, X. Q.; Wang, R.; Yu, L., Aggregation Behaviors of Dodecyl Sulfate-Based Anionic Surface Active Ionic Liquids in Water. *J. Phys. Chem. B* **2012**, *116* (3), 958-965.
159. Laughlin, R. G., Fundamentals of the Zwitterionic Hydrophilic Group. *Langmuir* **1991**, *7* (5), 842-847.
160. Wang, B.; Zhang, Q. G.; Yang, H. Z., Study on solid-liquid phase equilibria in ionic liquid - 2. The solubility of alkali bromide in ionic liquid 1-ethyl-3-methylimidazolium ethyl sulfate. *Fluid Phase Equilib.* **2007**, *254* (1-2), 163-166.

161. Albayrak, C.; Cihaner, A.; Dag, O., A New, Highly Conductive, Lithium Salt/Nonionic Surfactant, Lyotropic Liquid-Crystalline Mesophase and Its Application. *Chemistry-a European Journal* **2012**, *18* (14), 4190-4194.

162. Seredyuk, V.; Alami, E.; Nyden, M.; Holmberg, K.; Peresykin, A. V.; Menger, F. M., Adsorption of zwitterionic gemini surfactants at the air-water and solid-water interfaces. *Colloid Surface A*. **2002**, *203* (1-3), 245-258.

APENDIX B

PROPOSED EXPERIMENTS

B.1 Synthesis of $[C_nTA][C_nSO_4]$ without Small Counterions by Ion Exchange

It is well known that ILs with the same cations but different anions may have completely different properties in solubility and hydrophobicity.^{55, 163} Previously XPS results also shows the completely dissociation of counterions from surfactants into the bulk solution. Here, we propose to synthesize a novel surfactant by using ion exchange to remove the counterions of the mixed surfactants, that is $[C_nTA][C_nSO_4]$ without Br- and Na^+ counterions. Bales et al.¹⁶⁴ give the experimental details for the synthesis and more importantly, they suggested these novel surfactants can be in liquid state at room temperature, which means they are also ILs. We may call them surfactant ionic liquids which have a long alkyl chain in both cation and anion.

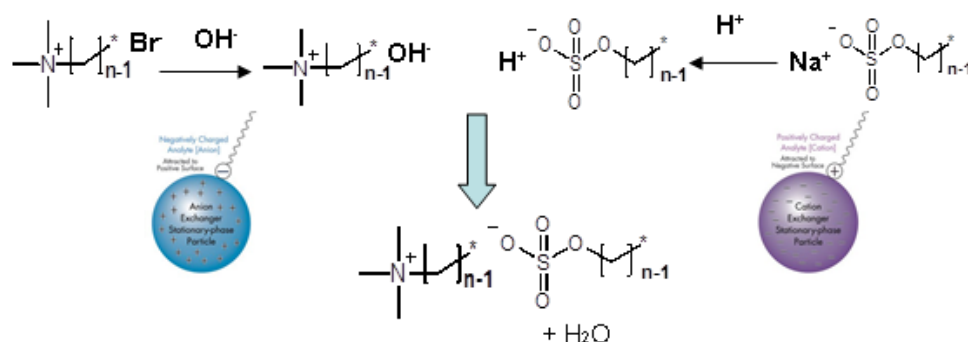


Figure B.1 Synthesis of $[C_nTA][C_nSO_4]$ by ion exchange.

We have started to synthesize $[\text{C}_{12}\text{TA}][\text{C}_{12}\text{SO}_4]$ which is composed the same alkyl chain length of SDS and C_{12}TAB by ion exchange (Figure B.1). The preliminary results show the $[\text{C}_{12}\text{TA}][\text{C}_{12}\text{SO}_4]$ is not liquid at room temperature (m.p. is above 100°C), which may due to the two long alkyl chains in the surfactant molecule, leading to strong hydrophobic attraction and large molecular weight. Therefore, $[\text{C}_6\text{TA}][\text{C}_6\text{SO}_4]$ is the next synthetic goal because it might have a much lower melting temperature.

In addition, the difference of $[\text{C}_n\text{TA}][\text{C}_n\text{SO}_4]$ and $\text{C}_n\text{TABr}/\text{NaC}_n\text{SO}_4$ is that the former one lack the counterion salt NaBr. And it is quite interesting to find that the solubility of NaBr in ILs is much smaller than that of $[\text{C}_{12}\text{TA}][\text{C}_{12}\text{SO}_4]$ from the preliminary results.

References

55. Kolbeck, C.; Cremer, T.; Lovelock, K. R. J.; Paape, N.; Schulz, P. S.; Wasserscheid, P.; Maier, F.; Steinruck, H. P., Influence of Different Anions on the Surface Composition of Ionic Liquids Studied Using ARXPS. *J. Phys. Chem. B* **2009**, *113* (25), 8682-8688.
163. Wang, H. Y.; Wang, J. J.; Zhang, S. B.; Xuan, X. P., Structural Effects of Anions and Cations on the Aggregation Behavior of Ionic Liquids in Aqueous Solutions. *J. Phys. Chem. B* **2008**, *112* (51), 16682-16689.
164. Bales, B. L.; Zana, R., Cloud point of aqueous solutions of tetrabutylammonium dodecyl sulfate is a function of the concentration of counterions in the aqueous phase. *Langmuir* **2004**, *20* (5), 1579-1581.

B.2 Different Ionic Liquids, Effect of Anions

Since surfactants and ionic liquids are the two major components in the system, after studying the effect of surfactant charge presentation in Appendix A, modification of ionic liquids could be also interesting to control the interface and aggregation behavior.

B.2.1. Ionic Liquids with Different Types of Anions

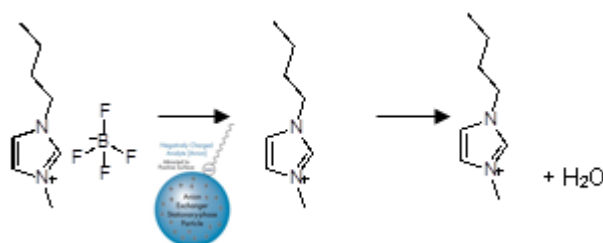


Figure B.2 Preparation of ILs with different anions by anion exchange.

The novel feature of ILs as solvents is the possibility to design one with the necessary properties for a specific application.¹⁸ These designer solvents can be reached from ionic liquids with different anions which can be simply prepared by using anion exchange resin which has been described by Wang et al¹⁶³ (see Figure B.2). This process can give a series of ionic liquids with the same imidazolium cation but different anions. The anion X can be Cl, Br, NO₃, CH₃COO, PF₆, Tf₂N, etc. And the latter two ILs with BmimBF₄ would be used as the hydrophobic ILs to be studied in section B2.2.

B.2.2. Comparison of Hydrophilic and Hydrophobic ILs

Hydrophobicity of ILs is mainly determined by the types of anion. It has been found that the air-liquid interfaces for hydrophobic ILs and hydrophilic ILs may be

quite different.⁷⁰ For example, water affects the surface of hydrophobic ionic liquids and not hydrophilic ones.¹⁶⁵ What's more, hydrophobic ionic liquids can be strikingly tuned to be hydrophilic by means of an electric field.¹⁶⁶ Here, we want to investigate and compare the properties of hydrophilic ILs and hydrophobic ILs, which is BMIMBF₄ and BMIMPF₆ or BMIMTf₂N. Since we have suggested that interfacial energy is the major factor affecting surfactant's solubility and aggregation, we are curious if hydrophobic ILs also follow the same trend by calculating the interfacial energy of BMIMPF₆. In addition, we are looking for a method to measure the interfacial energy directly to confirm the calculated results in Table 2.7.

B.2.3. pH Effect on Surface Tension and Aggregation

ILs have been explored to be a potential novel solvent and media for storage and chemical reactions. It would be of great importance to understand the proton activity in an ionic medium especially when a material or reaction is pH sensitive. MacFarlane et al.¹⁶⁷ have found that pH can be controlled by ionic liquid "buffers" in ionic liquid/water systems. And Dai et al.¹⁶⁸ pointed out that both the solubility and the CMC of charged surfactants decrease with pH. Although both of their work is conducted in ionic liquid aqueous solutions, we are interested in studying pH effect on surface tension and aggregation in a pure ionic liquid system (Figure B.3).

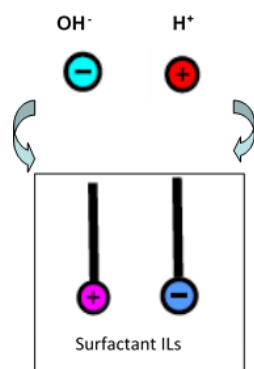


Figure B.3 Cartoon of pH effect on ionic liquids.

In order to establish a pH controlled IL system, the first choice is to use the synthesized $[\text{C}_n\text{TA}^+][\text{C}_n\text{SO}_4^-]$ surfactant ionic liquids in section B.1. The intermediate product in the ion exchange process, that is $[\text{C}_n\text{TA}^+][\text{OH}^-]$ or $\text{C}_n\text{SO}_4^-\text{H}^+$, can be added to control the pH in the IL system. In this case, there are only three types of ions in the system: cations and anions from ILs, the H^+ or OH^- ions. This non-water pH controlled ILs will be useful to study the fundamental of pH in a non-aqueous media and might show promising application in the future.

On the other hand, if the synthesis of surfactant ionic liquids in section B.1 is not successful (their melting temperature is much higher than RT), the backup plan is to use the most traditional ionic liquid ethylammonium nitrate EtAN. NaOH and HNO_3 can be used to control its pH. Another choice is $[\text{Bmim}][\text{Acetate}]$, because $[\text{Bmim}][\text{OH}^-]$ and Acetate acid are weak base and acid.

In this long term plan section, we are proposing to do the following experiments:

- Synthesize a series of ILs with different anions by ion exchange (from $[\text{Bmim}][\text{BF}_4]$ to $[\text{PF}_6^-]$, $[\text{Tf}_2\text{N}^-]$, and $[\text{Bmim}][\text{OH}^-]$ as the intermediate product)

- Similar studies on the hydrophobic ILs [Bmim][PF₆] or [Bmim][Tf₂N] by measuring the CMCs of surfactants and calculate the interfacial energy.
- Measure pH value in a non-water ILs by pH meter or pH indicator. (There is still a question that what is the physical meaning of pH value measured by pH meter?) Use [C₆TA][C₆SO₄] if it is liquid at room temperature, and [C₆TA][OH] and [C₆SO₄]H are used to control the pH. If a surfactant ionic liquid cannot be synthesized, use protic IL (EAN) instead.
- Measure the surface tension or surface composition of these novel pH controlled ILs by tensiometer or XPS.
- The same study by adding a pH sensitive polymer (such as polyacrylic acid and chitosan) into ILs.

B.2.4. References

18. Marsh, K. N.; Boxall, J. A.; Lichtenthaler, R., Room temperature ionic liquids and their mixtures - a review. *Fluid Phase Equilibr.* **2004**, *219* (1), 93-98.
70. Huddleston, J. G.; Visser, A. E.; Reichert, W. M.; Willauer, H. D.; Broker, G. A.; Rogers, R. D., Characterization and comparison of hydrophilic and hydrophobic room temperature ionic liquids incorporating the imidazolium cation. *Green Chem.* **2001**, *3* (4), 156-164.
163. Wang, H. Y.; Wang, J. J.; Zhang, S. B.; Xuan, X. P., Structural Effects of Anions and Cations on the Aggregation Behavior of Ionic Liquids in Aqueous Solutions. *J. Phys. Chem. B* **2008**, *112* (51), 16682-16689.
165. Rivera-Rubero, S.; Baldelli, S., Influence of water on the surface of hydrophilic and hydrophobic room-temperature ionic liquids. *J. Am. Chem. Soc.* **2004**, *126* (38), 11788-11789.
166. Sha, M. L.; Niu, D. X.; Dou, Q.; Wu, G. Z.; Fang, H. P.; Hu, J., Reversible tuning of the hydrophobic-hydrophilic transition of hydrophobic ionic liquids by means of an electric field. *Soft Matter* **2011**, *7* (9), 4228-4233.

167. MacFarlane, D. R.; Vijayaraghavan, R.; Ha, H. N.; Izgorodin, A.; Weaver, K. D.; Elliott, G. D., Ionic liquid "buffers"-pH control in ionic liquid systems. *Chem. Commun.* **2010**, *46* (41), 7703-7705.

168. Dai, Q.; Laskowski, J. S., The Krafft Point of Dodecylammonium Chloride - Ph Effect. *Langmuir* **1991**, *7* (7), 1361-1364.

B.3 Surface Dynamic by Compression Isotherms

The surface tension in the preliminary results is measured in passive isotherms which give static information, while compression isotherms can describe the dynamic reorientation information at the air/liquid interface. It will be worth to try compression isotherms for stable Langmuir monolayer of pure surfactants or their mixture in ILs. Appropriate surfactants can be chosen from small surfactants with a relatively long alkyl chain¹⁶⁹ (e.g. C₁₆TAB), block copolymer surfactants¹⁷⁰ (PEO-PBD, PEO-PS), polyelectrolyte (PSS, PAA, PEG-COOH, ELP, etc.) zwitterionic polymers or even novel ionic liquid polymers¹⁷¹. The transitions in a compression isotherm may give information about the transformation of surface structures and bulk aggregations, such as different shapes of micelles (disklike, rodlike, or sphere).

The first choice of materials in a compression isotherm would be C₁₆TAB or SC₁₆S on IL I because they are more likely to form Langmuir monolayer on the surface of ILs due to their limited solubility. The zwitterionic surfactants or even mixtures of the above two surfactants may be applied in the following experiments. If they could not form a Langmuir monolayer, a polymer surfactant such as PEO-PBD might be worth to try.

Here is the summary of the experiments that we propose to do by using Langmuir-Blodgett Trough:

Surface pressure-area isotherm at RT or 90°C, speed of 1A²/(molecule min)

- C₁₆TAB or SC₁₆S on IL I

- Their mixtures on IL I
- The Zwitterionic surfactant
- PEO-PBD

References

169. Tah, B.; Pal, P.; Mahato, M.; Talapatra, G. B., Aggregation Behavior of SDS/CTAB Catanionic Surfactant Mixture in Aqueous Solution and at the Air/Water Interface. *J. Phys. Chem. B* **2011**, *115* (26), 8493-8499.

170. Lerum, R. V.; Bermudez, H., Controlled Interfacial Assembly and Transfer of Brushlike Copolymer Films. *Chemphyschem* **2010**, *11* (3), 665-669.

171. Winterton, N., Solubilization of polymers by ionic liquids. *J. Mater. Chem.* **2006**, *16* (44), 4281-4293.

APENDIX C

PROCEDURES FOR XPS MEASUREMENTS

(Conte B551 with Jack Hirsh)

C.1 Sample Preparation

C.1.1 Five microliters of aqueous surfactant solutions were applied on the surface of 5 μ L of IL droplets using (oxygen-plasma-cleaned) silicon wafers as substrates. Samples were dried in a flowing nitrogen environment for 3 days at room temperature prior to conducting XPS measurement.

C.1.2 Note: The predissolution of the samples in water is not necessary if the surfactant can dissolve in IL at an elevated temperature and can be transfer to the silicon wafer substrate easily.

C.1.3 XPS data were recorded using a Physical Electronics Quantum 2000 Microprobe instrument with monochromatic Al X-ray at 50 W, and a 200 μ m spot area.

C.1.4 The samples on silicon wafer were fixed on the XPS sample holder stage. There are two different sample holders, one is for regular take-off angle of 45 degree and another is for various take-off angles.

C.2 Instrument Setup

C.2.1 On computer, open the software Phi. The map on the software console control window represents the structure of the instrument inside and the software can monitor every step in the instrument chamber. In the Prep Area, drag platen X (X is number 2 or 4 for regular take-off angle, ARS for angle dependent test) on the plate. Monitor the chamber pressure, when pressure reaches 8.2×10^2 Torr, open the vacuum side door and put the sample holder in the chamber and click "OK". After this, everything is controlled on the computer software.

C.2.2 Vacuum pressure of the chamber will go down. Wait for the vacuum to be under 2×10^{-6} . It will take about 20-30 min depending on the moisture content of the sample. During the time, change the platen information for each sample, such as filename (use LCdate_, such as LC072714_), sample description, and comments. Choose the folder to save the data.

C.2.3 When vacuum pressure is below 2×10^{-6} Torr, click "photo: Lo Mag" to take a photo of the sample plate, then drag the sample to sample stage, then the sample comes in. Wait until it doesn't move anymore.

C.2.4 On the Main control window, "locate area", clear all points (file name, prefix and comment)

C.2.5 Click on "sample handling", "reconfigure", double check the "platen X" is the right one.

C.2.6 Click "neutralizer", "electron and ion" choose "standby", "ion gun" choose "ion gun pump on, flow state on", then neutralizer, "electron and ion" choose "auto".

C.2.7 Change X-ray position, (just change to any of them to check the synchronize of the computer)

C.3 Sample Running

C.3.1 On Platen view window, drag the red arrow to the sample point of interest. Click “add points”, write the comments for the specific sample. Then you have to determine the height of the sample, for Si wafer, set $Z=24$ and click “auto Z” (on “pc compass” window wait until it’s finished, around 2 - 3 minutes). Check the height on the platen view by scrolling on the right on dot’s window. If the numbers are the same, turn the spot to green and turn “imaging” off on the small window (bottom right). If there are several substrates, you can also do a quick survey to check if the height is good. For most of the samples, you expect $\approx 10\,000$ counts.

C.3.2 Auto Z and survey scan can be done together. Choose “still mode”, then choose spot (click both left and right of the mouse), set the property, Z alignment, and add to queue.

C.3.3 Acquisition, there are several kind of acquisitions

C.3.3.1 Spectral acquisition \rightarrow one angle (45°)

C.3.3.2 Sputter depth profile \rightarrow deep analysis

C.3.3.3 Angle dependent \rightarrow different angles

C.3.4 On the spectral acquisition,

C.3.4.1 Pass energy \rightarrow the smaller the number, the higher the resolution. Choose 187.85 eV for survey scan and 46.95 eV for second scan.

C.3.4.2 Set the time. In the 1st fast scan, choose “survey“(Su), raise the number of sweeps (2 or 3) (high number for low concentration and for interesting elements). Normally, use 3 min and choose “200u50W15kV” resolution for the scan. In the 2nd scan, choose the element and don’t forget to put the same pass energy (46.95 eV) for each element. The number of sweeps we are using are as follows:

Elements	O	C	Si	N	S	Na	Br	F	B
# of sweeps	2	3	3	3	3	4	4	3	4

C.3.4.3 Add to queue, “acquire” or run the queue.

C.3.5 Identify peaks with multipack and XPS’s handbook

C.3.6 Sputter depth profile (1KV1x1) (.pro)

C.3.6.1 Number of cycles (5 is ok), the more you put cycles, the deeper you go.

C.3.6.2 You can queue several scans no matter what kind of.

C.4 Finishing

C.4.1 On the software, electron off, flow rate off. 30 seconds later, when pressure stable, diff pump off, and then ion gun off.

C.4.2 On the main control, drag the sample onto the prep area. When pressure (bottom right) reach $2E+2$ Torr, remove the sample holder from the plate. Click pump down on the intro and sign out the log book.

C.4.3 Analysis is based on the integration of the XPS peaks and atomic sensitivity factors below.

C.5 Atomic Sensitivity Factors

	C1s	N1s	S2p	Na1s	Br3d
ASF	0.314	0.499	0.717	1.102	1.149

APENDIX D

PROCEDURES FOR PGSE-NMR MEASUREMENTS

(LGRC with Weiguo Hu)

D.1 Sample preparation and fundamental

D.1.1 References: <http://www.chemistry.jhu.edu/NMR/dosy.pdf> and Weiguo's NMR tutorial handouts

D.1.2 All solutions were prepared by directly dissolving certain amount of SDS in [EMIM][EtSO₄] or D₂O. PGSE-NMR diffusion measurements were carried out on a 400 MHz Bruker NMR spectrometer equipped with a temperature controller. The self-diffusion measurements were performed with a Gaussian-shape pulsed field gradient stimulated echo, whose magnitude is 5.35 Gauss/mm. The diffusion time, Δ , between the two pulses was set between 200-500 ms, and the gradient pulse duration, δ , was set between 2 and 6 ms, depending on the diffusion coefficient of the mobile species. The diffusion coefficient value was determined from the intensity change equation:

$$I = I_0 e^{-D\gamma^2 g^2 \delta^2 (\Delta - \frac{\delta}{3})}$$

Here, I and I_0 are the areas of the signal obtained with or without gradient pulses respectively, D is the diffusion coefficient, γ is the gyromagnetic ratio of proton,

whose value is given by $2.675 \cdot 10^8 \text{ T}^{-1}\text{s}^{-1}$, g is the magnitude of the two gradient pulses.

D.1.3 0.5 mL or less of surfactant solutions are applied into NMR tubes. For surfactant/ionic liquid samples, because they are solid at RT, store the NMR tubes in 90 °C oven until the samples melted and flow into the bottom of the NMR tube. The height of NMR tube should be about 3-5 cm.

D.1.4 Note: There is no deuterated solvent in surfactant/IL samples in order to avoid their unknown influence. This NMR technique is special in 3 ways: 1) High temperature 2) Label free (i.e., no deuterated solvent) 3) Measuring diffusion coefficient

D.2 Instrument Setup and Optimizing Parameters

D.2.1 Because of high temperature, **ceramic spinner** is used instead of traditional plastic one. Place the NMR tube into the spinner and the center of sample should align with the mark on the spinner.

D.2.2 Use neat D₂O to lock (top shimming, roughly lock)

D.2.2.1 On computer, open the software.

D.2.2.2 Type “ej” to eject standard sample, “ij” to insert D₂O sample, “edc”-> “rsh shims.best”-> “lock”-> “lockdisp”-> “bsmsdisp” to manually shimming z, z2, z3 (this step is similar to regular NMR and critical for good signal) -> “ej” to eject the D₂O sample-> “ij” to inject IL sample.

D.2.2.3 Make sure take the NMR tube **cap off** to avoid the flux due to heating.
 (Cap off is not necessary for ILs because ILs will not evaporate, but to be consistent, we always take off the cap.)

D.2.3 Increase Temperature to 90 °C step by step (Source: Weiguo’s note, page 4)

D.2.3.1 “EDTE” to open a new window for temperature setup

Set the T_{Target} , change the HeaterMax and flow step by step according to the following chart. First set T_{Target} to be 310K, HeaterMax(%) to be 5%, Flow (l/hr) to be 400. Wait several minutes until temperature stable. Then T_{Target} to be 330K, 5%, 400. Then 344.55K, 10%, 535. The final T_{Target} is calculate by the equation below.

$$T_{\text{Target}} = 0.7482 * T_{\text{CALIB}} + 72.843 = 0.7482 * (273.15 + 90) + 72.843 = 344.55$$

T (°C)	T _{CALIB}	T _{Target}	HeaterMax(%)	Flow (l/hr)
23.7	296.7	294	off	270
44.8	317.8	310	5	400
72.8	345.8	330	5	400
97.9	370.9	350	10	535
109	382	360	10	670

D.2.4 When target temperature reached, “edc” name your sample -> “rpar”->choose user->diffusion 1D->read->OK->“get prosol”

D.2.5 Fid Shimming. (Further lock) acqu->gs->bsmsdisp (Turn off lock, sweep)
->manually change z,z2,z3 until the fid area to be maximum -> halt

D.2.6 “ased” to set D20 (big delta), P30 (little delta) and gpz6 (pulse strength) to be 2% -> rga -> zg -> efp -> apk

D.2.7 Edc -> Name 2 -> “ased” to set D20 (big delta), P30 (little delta) and gpz6 to be 95%, -> zg -> efp -> apk

D.2.8 Repeat 2.6 and 2.7 to adjust D20 and P30 to get perfect decay. Click “the symbol of multiply display”, choose one peak, drag the height of the peak and compare, check the scale until in the range of 1% to 5%.

D.3 Running the Diffusion Measurement

D.3.1 When optimal D20 and P30 parameters founded, edc -> Name 3 -> rpar -> 2d -> read -> OK -> “getprosol” -> change D20 and P30 by “ased”

D.3.2 “Xau dosy 2 95 16 l y y” to start the acquisition. It means the start value 2%, final value 95%, 16 steps, linear ramp, and start acquisition.

D.3.3 “xf2” -> phase correction by click the symbol, drug “R” to do phase correction and “ABS2” for automatic baseline correction.

D.3.4 “setdiffparm”. This will transfer D20 and P30 parameters into the appropriate parameters for the next processing step.

D.3.5 In analysis on the top tool bar, Dosy 2D, choose “T1/T2” -> extreme -> spectrum -> manual integration -> save export all peaks without regions -> Reexamine window -> Fitting -> choose area, show all calculation fitting -> report

D.4 Transfer data through ftp: Host: www.pse.umass.edu User: nmrusers PW: 2dc13f19

BIBLIOGRAPHY

1. Barrer, R. M., The viscosity of pure liquids. II. Polymerised ionic melts. *T Faraday Soc* **1943**, *39*, 0059-0066.
2. Walden, P., Molecular weights and electrical conductivity of several fused salts. *Bulletin de l'Academie Imperiale des Sciences de St.-Petersbourg* **1914**, 405-422.
3. Chum, H. L.; Koch, V. R.; Miller, L. L.; Osteryoung, R. A., Electrochemical Scrutiny of Organometallic Iron Complexes and Hexamethylbenzene in a Room-Temperature Molten-Salt. *J. Am. Chem. Soc.* **1975**, *97* (11), 3264-3265.
4. Wilkes, J. S.; Levisky, J. A.; Wilson, R. A.; Hussey, C. L., Dialkylimidazolium Chloroaluminate Melts - a New Class of Room-Temperature Ionic Liquids for Electrochemistry, Spectroscopy, and Synthesis. *Inorg. Chem.* **1982**, *21* (3), 1263-1264.
5. Fry, S. E.; Pienta, N. J., Effects of Molten-Salts on Reactions - Nucleophilic Aromatic-Substitution by Halide-Ions in Molten Dodecyltributylphosphonium Salts. *J. Am. Chem. Soc.* **1985**, *107* (22), 6399-6400.
6. Castner, E. W.; Wishart, J. F., Spotlight on ionic liquids. *J. Chem. Phys.* **2010**, *132* (12), -.
7. Greaves, T. L.; Drummond, C. J., Ionic liquids as amphiphile self-assembly media. *Chem. Soc. Rev.* **2008**, *37* (8), 1709--1726.
8. Rogers, R. D.; Seddon, K. R., Ionic liquids - Solvents of the future? *Science* **2003**, *302* (5646), 792-793.
9. Maier, F.; Cremer, T.; Kolbeck, C.; Lovelock, K. R. J.; Paape, N.; Schulz, P. S.; Wasserscheid, P.; Steinrueck, H.-P., Insights into the surface composition and enrichment effects of ionic liquids and ionic liquid mixtures. *Phys. Chem. Chem. Phys.* **2010**, *12* (8), 1905-1915.
10. Dobler, D.; Schmidts, T.; Klingenhofer, I.; Runkel, F., Ionic liquids as ingredients in topical drug delivery systems. *International Journal of Pharmaceutics* **2013**, *441* (1-2), 620-627.
11. He, Y. Y.; Li, Z. B.; Simone, P.; Lodge, T. P., Self-assembly of block copolymer micelles in an ionic liquid. *J. Am. Chem. Soc.* **2006**, *128* (8), 2745-2750.
12. Bai, Z. F.; He, Y. Y.; Lodge, T. P., Block copolymer micelle shuttles with tunable transfer temperatures between ionic liquids and aqueous solutions. *Langmuir* **2008**, *24* (10), 5284-5290.
13. Welton, T., Room-Temperature Ionic Liquids. Solvents for Synthesis and Catalysis. *Chemical Reviews* **1999**, *99* (8), 2071-2084.

14. Wasserscheid, P.; Keim, W., Ionic liquids - New "solutions" for transition metal catalysis. *Angew. Chem. Int. Edit.* **2000**, *39* (21), 3772--3789.
15. Yao, C.; Pitner, W. R.; Anderson, J. L., Ionic Liquids Containing the Tris(pentafluoroethyl)trifluorophosphate Anion: a New Class of Highly Selective and Ultra Hydrophobic Solvents for the Extraction of Polycyclic Aromatic Hydrocarbons Using Single Drop Microextraction. *Anal. Chem.* **2009**, *81* (12), 5054-5063.
16. Greaves, T. L.; Drummond, C. J., Protic ionic liquids: Properties and applications. *Chem. Rev.* **2008**, *108* (1), 206-237.
17. Aliaga, C.; Santos, C. S.; Baldelli, S., Surface chemistry of room-temperature ionic liquids. *Phys. Chem. Chem. Phys.* **2007**, *9* (28), 3683-3700.
18. Marsh, K. N.; Boxall, J. A.; Lichtenthaler, R., Room temperature ionic liquids and their mixtures - a review. *Fluid Phase Equilib.* **2004**, *219* (1), 93-98.
19. Chiappe, C.; Pieraccini, D., Ionic liquids: solvent properties and organic reactivity. *J. Phys. Org. Chem.* **2005**, *18* (4), 275-297.
20. Fletcher, K. A.; Pandey, S., Surfactant aggregation within room-temperature ionic liquid 1-ethyl-3-methylimidazolium bis(trifluoromethylsulfonyl)imide. *Langmuir* **2004**, *20* (1), 33-36.
21. Zheng, L. Q.; Li, N.; Zhang, S. H.; Wu, J. P.; Li, X. W.; Yu, L., Aggregation behavior of a fluorinated surfactant in 1-butyl-3-methylimidazolium ionic liquids. *J. Phys. Chem. B* **2008**, *112* (39), 12453-12460.
22. Li, N.; Zhang, S. H.; Zheng, L. Q.; Dong, B.; Li, X. W.; Yu, L., Aggregation behavior of long-chain ionic liquids in an ionic liquid. *Phys. Chem. Chem. Phys.* **2008**, *10* (30), 4375-4377.
23. Ogino, K.; Kakihara, T.; Abe, M., Estimation of the Critical Micelle Concentrations and the Aggregation Numbers of Sodium Alkyl Sulfates by Capillary-Type Isotachopheresis. *Colloid Polym. Sci.* **1987**, *265* (7), 604-612.
24. Patrascu, C.; Gauffre, F.; Nallet, F.; Bordes, R.; Oberdisse, J.; de Lauth-Viguerie, N.; Mingotaud, C., Micelles in ionic liquids: Aggregation behavior of alkyl poly(ethyleneglycol)-ethers in 1-butyl-3-methyl-imidazolium type ionic liquids. *Chemphyschem* **2006**, *7* (1), 99-101.
25. Anderson, J. L.; Pino, V.; Hagberg, E. C.; Sheares, V. V.; Armstrong, D. W., Surfactant solvation effects and micelle formation in ionic liquids. *Chemical Communications* **2003**, (19), 2444-2445.

26. Bhattacharya, S.; Haldar, J.; Aswal, V. K.; Goyal, P. S., Molecular modulation of surfactant aggregation in water: Effect of the incorporation of multiple headgroups on micellar properties. *Angew. Chem. Int. Edit.* **2001**, *40* (7), 1228-+.
27. Sedev, R., Surface tension, interfacial tension and contact angles of ionic liquids. *Curr. Opin. Colloid In.* **2011**, *16* (4), 310-316.
28. Israelachvili, J. N., *Intermolecular and surface forces*. Academic Press: San Diego, 1992.
29. Anderson, J. L.; Pino, V.; Hagberg, E. C.; Sheares, V.; Armstrong, D. W., Surfactant solvation effects and micelle formation in ionic liquids. *Chem. Commun.* **2003**, (19), 2444-2445.
30. Li, N.; Zhang, S.; Zheng, L.; Wu, J.; Li, X.; Yu, L., Aggregation behavior of a fluorinated surfactant in 1-butyl-3-methylimidazolium ionic liquids. *J. Phys. Chem. B* **2008**, *112* (39), 12453-12460.
31. Li, N.; Zhang, S.; Zheng, L.; Inoue, T., Aggregation behavior of a fluorinated surfactant in 1-butyl-3-methylimidazolium bis(trifluoromethylsulfonyl)imide ionic liquid. *Langmuir* **2009**, *25* (18), 10473-82.
32. Santos, C. S.; Baldelli, S., Gas-liquid interface of room-temperature ionic liquids. *Chem. Soc. Rev.* **2010**, *39* (6), 2136-2145.
33. Hayes, R.; Warr, G. G.; Atkin, R., At the interface: solvation and designing ionic liquids. *Phys. Chem. Chem. Phys.* **2010**, *12* (8), 1709-1723.
34. Gannon, T. J.; Law, G.; Watson, P. R.; Carmichael, A. J.; Seddon, K. R., First observation of molecular composition and orientation at the surface of a room-temperature ionic liquid. *Langmuir* **1999**, *15* (24), 8429-8434.
35. Law, G.; Watson, P. R., Surface orientation in ionic liquids. *Chem. Phys. Lett.* **2001**, *345* (1-2), 1-4.
36. Baldelli, S., Influence of water on the orientation of cations at the surface of a room-temperature ionic liquid: A sum frequency generation vibrational spectroscopic study. *J. Phys. Chem. B* **2003**, *107* (25), 6148-6152.
37. Sloutskin, E.; Ocko, B. M.; Tamam, L.; Kuzmenko, I.; Gog, T.; Deutsch, M., Surface layering in ionic liquids: An X-ray reflectivity study (vol 127, pg 7796, 2005). *J. Am. Chem. Soc.* **2005**, *127* (51), 18333-18333.
38. Santos, C. S.; Baldelli, S., Surface orientation of 1-methyl-, 1-ethyl-, and 1-butyl-3-methylimidazolium methyl sulfate as probed by sum-frequency generation vibrational spectroscopy. *J. Phys. Chem. B* **2007**, *111* (18), 4715-4723.

39. Waring, C.; Bagot, P. A. J.; Slattery, J. M.; Costen, M. L.; McKendrick, K. G., O((3)P) Atoms as a Probe of Surface Ordering in 1-Alkyl-3-methylimidazolium-Based Ionic Liquids. *J. Phys. Chem. Lett.* **2010**, *1* (1), 429-433.
40. Niga, P.; Wakeham, D.; Nelson, A.; Warr, G. G.; Rutland, M.; Atkin, R., Structure of the Ethylammonium Nitrate Surface: An X-ray Reflectivity and Vibrational Sum Frequency Spectroscopy Study. *Langmuir* **2010**, *26* (11), 8282-8288.
41. Wang, Y. T.; Voth, G. A., Unique spatial heterogeneity in ionic liquids. *J. Am. Chem. Soc.* **2005**, *127* (35), 12192-12193.
42. Bhargava, B. L.; Balasubramanian, S., Layering at an ionic liquid-vapor interface: A molecular dynamics simulation study of [bmim][PF(6)]. *J. Am. Chem. Soc.* **2006**, *128* (31), 10073-10078.
43. Sloutskin, E.; Lynden-Bell, R. M.; Balasubramanian, S.; Deutsch, M., The surface structure of ionic liquids: Comparing simulations with x-ray measurements. *J. Chem. Phys.* **2006**, *125* (17).
44. Wang, Y.; Jiang, W.; Yan, T.; Voth, G. A., Understanding ionic liquids through atomistic and coarse-grained molecular dynamics simulations. *Accounts Chem. Res.* **2007**, *40* (11), 1193-1199.
45. Lynden-Bell, R. M.; Del Popolo, M. G.; Youngs, T. G. A.; Kohanoff, J.; Hanke, C. G.; Harper, J. B.; Pinilla, C. C., Simulations of ionic liquids, solutions, and surfaces. *Accounts Chem. Res.* **2007**, *40* (11), 1138-1145.
46. Chen, L. G.; H., S. S.; Bermudez, H., Characterization of Self-assembled Amphiphiles in Ionic Liquids. Paul, B. K., Ed. Wiley: 2014.
47. Tariq, M.; Freire, M. G.; Saramago, B.; Coutinho, J. A. P.; Lopes, J. N. C.; Rebelo, L. P. N., Surface tension of ionic liquids and ionic liquid solutions. *Chem. Soc. Rev.* **2012**, *41* (2), 829-868.
48. Inoue, T.; Higuchi, Y.; Misono, T., Differential scanning calorimetric study of nonionic surfactant mixtures with a room temperature ionic liquid, bmimBF(4). *J. Colloid. Interf. Sci.* **2009**, *338* (1), 308-311.
49. Tsujii, K.; Mino, J., Krafft Point Depression of Some Zwitterionic Surfactants by Inorganic Salts. *J. Phys. Chem.* **1978**, *82* (14), 1610-1614.
50. Rico, I.; Lattes, A., Formamide, a Water Substitute .12. Krafft Temperature and Micelle Formation of Ionic Surfactants in Formamide. *J. Phys. Chem.* **1986**, *90* (22), 5870-5872.
51. Smith, E. F.; Villar Garcia, I. J.; Briggs, D.; Licence, P., Ionic liquids in vacuo; solution-phase X-ray photoelectron spectroscopy. *Chem. Commun.* **2005**, (45), 5633-5635.

52. Smith, E. F.; Rutten, F. J. M.; Villar-Garcia, I. J.; Briggs, D.; Licence, P., Ionic liquids in vacuo: Analysis of liquid surfaces using ultra-high-vacuum techniques. *Langmuir* **2006**, *22* (22), 9386-9392.
53. Gottfried, J. M.; Maier, F.; Rossa, J.; Gerhard, D.; Schulz, P. S.; Wasserscheid, P.; Steinruck, H. P., Surface studies on the ionic liquid 1-ethyl-3-methylimidazolium ethylsulfate using X-ray photoelectron spectroscopy (XPS). *Z. Phys. Chem.* **2006**, *220* (10-11), 1439-1453.
54. Lockett, V.; Sedev, R.; Bassell, C.; Ralston, J., Angle-resolved X-ray photoelectron spectroscopy of the surface of imidazolium ionic liquids. *Phys. Chem. Chem. Phys.* **2008**, *10* (9), 1330-1335.
55. Kolbeck, C.; Cremer, T.; Lovelock, K. R. J.; Paape, N.; Schulz, P. S.; Wasserscheid, P.; Maier, F.; Steinruck, H. P., Influence of Different Anions on the Surface Composition of Ionic Liquids Studied Using ARXPS. *J. Phys. Chem. B* **2009**, *113* (25), 8682-8688.
56. Lovelock, K. R. J.; Kolbeck, C.; Cremer, T.; Paape, N.; Schulz, P. S.; Wasserscheid, P.; Maier, F.; Steinruck, H. P., Influence of Different Substituents on the Surface Composition of Ionic Liquids Studied Using ARXPS. *J. Phys. Chem. B* **2009**, *113* (9), 2854-2864.
57. Lovelock, K. R. J.; Villar-Garcia, I. J.; Maier, F.; Steinruck, H. P.; Licence, P., Photoelectron Spectroscopy of Ionic Liquid-Based Interfaces. *Chem. Rev.* **2010**, *110* (9), 5158-5190.
58. http://www.ntt-at.com/product/x-ray_focus/.
59. Chen, L. G.; Lerum, R. V.; Aranda-Espinoza, H.; Bermudez, H., Surfactant-Mediated Ion Exchange and Charge Reversal at Ionic Liquid Interfaces. *J. Phys. Chem. B* **2010**, *114* (35), 11502-11508.
60. Chen, L. G.; Bermudez, H., Probing the interface of charged surfactants in ionic liquids by XPS. In *ACS Symposium Series 1117*, Visser, A. E., Ed. American Chemical Society: Washington, DC, 2012; pp 289-302.
61. <http://mestrelab.com/resources/dosy/>.
62. Pettersson, E.; Topgaard, D.; Stilbs, P.; Soderman, O., Surfactant/nonionic polymer interaction. a NMR diffusometry and NMR electrophoretic investigation. *Langmuir* **2004**, *20* (4), 1138-1143.
63. Kunze, M.; Jeong, S.; Paillard, E.; Schonhoff, M.; Winter, M.; Passerini, S., New Insights to Self-Aggregation in Ionic Liquid Electrolytes for High-Energy Electrochemical Devices. *Advanced Energy Materials* **2011**, *1* (2), 274-281.
64. Pramanik, R.; Sarkar, S.; Ghatak, C.; Rao, V. G.; Sarkar, N., Ionic Liquid Containing Microemulsions: Probe by Conductance, Dynamic Light Scattering, Diffusion-Ordered Spectroscopy NMR Measurements, and Study of Solvent Relaxation Dynamics. *J. Phys. Chem. B* **2011**, *115* (10), 2322-2330.

65. Chen, L. G.; Bermudez, H., Solubility and Aggregation of Charged Surfactants in Ionic Liquids. *Langmuir* **2012**, *28* (2), 1157-1162.
66. Evans, D. F.; Yamauchi, A.; Roman, R.; Casassa, E. Z., Micelle Formation in Ethylammonium Nitrate, a Low-Melting Fused Salt. *J. Colloid. Interf. Sci.* **1982**, *88* (1), 89-96.
67. Gao, L. C.; McCarthy, T. J., Ionic liquids are useful contact angle probe fluids. *J. Am. Chem. Soc.* **2007**, *129* (13), 3804-+.
68. Gao, L. C.; McCarthy, T. J., Ionic liquid marbles. *Langmuir* **2007**, *23* (21), 10445-10447.
69. Sanchez, L. G.; Espel, J. R.; Onink, F.; Meindersma, G. W.; de Haan, A. B., Density, Viscosity, and Surface Tension of Synthesis Grade Imidazolium, Pyridinium, and Pyrrolidinium Based Room Temperature Ionic Liquids. *J. Chem. Eng. Data* **2009**, *54* (10), 2803-2812.
70. Huddleston, J. G.; Visser, A. E.; Reichert, W. M.; Willauer, H. D.; Broker, G. A.; Rogers, R. D., Characterization and comparison of hydrophilic and hydrophobic room temperature ionic liquids incorporating the imidazolium cation. *Green Chem.* **2001**, *3* (4), 156-164.
71. Nakayama, H.; Shinoda, K., Effect of Added Salts on Solubilities and Krafft Points of Sodium Dodecyl Sulfate and Potassium Perfluoro-Octanoate. *B. Chem. Soc. Jpn.* **1967**, *40* (8), 1797-&.
72. Luczak, J.; Jungnickel, C.; Joskowska, M.; Thoming, J.; Hupka, J., Thermodynamics of micellization of imidazolium ionic liquids in aqueous solutions. *J. Colloid. Interf. Sci.* **2009**, *336* (1), 111-116.
73. Shinoda, K.; Hutchinson, E., Pseudo-Phase Separation Model for Thermodynamic Calculations on Micellar Solutions. *J. Phys. Chem.* **1962**, *66* (4), 577-&.
74. Bales, B. L.; Benraou, M.; Zana, R., Krafft temperature and micelle ionization of aqueous solutions of cesium dodecyl sulfate. *J. Phys. Chem. B* **2002**, *106* (35), 9033-9035.
75. Nakayama, H.; Shinoda, K.; Hutchins.E, Effect of Added Alcohols on Solubility and Krafft Point of Sodium Dodecyl Sulfate. *J. Phys. Chem.* **1966**, *70* (11), 3502-&.
76. Rosen, M. J., *Surfactants and interfacial phenomena*. Wiley-interscience: New York, 1989.
77. Bae, S.; Haage, K.; Wantke, K.; Motschmann, H., On the factor in Gibbs equation for ionic surfactants. *J. Phys. Chem. B* **1999**, *103* (7), 1045-1050.
78. Gao, Y. N.; Li, N.; Li, X. W.; Zhang, S. H.; Zheng, L. Q.; Bai, X. T.; Yu, L., Microstructures of Micellar Aggregations Formed within 1-Butyl-3-methylimidazolium Type Ionic Liquids. *J. Phys. Chem. B* **2009**, *113* (1), 123-130.

79. Good, R. J.; Elbing, E., Generalization of Theory for Estimation of Interfacial Energies. *Ind. Eng. Chem.* **1970**, *62* (3), 54-&.
80. Fowkes, F. M., Attractive Forces at Interfaces. *Ind. Eng. Chem.* **1964**, *56* (12), 40-&.
81. Girifalco, L. A.; Good, R. J., A Theory for the Estimation of Surface and Interfacial Energies .1. Derivation and Application to Interfacial Tension. *J. Phys. Chem.* **1957**, *61* (7), 904-909.
82. Ueno, K.; Inaba, A.; Kondoh, M.; Watanabe, M., Colloidal stability of bare and polymer-grafted silica nanoparticles in ionic liquids. *Langmuir* **2008**, *24* (10), 5253-5259.
83. Smith, J. A.; Werzer, O.; Webber, G. B.; Warr, G. G.; Atkin, R., Surprising Particle Stability and Rapid Sedimentation Rates in an Ionic Liquid. *J. Phys. Chem. Lett.* **2010**, *1* (1), 64-68.
84. Reichardt, C., Pyridinium N-phenoxide betaine dyes and their application to the determination of solvent polarities part 29 - Polarity of ionic liquids determined empirically by means of solvatochromic pyridinium N-phenolate betaine dyes. *Green Chem.* **2005**, *7* (5), 339-351.
85. Ueno, K.; Tokuda, H.; Watanabe, M., Ionicity in ionic liquids: correlation with ionic structure and physicochemical properties (vol 8, pg 1649, 2010). *Phys. Chem. Chem. Phys.* **2010**, *12* (45), 15133-15134.
86. Behera, K.; Om, H.; Pandey, S., Modifying Properties of Aqueous Cetyltrimethylammonium Bromide with External Additives: Ionic Liquid 1-Hexyl-3-methylimidazolium Bromide versus Cosurfactant n-Hexyltrimethylammonium Bromide. *J. Phys. Chem. B* **2009**, *113* (3), 786-793.
87. Behera, K.; Pandey, S., Concentration-dependent dual behavior of hydrophilic ionic liquid in changing properties of aqueous sodium dodecyl sulfate. *J. Phys. Chem. B* **2007**, *111* (46), 13307-13315.
88. Chen, L. G.; Bermudez, H., Charge Screening between Anionic and Cationic Surfactants in Ionic Liquids. *Langmuir* **2013**, *29* (9), 2805-2808.
89. Holland, P. M.; Rubingh, D. N., Mixed Surfactant Systems - an Overview. *Acs Symposium Series* **1992**, *501*, 2-30.
90. Ong, C. P.; Ng, C. L.; Lee, H. K.; Li, S. F. Y., The Use of Mixed Surfactants in Micellar Electrokinetic Chromatography. *Electrophoresis* **1994**, *15* (10), 1273-1275.
91. Shiloach, A.; Blankshtein, D., Measurement and prediction of ionic/nonionic mixed micelle formation and growth. *Langmuir* **1998**, *14* (25), 7166-7182.
92. Kume, G.; Gallotti, M.; Nunes, G., Review on anionic/cationic surfactant mixtures. *Journal of Surfactants and Detergents* **2008**, *11* (1), 1-11.

93. Clint, J. H., Micellization of Mixed Nonionic Surface-Active Agents. *Journal of the Chemical Society-Faraday Transactions I* **1975**, 71 (6), 1327-1334.
94. Holland, P. M.; Rubingh, D. N., Nonideal Multicomponent Mixed Micelle Model. *J. Phys. Chem.* **1983**, 87 (11), 1984-1990.
95. Motomura, K.; Yamanaka, M.; Aratono, M., Thermodynamic Consideration of the Mixed Micelle of Surfactants. *Colloid Polym. Sci.* **1984**, 262 (12), 948-955.
96. Puvvada, S.; Blankschtein, D., Thermodynamic Description of Micellization, Phase-Behavior, and Phase-Separation of Aqueous-Solutions of Surfactant Mixtures. *J. Phys. Chem.* **1992**, 96 (13), 5567-5579.
97. Shiloach, A.; Blankschtein, D., Predicting micellar solution properties of binary surfactant mixtures. *Langmuir* **1998**, 14 (7), 1618-1636.
98. Bakshi, M. S.; Sachar, S.; Mahajan, N.; Kaur, I.; Kaur, G.; Singh, N.; Sehgal, P.; Doe, H., Mixed-micelle formation by strongly interacting surfactant binary mixtures: effect of head-group modification. *Colloid Polym. Sci.* **2002**, 280 (11), 990-1000.
99. Wasserscheid, P.; Keim, W., Ionic liquids - New "solutions" for transition metal catalysis. *Angew. Chem. Int. Edit.* **2000**, 39 (21), 3772-3789.
100. Sakai, H.; Saitoh, T.; Misono, T.; Tsuchiya, K.; Sakai, K.; Abe, M., Nonionic Surfactant Mixtures in an Imidazolium-Type Room-Temperature Ionic Liquid. *Journal of Oleo Science* **2011**, 60 (11), 563-567.
101. Jiang, L. X.; Bin Huang, J.; Bahramian, A.; Li, P. X.; Thomas, R. K.; Penfold, J., Surface Behavior, Aggregation and Phase Separation of Aqueous Mixtures of Dodecyl Trimethylammonium Bromide and Sodium Oligoarene Sulfonates: the Transition to Polyelectrolyte/Surfactant Behavior. *Langmuir* **2012**, 28 (1), 327-338.
102. Schick, M. J., Effect of Temperature on Critical Micelle Concentration of Nonionic Detergents - Thermodynamics of Micelle Formation. *J. Phys. Chem.* **1963**, 67 (9), 1796-&.
103. Kamenka, N.; Chorro, M.; Talmon, Y.; Zana, R., Study of Mixed Aggregates in Aqueous-Solutions of Sodium Dodecyl-Sulfate and Dodecyltrimethylammonium Bromide. *Colloids and Surfaces* **1992**, 67, 213-222.
104. Rosen, M. J.; Murphy, D. S., Synergism in Binary-Mixtures of Surfactants .5. 2-Phase Liquid Liquid-Systems at Low Surfactant Concentrations. *J. Colloid. Interf. Sci.* **1986**, 110 (1), 224-236.

105. Rubingh, D. N., Mixed Micelle Solutions. In *Solution Chemistry of Surfactants*, Mittal, K. L., Ed. Plenum Press: New York, 1979; Vol. 1, pp 337-354.
106. Lopez-Fontan, J. L.; Suarez, M. J.; Mosquera, V.; Sarmiento, F., Micellar behavior of n-alkyl sulfates in binary mixed systems. *J. Colloid. Interf. Sci.* **2000**, *223* (2), 185-189.
107. Frank, H. S.; Thompson, P. T., Fluctuations and the Limit of Validity of the Debye-Huckel Theory. *J. Chem. Phys.* **1959**, *31* (4), 1086-1095.
108. Cui, X. H.; Jiang, Y.; Yang, C. S.; Lu, X. Y.; Chen, H.; Mao, S. Z.; Liu, M. L.; Yuan, H. Z.; Luo, P. Y.; Du, Y. R., Mechanism of the Mixed Surfactant Micelle Formation. *J. Phys. Chem. B* **2010**, *114* (23), 7808-7816.
109. Singh, S.; Simmons, B. A.; Vogel, K. P., Visualization of Biomass Solubilization and Cellulose Regeneration During Ionic Liquid Pretreatment of Switchgrass. *Biotechnology and Bioengineering* **2009**, *104* (1), 68-75.
110. Han, X.; Armstrong, D. W., Ionic liquids in separations. *Accounts Chem. Res.* **2007**, *40* (11), 1079-1086.
111. Ueno, K.; Watanabe, M., From Colloidal Stability in Ionic Liquids to Advanced Soft Materials Using Unique Media. *Langmuir* **2011**, *27* (15), 9105-9115.
112. Fileti, E. E.; Chaban, V. V., Imidazolium Ionic Liquid Helps to Disperse Fullerenes in Water. *J. Phys. Chem. Lett.* **2014**, *5* (11), 1795-1800.
113. Comelles, F.; Ribosa, I.; Gonzalez, J. J.; Garcia, M. T., Interaction of Nonionic Surfactants and Hydrophilic Ionic Liquids in Aqueous Solutions: Can Short Ionic Liquids Be More Than a Solvent? *Langmuir* **2012**, *28* (41), 14522-14530.
114. Hao, J. C.; Song, A. X.; Wang, J. Z.; Chen, X.; Zhuang, W. C.; Shi, F.; Zhou, F.; Liu, W. M., Self-assembled structure in room-temperature ionic liquids. *Chemistry-a European Journal* **2005**, *11* (13), 3936-3940.
115. Khandavalli, S.; Rothstein, J. P., Extensional rheology of shear-thickening fumed silica nanoparticles dispersed in an aqueous polyethylene oxide solution. *Journal of Rheology* **2014**, *58* (2), 411-431.
116. Bakshi, M. S.; Kaura, A.; Miller, J. D.; Paruchuri, V. K., Sodium dodecyl sulfate-poly(amidoamine) interactions studied by AFM imaging, conductivity, and Krafft temperature measurements. *J. Colloid. Interf. Sci.* **2004**, *278* (2), 472-477.

117. Macchioni, A.; Ciancaleoni, G.; Zuccaccia, C.; Zuccaccia, D., Determining accurate molecular sizes in solution through NMR diffusion spectroscopy. *Chem. Soc. Rev.* **2008**, *37* (3), 479-489.
118. Maier, F.; Gottfried, J. M.; Rossa, J.; Gerhard, D.; Schulz, P. S.; Schwieger, W.; Wasserscheid, P.; Steinruck, H. P., Surface enrichment and depletion effects of ions dissolved in an ionic liquid: an X-ray photoelectron spectroscopy study. *Angew. Chem. Int. Edit.* **2006**, *45* (46), 7778-7780.
119. Hofft, O.; Bahr, S.; Himmerlich, M.; Krischok, S.; Schaefer, J. A.; Kempter, V., Electronic structure of the surface of the ionic liquid [EMIM][Tf2N] studied by metastable impact electron spectroscopy (MIES), UPS, and XPS. *Langmuir* **2006**, *22* (17), 7120-7123.
120. Law, G.; Watson, P. R.; Carmichael, A. J.; Seddon, K. R.; Seddon, B., Molecular composition and orientation at the surface of room-temperature ionic liquids: Effect of molecular structure. *Phys. Chem. Chem. Phys.* **2001**, *3* (14), 2879-2885.
121. Caporali, S.; Bardi, U.; Lavacchi, A., X-ray photoelectron spectroscopy and low energy ion scattering studies on 1-butyl-3-methyl-imidazolium bis(trifluoromethane) sulfonimide. *J Electron Spectrosc* **2006**, *151* (1), 4-8.
122. Romero, C.; Baldelli, S., Sum frequency generation study of the room-temperature ionic liquids/quartz interface. *J. Phys. Chem. B* **2006**, *110* (12), 6213-6223.
123. Jeon, Y.; Sung, J.; Bu, W.; Vaknin, D.; Ouchi, Y.; Kim, D., Interfacial Restructuring of Ionic Liquids Determined by Sum-Frequency Generation Spectroscopy and X-Ray Reflectivity. *J Phys Chem C* **2008**, *112* (49), 19649-19654.
124. Sloutskin, E.; Ocko, B. M.; Taman, L.; Kuzmenko, I.; Gog, T.; Deutsch, M., Surface, layering in ionic liquids: An X-ray reflectivity study. *J. Am. Chem. Soc.* **2005**, *127* (21), 7796-7804.
125. Law, G.; Watson, P. R., Surface tension measurements of N-alkylimidazolium ionic liquids. *Langmuir* **2001**, *17* (20), 6138-6141.
126. Carvalho, P. J.; Freire, M. G.; Marrucho, I. M.; Queimada, A. J.; Coutinho, J. A. P., Surface tensions for the 1-alkyl-3-methylimidazolium bis(trifluoromethylsulfonyl)imide ionic liquids. *J. Chem. Eng. Data* **2008**, *53* (6), 1346-1350.
127. Ghatee, M. H.; Zolghadr, A. R., Surface tension measurements of imidazolium-based ionic liquids at liquid-vapor equilibrium. *Fluid Phase Equilibr.* **2008**, *263* (2), 168-175.
128. Niedermaier, I.; Kolbeck, C.; Taccardi, N.; Schulz, P. S.; Li, J.; Drewello, T.; Wasserscheid, P.; Steinruck, H. P.; Maier, F., Organic Reactions in Ionic Liquids Studied by in Situ XPS. *Chemphyschem* **2012**, *13* (7), 1725-1735.

129. Hurisso, B. B.; Lovelock, K. R. J.; Licence, P., Amino acid-based ionic liquids: using XPS to probe the electronic environment via binding energies. *Phys. Chem. Chem. Phys.* **2011**, *13* (39), 17737-17748.
130. Silvester, D. S.; Broder, T. L.; Aldous, L.; Hardacre, C.; Crossley, A.; Compton, R. G., Using XPS to determine solute solubility in room temperature ionic liquids. *Analyst* **2007**, *132* (3), 196-198.
131. Liu, Q. B.; Janssen, M. H. A.; van Rantwijk, F.; Sheldon, R. A., Room-temperature ionic liquids that dissolve carbohydrates in high concentrations. *Green Chem.* **2005**, *7* (1), 39-42.
132. Jacquemin, J.; Husson, P.; Majer, V.; Padua, A. A. H.; Gomes, M. F. C., Thermophysical properties, low pressure solubilities and thermodynamics of solvation of carbon dioxide and hydrogen in two ionic liquids based on the alkylsulfate anion. *Green Chem.* **2008**, *10* (9), 944-950.
133. Domanska, U., Solubilities and thermophysical properties of ionic liquids. *Pure Appl Chem* **2005**, *77* (3), 543-557.
134. Swatloski, R. P.; Spear, S. K.; Holbrey, J. D.; Rogers, R. D., Dissolution of cellulose with ionic liquids. *J. Am. Chem. Soc.* **2002**, *124* (18), 4974-4975.
135. Blesic, M.; Lopes, J. N. C.; Gomes, M. F. C.; Rebelo, L. P. N., Solubility of alkanes, alkanols and their fluorinated counterparts in tetraalkylphosphonium ionic liquids. *Phys. Chem. Chem. Phys.* **2010**, *12* (33), 9685-9692.
136. Roscioli, J. R.; Nesbitt, D. J., State-Resolved Scattering at Room-Temperature Ionic Liquid-Vacuum Interfaces: Anion Dependence and the Role of Dynamic versus Equilibrium Effects. *J. Phys. Chem. Lett.* **2010**, *1* (4), 674-678.
137. Jones, R. A. L., *Soft condensed matter*. Oxford University Press: Oxford, 2002.
138. Fernandez, A.; Torrecilla, J. S.; Garcia, J.; Rodriguez, F., Thermophysical properties of 1-ethyl-3-methylimidazolium ethylsulfate and 1-butyl-3-methylimidazolium methylsulfate ionic liquids. *J. Chem. Eng. Data* **2007**, *52* (5), 1979-1983.
139. Sarkar, S.; Pramanik, R.; Ghatak, C.; Setua, P.; Sarkar, N., Probing the Interaction of 1-Ethyl-3-methylimidazolium Ethyl Sulfate ([Emim][EtSO₄]) with Alcohols and Water by Solvent and Rotational Relaxation. *J. Phys. Chem. B* **2010**, *114* (8), 2779-2789.
140. Kazarian, S. G.; Cammarata, L.; Salter, P. A.; Welton, T., Molecular states of water in room temperature ionic liquids. *Phys. Chem. Chem. Phys.* **2001**, *3* (23), 5192-5200.
141. Hanke, C. G.; Lynden-Bell, R. M., A simulation study of water-dialkylimidazolium ionic liquid mixtures. *J. Phys. Chem. B* **2003**, *107* (39), 10873-10878.

142. Su, Z. H.; Wu, D. C.; Hsu, S. L.; McCarthy, T. J., Adsorption of end-functionalized poly(ethylene oxide)s to the poly(ethylene oxide)-air interface. *Macromolecules* **1997**, *30* (4), 840-845.
143. Hougen, O. A., *Chemical Process Principles*. Wiley: New York, 1954.
144. Felder, R. M.; Rousseau, R. W., *Elementary Principles of Chemical Processes*. John Wiley: New York, 1999.
145. Rebelo, L. P. N.; Lopes, J. N. C.; Esperanca, J. M. S. S.; Guedes, H. J. R.; Lachwa, J.; Najdanovic-Visak, V.; Visak, Z. P., Accounting for the unique, doubly dual nature of ionic liquids from a molecular thermodynamic, and modeling standpoint. *Accounts Chem. Res.* **2007**, *40* (11), 1114-1121.
146. Strutt, J. W., *Philos. Mag.* **1899**, (48), 321-337.
147. Gomez-Diaz, D.; Navaza, J. M.; Sanjurjo, B., Density, kinematic viscosity, speed of sound, and surface tension of hexyl, octyl, and decyl trimethyl ammonium bromide aqueous solutions. *J. Chem. Eng. Data* **2007**, *52* (3), 889-891.
148. Mukerjee P, M. K., *Critical micellar concentration of aqueous surfactant systems*. National Bureau of Standards: Washington, 1971.
149. Mosquera, V.; del Rio, J. M.; Attwood, D.; Garcia, M.; Jones, M. N.; Prieto, G.; Suarez, M. J.; Sarmiento, F., A study of the aggregation behavior of hexyltrimethylammonium bromide in aqueous solution. *J. Colloid. Interf. Sci.* **1998**, *206* (1), 66-76.
150. Lynden-Bell, R. M., Screening of pairs of ions dissolved in ionic liquids. *Phys. Chem. Chem. Phys.* **2010**, *12* (8), 1733-1740.
151. Angell, C. A.; Byrne, N.; Belieres, J. P., Parallel developments in aprotic and protic ionic liquids: Physical chemistry and applications. *Accounts Chem. Res.* **2007**, *40* (11), 1228-1236.
152. Triolo, A.; Russina, O.; Bleif, H. J.; Di Cola, E., Nanoscale segregation in room temperature ionic liquids. *J. Phys. Chem. B* **2007**, *111* (18), 4641-4644.
153. Bhargava, B. L.; Balasubramanian, S., Layering at an ionic liquid-vapor interface: A molecular dynamics simulation study of [bmim][PF6]. *J. Am. Chem. Soc.* **2006**, *128* (31), 10073-10078.
154. Hoyer, H. W.; Zoellner, M.; Marmo, A., Some Colloidal Properties of Decyl-and Dodecyltrimethylammonium Dodecyl Sulfate. *J. Phys. Chem.* **1961**, *65* (10), 1804-&.
155. Fernandes, R. M. F.; Marques, E. F.; Silva, B. F. B.; Wang, Y. J., Micellization behavior of a cationic surfactant with high solubility mismatch Composition, temperature, and salt effects. *Journal of Molecular Liquids* **2010**, *157* (2-3), 113-118.

156. Gilanyi, T.; Meszaros, R.; Varga, I., Phase transition in the adsorbed layer of cationic surfactants at the air/solution interface. *Langmuir* **2000**, *16* (7), 3200-3205.
157. Behera, K.; Pandey, S., Ionic liquid induced changes in the properties of aqueous zwitterionic surfactant solution. *Langmuir* **2008**, *24* (13), 6462-6469.
158. Jiao, J. J.; Dong, B.; Zhang, H. N.; Zhao, Y. Y.; Wang, X. Q.; Wang, R.; Yu, L., Aggregation Behaviors of Dodecyl Sulfate-Based Anionic Surface Active Ionic Liquids in Water. *J. Phys. Chem. B* **2012**, *116* (3), 958-965.
159. Laughlin, R. G., Fundamentals of the Zwitterionic Hydrophilic Group. *Langmuir* **1991**, *7* (5), 842-847.
160. Wang, B.; Zhang, Q. G.; Yang, H. Z., Study on solid-liquid phase equilibria in ionic liquid - 2. The solubility of alkali bromide in ionic liquid 1-ethyl-3-methylimidazolium ethyl sulfate. *Fluid Phase Equilib.* **2007**, *254* (1-2), 163-166.
161. Albayrak, C.; Cihaner, A.; Dag, O., A New, Highly Conductive, Lithium Salt/Nonionic Surfactant, Lyotropic Liquid-Crystalline Mesophase and Its Application. *Chemistry-a European Journal* **2012**, *18* (14), 4190-4194.
162. Seredyuk, V.; Alami, E.; Nyden, M.; Holmberg, K.; Peresykin, A. V.; Menger, F. M., Adsorption of zwitterionic gemini surfactants at the air-water and solid-water interfaces. *Colloid Surface A*. **2002**, *203* (1-3), 245-258.
163. Wang, H. Y.; Wang, J. J.; Zhang, S. B.; Xuan, X. P., Structural Effects of Anions and Cations on the Aggregation Behavior of Ionic Liquids in Aqueous Solutions. *J. Phys. Chem. B* **2008**, *112* (51), 16682-16689.
164. Bales, B. L.; Zana, R., Cloud point of aqueous solutions of tetrabutylammonium dodecyl sulfate is a function of the concentration of counterions in the aqueous phase. *Langmuir* **2004**, *20* (5), 1579-1581.
165. Rivera-Rubero, S.; Baldelli, S., Influence of water on the surface of hydrophilic and hydrophobic room-temperature ionic liquids. *J. Am. Chem. Soc.* **2004**, *126* (38), 11788-11789.
166. Sha, M. L.; Niu, D. X.; Dou, Q.; Wu, G. Z.; Fang, H. P.; Hu, J., Reversible tuning of the hydrophobic-hydrophilic transition of hydrophobic ionic liquids by means of an electric field. *Soft Matter* **2011**, *7* (9), 4228-4233.
167. MacFarlane, D. R.; Vijayaraghavan, R.; Ha, H. N.; Izgorodin, A.; Weaver, K. D.; Elliott, G. D., Ionic liquid "buffers"-pH control in ionic liquid systems. *Chem. Commun.* **2010**, *46* (41), 7703-7705.

168. Dai, Q.; Laskowski, J. S., The Krafft Point of Dodecylammonium Chloride - Ph Effect. *Langmuir* **1991**, *7* (7), 1361-1364.
169. Tah, B.; Pal, P.; Mahato, M.; Talapatra, G. B., Aggregation Behavior of SDS/CTAB Catanionic Surfactant Mixture in Aqueous Solution and at the Air/Water Interface. *J. Phys. Chem. B* **2011**, *115* (26), 8493-8499.
170. Lerum, R. V.; Bermudez, H., Controlled Interfacial Assembly and Transfer of Brushlike Copolymer Films. *Chemphyschem* **2010**, *11* (3), 665-669.
171. Winterton, N., Solubilization of polymers by ionic liquids. *J. Mater. Chem.* **2006**, *16* (44), 4281-4293.